High-Resolution Geophysical Imaging and Characterization of Severe Landslides Vicinities at South-Eastern Nigeria for Uni-Vario-Seasonal Degradation Monitoring and Civil Engineering Remediation

Edward Emenike CHIKWELU

2021

High-Resolution Geophysical Imaging and Characterization of Severe Landslides Vicinities at South-Eastern Nigeria for Uni-Vario-Seasonal Degradation Monitoring and Civil Engineering Remediation

By

Edward Emenike CHIKWELU
Student No: 217052231

Supervisor: Professor Naven Chetty

Submitted in partial fulfillment of the academic requirements for the degree of

Doctor of Philosophy

School of Chemistry and Physics,

College of Agriculture, Engineering, and Science,

University of KwaZulu-Natal,

Pietermaritzburg Campus, South Africa

2021

ABSTRACT

This research work used high-resolution geophysical methods to explore the near surface of severe gully-erosion sites. The erosion that mesmerized the environment as landslides is the major landscaping challenge facing Anambra Basin in the South Eastern Nigeria. The geophysical techniques used include electrical resistivity tomography (ERT), induced polarization (IP), vertical electrical sounding (VES), and geotechnical analysis to study the subsurface conditions of severe gullies. Principally Wenner, Schlumberger, and dipole-dipole are the geophysical tomography technique used during the survey, depending on the peculiarity of each selected site. Geotechnical data analysis was used to confirm the results of vertical electrical sounding at a specific location, with the aid of resistivity formations. The geodynamics of the sites as related to rocks' susceptibility to failure, and the mechanisms of slope failure was investigated, and foundation depths of the immediate surroundings of the Nanka gully were studied using geotechnical data. The surrounding and the subsurface of the eroded portions were monitored through imaging and analysis across the basin to measure hydrological contribution to the gully risks and other prevailing factors. The geoelectrical data was acquired with the ABEM Terrameter SAS 4000 and the ABEM LUND ES464 electrode selection system (using resistivity method) and processed with the RES2DINV software to produce 2D subsurface images. The VES resistivity curve matching was developed by a partial curve matching technique; and interpreted by Minitab 18 software to produce subsurface contour maps. In addition, the subsurface contour maps were qualitatively analysed with mapped surface geology and information on current geological typical rocks. In the geotechnical analysis, Spangler and Handy sampling techniques were used to collect eighteen (18) samples from dug gully walls, and the laboratory tests were to ascertain the soil properties index. The results of the models indicate that the study area is mainly clayey and sandstone formations that exhibited low resistivity values corresponding to the shale layers and groundwater zones. Many features that may lead to slope failure are present in the study areas, such as fractures, boulders, weak zone, and saturated zone. The results also showed that the soils in the study areas are friable hence easily washed off whenever there is storm water runoff from the surface, making the landslide active over the years despite every protective precaution put in place. In conclusion, this research work has identified lithologies, structural deformations, and distinguishing clayey zones from water-saturated zones, proving that the geophysical technique is the most successful tool in the landslide investigation.

PREFACE

The research work was undertaken by Chikwelu Edward Emenike, Department of Physics, School of Chemistry and Physics of the College of Agriculture, Engineering and Science, University of KwaZulu-Natal, Pietermaritzburg campus, South Africa. The research was financially supported by my personal effort and help from beloved friends.

This thesis is the original work carried out by me and has never been presented in any form to another university. However, while the works of other writers were carefully cited and recognized in the text, the results were derived from field investigations undertaken by the author.

Chikwelu Edward Emenike (Student): Signature █████████ ..….Date:….. 01/12/2021…

Professor Naven Chetty (Supervisor): Signature █████████ ….. Date:……01/12/2021….

DECLARATION 1: PLAGIARISM

I, Chikwelu Edward Emenike, declare that:

(i) the research reported in this dissertation, except where otherwise indicated or acknowledged, is my original work;

(ii) this dissertation has not been submitted in full or in part for any degree or examination to any other university;

(iii) this dissertation does not contain other persons' data, pictures, graphs or other information, unless specifically acknowledged as being sourced from other persons;

(iv) this dissertation does not contain other persons' writing, unless specifically acknowledged as being sourced from other researchers. Where other written sources have been quoted, then:

a) their words have been re-written but the general information attributed to them has been referenced;

b) where their exact words have been used, their writing has been placed inside quotation marks, and referenced;

(v) where I have used material for which publications followed, I have indicated in detail my role in the work;

(vi) this dissertation is primarily a collection of material, prepared by myself, published as journal articles or presented as a poster and oral presentations at conferences. In some cases, additional material has been included;

(vii) this dissertation does not contain text, graphics or tables copied and pasted from the Internet, unless specifically acknowledged, and the source being detailed in the dissertation and in the References sections.

Signature (Student):.. …………………………Date: 1st December, 2021

DECLARATION 2: 3-PUBLICATIONS

I, Chikwelu Edward Emenike, declare that contributions to publications that are part of the research work are presented as chapters in this thesis.

i.   Chikwelu Edward Emenike & Naven. Chetty: Assessment of the subsurface conditions of a landslide in South-Eastern Nigeria, by using geotechnical results for a proper understanding of the geo-electrical sounding findings. International Journal of Applied Science and Engineering. ID IJASE-2021-090 (Under review).

ii. Chikwelu Edward Emenike & Naven Chetty: The application of the geophysical methods in the study of slope instability at four major landslides in South-Eastern, Nigeria. (Submitted for publication).

iii. Chikwelu Edward Emenike & Naven Chetty (2021): Use of Electrical Resistivity Tomography in investigating the internal structure of a landslide and its groundwater characterization (Nanka Landslide, Anambra State, Nigeria). *Journal of Applied Science and Engineering, 25*(4), 663-672. (Published).

Signature (Student): ………………………………..Date: 1st December, 2021.

CONFERENCE CONTRIBUTION

i. Chikwelu Edward Emenike & Naven Chetty: Use of electrical resistivity tomography in investigating the internal structure of the landslide and its groundwater characterization (Nanka Landslide, Anambra State, Nigeria). Flash presentation at the Postgraduate Research and Innovation Symposium (Online), College of Agriculture, Engineering, and Science, University of KwaZulu-Natal, South Africa, 10th to 11th December, 2020.

Signature (Student): …………………………….Date: 1st December, 2021.

DEDICATION

This research work is dedicated to my parents Mr. and Mrs. Bernard N. Chikwelu, my wife, Mrs. Chikwelu Chidimma Patience, my Children, and my friend Rev. Fr. Christian Ossy Odionye.

ACKNOWLEDGMENTS

TABLE OF CONTENTS

LIST OF ABBREVIATION AND SYMBOLS

1D	One-dimensional
2D	Two-dimensional
3D	Three-dimensional
4D	Four-dimensional
ASTM	American Society for Testing Materials
Cc	Current Coefficient
CPT	Current Procedural Terminology
Cr	Relative Consistency
DC	Direct Current
ERT	Electrical Resistivity Tomography
EM	Electromagnetic
FCT	Federal Capital Territory
GIS	Geographic Information System
GPR	Ground Penetration Radar
GRM	General Reciprocal Method
HOV	High Occupancy Vehicles
HSP	Horizontal Seismic Profiling
H/V	Horizontal and Vertical Components
I	Current
IP	Induced Polarization
LI	Liquidity Index
NE-SNW	North East – South West
NPC	National Population Commission

PI	Plastic Index
PL	Plastic Limit
P-S	Primary – Secondary
SLIDE	Slope Infiltration Distributed Equilibrium
SP	Self-Potential
SWM	Surface Wave Method
VES	Vertical Electrical Sounding
VLF	Very Low Frequency
VSP	Vertical Seismic Profiling
Wn	Natural Moisture Content

LIST OF TABLES

LIST OF FIGURES

CHAPTER 1: INTRODUCTION

1.1 General Introduction

The most valuable resource of the earth is the soil, and it sustains both plants and animals for their growth and development. Therefore, any harm to the soil poses dangers to both plant and animal life. Landslide is a well-known environmental problem to the people of South-Eastern Nigeria (Akinbile, 2017). Landslide may be considered a severe natural hazard due to its unpredictable occurrence. It leads to significant economic losses and even fatalities to life and properties in the affected areas. Landslide events in many parts of South-Eastern Nigeria often result from weathering, poor drainage system, consequent civil engineering infrastructure failure, intense rainfall, and other human activities involving deforestation (Okoyeh *et al*, 2014). There is a need for annual monitoring of the landslide therein using modern geophysical equipment to provide pre-information on the underlying conditions. Again, the washing away of the top layer of soil degraded its fertility, and unless suitable precautional measures are adopted, the sloping zone will begin to slip. According to Adeola *et al* (2016), it is critical to detect and analyze gully erosion in greater depth in order to get a better understanding of land sliding processes and plan future repair. Information generated could possibly be used to improve current landslide hazards and prevent occurrences.

Landslides modify the shape and internal structure of the compacted landmass in terms of rock properties and groundwater formation (Miko S. *et al*., 2017). Anambra Basin is located in the Southern Basin Trough which has a synclinal sedimentary structure with about 500 m of Upper Cretaceous. It is the most affected zone in Nigeria by landslides. It consists of coarsening upward sequences with thick, dark grey shale of the base, grading upward through siltstones into thin, textually mature sandstone (Jahantigh & Pessarakli, 2011; Ojo & Akande, 2012).

Geological mapping of the surface area affected by the landslide is usually done by observation of aerial photographs or remote-sensing images that portrays the topographical expression of the landslide (Azwin *et al*., 2013). However, according to Xu *et al*., (2017), if the landslide is old or inactive, its morphologic characteristics and limits may have been eroded therefore surface observations and measurements must be supported by depth reconnaissance. In addition, the study of the sliding mass down to the undisturbed rock or soil is required for the determination of the 3D shape of the unstable body. Traditional geotechnical methods, which primarily include trenching, penetration tests (when possible), and boreholes (Fell *et al*, 2005), allow for a detailed geological description and mechanical characterization of the material,

identifying the vertical border of the slide as well as the parameters required for slope stability analysis (Zanial *et al*., 2012). These techniques only provide precise information, and their application is restricted due to the difficulties of drilling onto steep and unstable slopes (Zanial *et al*., 2012). The drilling method is a good one but require many drilling points for better information and knowledge, which increases the time, cost, and labour of the research. This method only provides single knowledge per drilling point and is unable to reveal what is happening at the next point (single-point information 1D). Yalcin (2011) used the application of geodynamic mapping and geological structure mapping by a visible observation survey based on existing damaged features caused by a movement and outcrop of rock, which still has some limitations.

Geo-techniques offer subsurface information on the change of physical variables with different spatial (dimensional) coordinates after data processing. One-dimensional data represents a horizontal or vertical profile, two-dimensional or three-Dimensional data stands for geophysical inversion (imaging), and while four-dimensional data stands for three-dimensional with time (Fomel, 2007; Sharma, 1997).

Recently, landslide vulnerability mapping has been made possible by the usability and variety of remote sensing data and thematic layers as causative factors data through Geographic Information System (GIS) and other geoscientific methods (Shahabi & Hashim, 2015). Almost all the landslides that occurred recently are referred to as significant geomorphic processes that usually form an important landscaping aspect in the tropical humid mountains of the surroundings (Thomas, 2001). The cloudy and rainy weather conditions are usually unfavourable for optical remote sensing data (Razak *et al*, 2011). As a result, different ideas and precise data analysis are required to reveal the landslide susceptibility mapping in the tropical environment of South-Eastern Nigeria (Thomas, 2001). Due to the persistent nature and occurrence of the landslide in South-Eastern Nigeria, there is a need for geoengineering investigation and analysis of data from the affected area, to foresee the effect of this natural disaster and prevent the devastation of the environment.

1.2 Research Motivation

Although with a thorough study and constant monitoring, determining the stability and calculating the landslide risk might be difficult. This is especially true for areas with few indicators of impending collapses, such as areas with dump-clay. Dump-clay-induced slides can quickly develop, resulting in complete damage (there is nothing more to be measured

afterward). Preliminary surveying methods, such as geological mapping, geotechnical and geophysical techniques, must be adapted to the features of the ground investigations. The combination of geotechnical and geoelectrical methods in landslides faces numerous well-known challenges, including determining the 2D geometry of the site with regard to the weak and failure surface, as well as differentiating the groundwater boundaries (Ojo & Akande, 2012). However, combinations of these variables are associated with varying degrees of landslide menace, particularly in dump-clay areas.

The internal architecture of landslide-prone terrain frequently differs from adjacent stable regions in terms of hydrogeological and geological characteristics (Grandjean, 2012). In turn, this difference can result in physic-mechanical characteristics changes. The inquiry down to the undisturbed rock or soil is required to define the unstable 2D body shape (Carreira *et al.*, 2010). The main advantages of geophysical techniques, as previously stated, are their flexibility and relative simplicity of deployment in a homogenous environment, even on steep terrain. Grandjean *et al.*, (2007) observed that the main disadvantages of geophysical methods are the non-similarity of solution from a distinctive set of data and provision of physic-mechanical parameters rather than geological properties. Needful to note, however, that virtually all of the benefits of geophysical methods are also downsides of geotechnical procedures, underlining the complementary nature of the two investigative techniques (Grandjean, 2012; McCann & Forster, 1990).

The geophysical approach is the best instrument for determining the feasibility of survey operations and obtaining landslides information. It can also be used more thoroughly in the ground-proofing, which is always necessary, to map the relevant properties, both laterally and vertically, and preferably in a quantitative manner for use by geo-technicians. Finally, both geophysical and geotechnical approaches are crucial in monitoring temporal parameter variations, if any, with the former calibration measurements and the latter for spatial variability.

Instead of employing the various geophysical approaches independently, it is necessary to look at the possibilities of developing an integrated strategy aimed to resolve a specific environmental challenge, (Ghose 2010). Based on the underlying physics, it may be needed to merge multiple approaches or disciplines under certain boundary conditions to solve a near-surface soil features problem accurately and efficiently (Ghose & Slob, 2006). This technique differs thematically from other interdisciplinary inclusion performed at the stage of interpretation (processing data independently before being combined and interpreted) or

inversion stochastic (inversion of several datasets at the same time using quantitative or empirical correlation), as done recently (Zhubayev & Ghose, 2011). These efforts to combine different methods for achieving a certain objective were qualitative. Such physics-based integration, according to Ghose (2010), yet to be applied in deep-clay areas in Nigeria, and the underlying knowledge needs to be established to get a better quantitative understanding. The integration of the geophysical and geotechnical methods used in this research work will constitute a part of the global effect in landslide investigation. The ERT/IP results will unveil the subsurface conditions of the major landslides in South-Eastern Nigeria and their remediation for future occurrence.

1.3 Aim and Objectives

This research is aimed at using a high-resolution geophysical imaging and geotechnical data to characterize the vicinities of severe landslides at the Anambra State Basin in the South-Eastern part of Nigeria.

The objectives of the research include:

1. To carry out a high-resolution 2D geoelectrical tomography using Wenner and Dipole-dipole techniques at the selected sites.

2. To determine the groundwater condition through Vertical Electrical Sounding iso-resistivity contour maps and to deduce the lithological component of the slides subsurface.

3. To determine the vertical and horizontal subsurface conditions of the area by interpreting the vertical electrical sounding data along with geotechnical field data.

4. To carry out any other affordable geophysical tomography technique, which is found complementary to the geoelectrical tomography at similar survey lines. This includes the soil composition test on the soil samples at different depths from sliding site.

5. To calculate the bearing capacity and other relevant parameters of the landslides' boundaries and vicinities at each site for civil engineering use.

6. To calculate the expected bearing pressure and other relevant parameters commensurate for civil constructions of roads, culverts and bridges, low and high-rise superstructures at the landslide's vicinities.

1.4 Location and Population of South-Eastern Nigeria

Figure 1.1 shows the Six (6) geopolitical zones in Nigeria. South-Eastern Nigeria is one of Nigeria's six geopolitical zones, comprised of six states; Anambra, Abia, Enugu, Imo, and Ebonyi. Other zones are North-West, North-East, North-Central, South-West, and South-South. The lower Niger River divided the zones into two sections; the East (encompassed the majority of the zone), and the West (encompassed the remaining parts).

Figure 1.1: The map of Nigeria showing Six (6) Geopolitical Zones (Okali *et al.*, 2001).

The South-Eastern Nigeria covers about 76,358 square kilometres east of the Lower Niger and south of the Benue Valley (Okali *et al.*, 2001). The zone is situated between 4 and 7 degrees north of the Equator and between 7 and 9 degrees east of the Equator. This zone is one of the country's most populated areas, and in 2016 the population was about 21,955,414 million people based on the approved 3.22% annual population growth rate by the 'National Population Commission 2016' (Ezeah *et al.*, 2013). Up to 69.91% of the people population lives in remote areas. Except for the metropolitan node of Port Harcourt, which is surrounded by a belt with high population density, the most heavily populated belt spreads through the area from Onitsha across Calabar to Awka-Orlu-Owerri, with population density dropping both at the north-east and at the south-west (Okali *et al.*, 2001). A high birth rate, a decreasing mortality rate, a steady rise in life expectancy, and a decrease in illiteracy rate are other demographic features of the population. This area is in the tropical rainforest zone of Nigeria, which has been replaced with derived savannah by human activities such as deforestation, bush burning, and intensive agriculture (Okali *et al.*, 2001). Most of the forestland has been turned for agriculture and the oil palm plantation. With no need for irrigation, the runoff water supports farming operations. It also encourages luxuriant forests and the recharging of deep and surface water sources beyond farmlands. The research focus is within the Anambra Sedimentary Basin, which is covered by the Nanka Formation. Nanka Formation is an unconsolidated sand deposit forming part of the Eocene deposit zone, underlain by the marine Imo shale of Paleocene age and overlain by the paralic Ogwashi-Asaba Formation of Oligocene (Adegoke *et al*, 2016; Onyewuchi & Ugwu, 2017).

1.5 Climate and Vegetation

The study area's vegetation is within the West African rainforest belt as shown in Figure 1.2, but notable amount of the parts has been subjected to massive deforestation prompted by anthropogenic activities, because, reducing some parts to savannah vegetation (Nwagbara & Ibe, 2015). In some places, (For example: - Anambra State) the heavy rainforest has equally given way to light rainforest as a result of human activities on the environment. Tall trees with canopy strata, thick undergrowth, and shrubs characterize the vegetation of the Tropical Rainforest. The landscape is dominated by oil palms and other species of trees found in the area include iroko, mango, mahogany, and oil bean (Nwagbara & Ibe, 2015).

The climate of South-Eastern Nigeria is an equatorial tropical rainforest type. Again, the area is heavily influenced by two climate conditions, namely the rainy season and the dry season.

The rainy season, as the name indicates, begins from April to October and is marked by thunderstorms, whereas the dry season occurs from November to March and is marked by high temperatures and a dusty environment. The rainy season is indeed characterized by relatively high temperature (33^0C) and high relative humidity (85%). The dry season is characterized by chilly, dry Harnatan winds. This significantly lowers the temperature in the months of December and January. The annual rainfall cycle includes both dry and wet seasons. Total annual rainfall according to (Chinweze, 2017; Osadebe *et al.*, 2014) is about 1800 mm. In the study areas, the total annual rainfall during the rainy season in the area leads to high soil saturation over a long period within the year. Excessive evaporation, low relative humidity (26%), low rainfall, and general dryness are its defining characteristics. These result in the drying of vegetable cover and subsequent bush burning that causes high fire accidents, the shedding of leaves by deciduous trees, the harvesting of farm produce, and so on (Chinwez, 2017; Peltzer *et al.*, 2010).

Climate variability has increased rainfall intensity resulting in massive flooding and storms that have also aggravated environmental and land degradation problems in the South-Eastern Nigeria. Land degradation problems such as gully erosion affect lands, soils and vegetation, water and landscape resources in areas where it is prevalent.
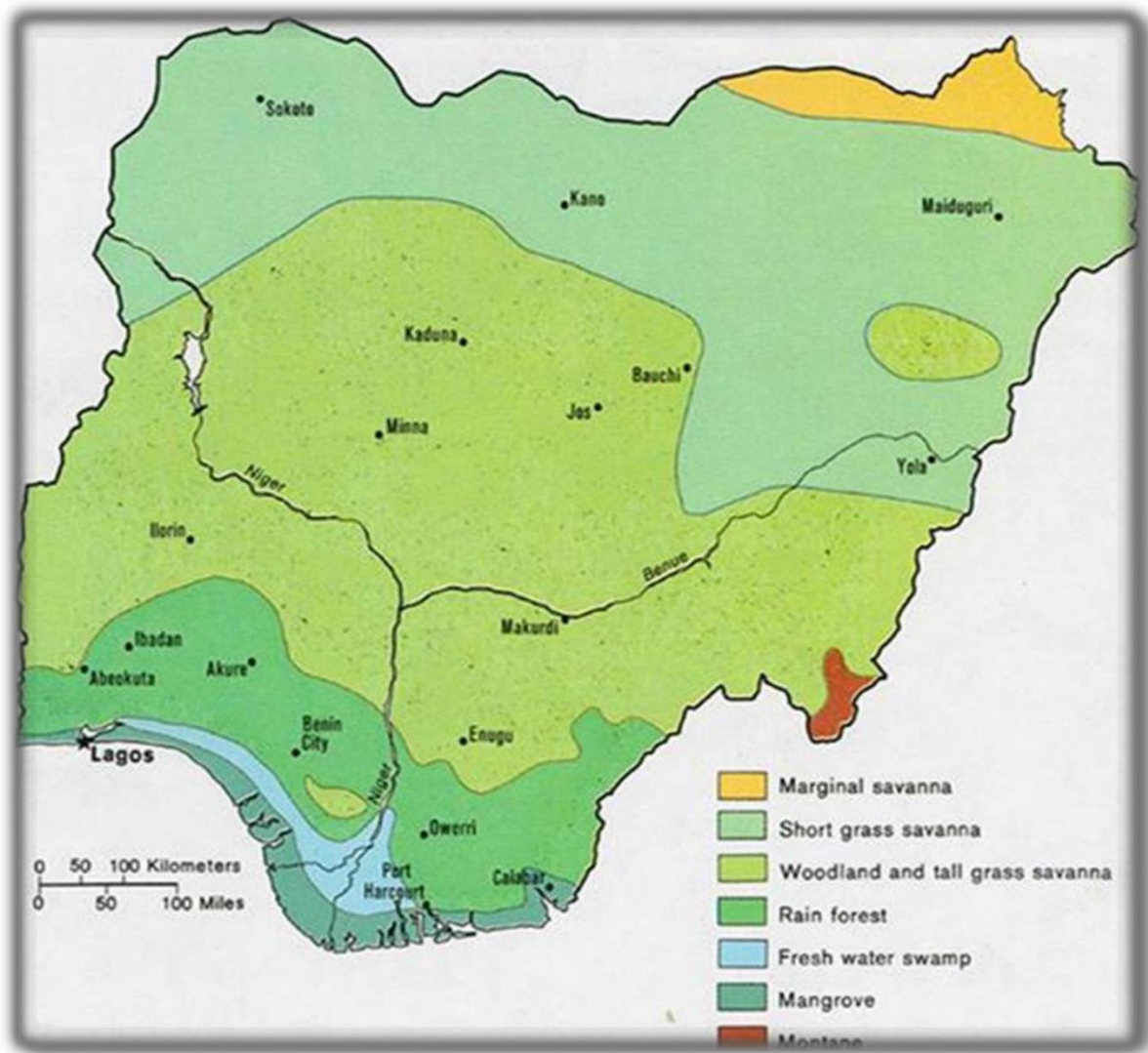
Figure 1.2: Vegetation map of Nigeria (Oni, Jimoh, & Adebisi, 2014).

1.6 Topography and Drainage

The area's topographic features have a distinct influence on the potential for erosion. The study areas have high terrain with noticeable rolling. These study areas also have long steep slopes that enhance the speed of runoff that gather momentum to produce the force that quickly detaches and transports soil particles, resulting in gullies. This (previously) lush green land is currently transforming into the arid terrible ground that is unfit for farming, unsafe for human settlement, and on its road to becoming a piece of useable land.

The soil type in the study area is typically loose, non-compactible and highly erodible. The nature of the soil hastens the erosion process more when exposed to external forces such as flooding and human disturbances.

The Anambra River, which drains into river Niger, is the main drainage system for the state. In the area, the river's natural flow patterns and streams form a dendritic drainage pattern (Amangabara, 2015), which makes the areas to be well drained. Two types of structures are generally identifiable in the state, namely sedimentation basins, and uplifts.

1.7 Accessibility and Road Network

A comprehensive and organised transportation system that ensure steady movement of goods and services defines a societal quality of life. Oni *et al* (2014), further asserts that the transportation system involves the movement of materials, people, ideas, goods, and services from one location to another, leading to the spatial distribution of resources. The transportation, movement of goods and services are mandatory features of modern life due to its multidimensional functions, the unavoidability of communication, and dynamic structure. A road may be described as the lifeblood of contemporary civilization and social contact; as a result, the intra- and inter-regional road network of a place sharpen its economic growth. Human settlements are naturally heterogeneous but are symbiotic. The marketplace and other critically influencing factors such as the mode of transit, the socioeconomic characteristics, the distance, location, and product range are important parts of the system. The road network, as one of the oldest infrastructures, occupies an important location in antique and modern times in modernization, sustainable development, and daily work.

South-Eastern Nigeria's well-structured road network is causing a slew of transportation issues, including making it difficult to get to and around busy marketplace (Chinweze 2017). Some of these markets are located in historically and culturally significant areas, which contribute to

the large volume of traffic that surrounds them. The state vehicle traffic fleet composition reveals the road transport pattern in Anambra State, with private automobiles accounting for 36.18 percent of total daily vehicle traffic, minibuses accounting for 39.60 percent, and lorries of various types accounting for the remaining percent (Ikegbunam, 2014). The area of study can be accessed through the Awka-Ekwulobia road including several footpaths connecting the adjoining villages. The study areas are also connected to the surrounding villages by several footpaths. Some roads connecting different areas of the villages are over 100 years old and facilitate movement in the study area.

1.8 Groundwater flow system in South-eastern Nigeria

The steady-state regional groundwater flow network diagram in Figure 1.3, derived from hydraulic head data in several smaller South-Eastern Nigeria drainage basins. It also showed the steady-state regional groundwater flow network.
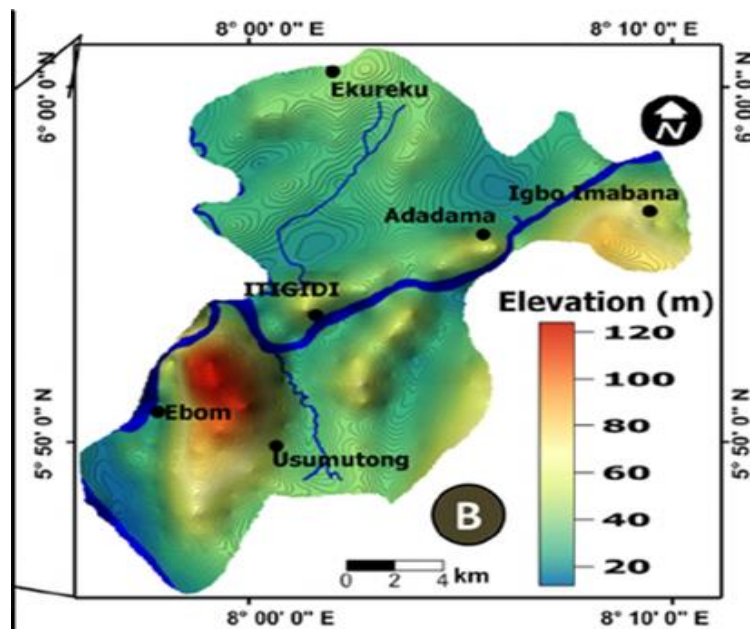
Figure 1.3: The steady-state groundwater flow network across South-Eastern, Nigeria (Oni *et al.*, 2014).

The indicated regions of local, intermediate, and regional groundwater flow systems correspond to three distinct basin hydraulic systems, namely an upper system with hydrostatic forming pressures, a middle system with pressures only slightly higher than the hydrostatic pressure, and a relatively deep system with abnormally high forming pressures (Onyekuru *et al.*, 2010). The south-eastern flow systems discharge into the Niger River, Cross River and Anambra, while the intermediate flow drains into their small tributaries (Amadi *et al.*, 2012; Onyekuru *et al.*, 2010). Minor and usually seasonal streams are associated with local groundwater flow systems. Local relief is negligible at the basin's centre, along the coast, and thus south-eastern flow systems predominate in these areas. The distribution of fluid potential in the upper and middle hydro-stratigraphic units is presented to illustrate that hydraulic heads and fluid energies are the highest at the edge of the basin to the east where the unit's major aquifers are exposed, and much lower at the centre of the basin to the southwest where the aquifer is confined (Michael *et al.*, 2003).

According to Ao *et al.*, (2015), Anambra Basin is one of the most economically strategic watersheds in South-Eastern Nigeria and occupies an area of about 95,000km^2. It does only have abundant water resources but also has oil and gas deposit potential.

1.9 The structure of the thesis

The structural arrangement of this thesis is laid out in six (6) chapters. Chapter 1 gives a general introduction to this work, background possibilities and challenges, aims and objectives of the research, the location and population of South-Eastern Nigeria, climate and vegetation, topography and drainage, accessibility and road network, and groundwater flow system in South-Eastern Nigeria.

Chapter 2 reviewed the related literature of the landslides menace and its significant effect in South-Eastern Nigeria. The geology of Nigeria, that is made up of three major components, namely the Sedimentary Basins, Young Granites, and Basement Complex, is also discussed. This chapter covered the Anambra Sedimentary Basin, produced by sedimentation that began after the break of South America from Africa during the Aptian/Albian era, influenced by three major tectonic processes.

Chapter 3 discusses journal article, which focuses on the assessment of the subsurface conditions of a landslide in South-Eastern Nigeria, by using geotechnical results for a proper understanding of the geo-electrical sounding findings. Eighteen (18) soil samples for analysis

were collected from dug holes at different marked depths and locations using geotechnical methods. Analysed data from the geotechnical investigation were used to interpret geoelectrical method (with Schlumberger configuration) findings, which include topsoil, subsoil, vertical geo-electric section, regolith, bedrock, and rock fragment Maps. The soil in the study area is friable according to the results, hence easily washed off when storm water or rainfall runoff drains away the surface, making the slide active over the years, defying every preventive measure put in place.

The application of the geophysical methods in the analysis of slope instability at four major landslides in South-Eastern Nigeria is the focus of chapter 4. The dipole-dipole array of the geoelectrical method (2D electrical resistivity tomography and induced polarization (IP) were used for this research due to its relatively high lateral and vertical resolution. The results showed that there are examples of features that might prompt a slope failure; boulders, weak / water-saturation zone, present.

In order to investigate the internal structure of the Nanka landslide and its groundwater characterization in Chapter 5, electrical resistivity tomography was used. The Wenner array was used at the survey site for collection of data from eleven (11) profiles due to its ability to obtain deeper profile data, and the apparent resistivities data are easily calculated. The formation of the Nanka landslide is related to the terrain morphology, environment factors, rainfall, and other features such as fractures and boulders, which led to slope failure (Akinbile, 2017).

Finally, Chapter 6 outlines the key findings of the dissertation and conclusions of the research, based on each chapter, and offers some recommendations for potential research work.

Bibliography

Adegoke, O. S., Oyebamiji, A., Edet, J. J., Osterloff, P., & Ulu, O. K. (2016). *Cenozoic foraminifera and calcareous nannofossil biostratigraphy of the Niger delta*: Elsevier.

Adeola, F. O., Ubom, O., & Adeyemi, O. (2016). Estimating Soil Loss from Soil Eros ion-Induced Land Degradation in Uyo Metropolis, Nigeria Using Remote Sensing Techniques and GIS. *Ife Research Publications in Geography, 12*(1), 120-137.

Akinbile, C. (2017). Soil Erosion in South Eastern Nigeria: A Review. *Scientific Research Journal (SCIRJ), V*, 30-37.

Amadi, A. N., Olasehinde, P. I., Yisa, J., Okosun, E. A., Nwankwoala, H. O., & Alkali, Y. B. (2012). Geostatistical assessment of groundwater quality from coastal aquifers of Eastern Niger Delta, Nigeria. *Geosciences, 2(3)*, 51-59.

Amangabara, G. (2015). Drainage morphology of Imo basin in the Anambra–Imo river basin area, of Imo state, southern Nigeria. *Journal of Geography, Environment and Earth Science International, 3*(1), 1-11.

Ao, O.-B., Adebayo, O., Madukwe, H., & Aturamu, A. (2015). Palynological and Sequence Stratigraphy Characterization of the Early-Late Campanian Nkporo Shale, Orekpekpe-Imiegba Area, Anambra Basin, Nigeria. *European Journal of Basic and Sciences, Vol. 2*, 1-15.

Azwin, I. N., Saad, R., & Nordiana, M. (2013). Applying the Seismic Refraction Tomography for Site Characterization. *APCBEE Procedia, 5*, 227-231. Retrieved from http://www.sciencedirect.com/science/article/pii/S2212670813000407. doi:https://doi.org/10.1016/j.apcbee.2013.05.039

Carreira, P. M., Marques, J. M., Pina, A., Gomes, A. M., Fernandes, P. A. G., & Santos, F. M. (2010). Groundwater assessment at Santiago Island (Cabo Verde): a multidisciplinary approach to a recurring source of water supply. *Water Resources Management, 24*(6), 1139-1159.

Chinweze, C. (2017). *Erosion and Climate Change Challenges: Anambra State Nigeria, Case Study* Paper presented at the IAIA17 Conference. https://conferences.iaia.org/2017/uploads/presentations/IAIA17%20Erosion_Chizoba.pdf

Ezeah, P., Iyanda, C. C., & Nwangw, C. (2013). Challenges of national population census and sustainable development in Nigeria: A theoretical exposition. *IOSR Journal Of Humanities And Social Science (IOSR-JHSS), 18*(1), 50-56.

Fell, R., Ho, K., Lacasse, S., & Leroi, E. (2005). *A framework for landslide risk assessment and management*.

Fomel, S. (2007). Shaping regularization in geophysical-estimation problems. *Geophysics, 72*(2), R29-R36.

Ghose, R. (2010). *Possibilities for multidisciplinary, integrated approaches in near-surface geophysics.* Paper presented at the 72nd EAGE Conference and Exhibition-Workshops and Fieldtrips.

Ghose, R., & Slob, E. (2006). Quantitative integration of seismic and GPR reflections to derive unique estimates for water saturation and porosity in subsoil. *Geophysical Research Letters, 33*(5).

Grandjean, A., Adnot, J., & Binet, G. (2012). A review and an analysis of the residential electric load curve models. *Renewable and Sustainable energy reviews, 16*(9), 6539-6565.

Grandjean, G., Malet, J.-P., Bitri, A., & Méric, O. (2007). Geophysical data fusion by fuzzy logic for imaging the mechanical behaviour of mudslides. *Bulletin de la Société géologique de France, 178*(2), 127-136.

Ikegbunam, F. I. (2014). Onitsha Urban Road Transport System: Implications for Urban Transport Planning. *International Journal of Applied, 4*(4).

Jahantigh, M., & Pessarakli, M. (2011). Causes and Effects of Gully Erosion on Agricultural Lands and the Environment. *Communications in Soil Science and Plant Analysis, 42*, 2250-2255. doi:10.1080/00103624.2011.602456

McCann, D., & Forster, A. (1990). Reconnaissance geophysical methods in landslide investigations. *Engineering Geology, 29*(1), 59-78.

Michael, K., Machel, H. G., & Bachu, S. (2003). New insights into the origin and migration of brines in deep Devonian aquifers, Alberta, Canada. *Journal of Geochemical Exploration, 80*(2-3), 193-219.

Mikoš, M., Vilímek, V., Yin, Y., & Sassa, K. (2017). *Advancing Culture of Living with Landslides: Volume 5 Landslides in Different Environments*: Springer International Publishing.

Nwagbara, M., & Ibe, O. (2015). Climate change and soil conditions in the tropical rainforest of Southeastern Nigeria. *Journal of Geography and Earth Sciences, 3*(1), 99-106.

Ojo, O., & Akande, S. (2012). Sedimentary Facies Relationships and Depositional Environments of the Maastrichtian Enagi Formation, Northern Bida Basin, Nigeria. *Journal of Geography and Geology, 4*. doi:10.5539/jgg.v4n1p136

Okali, D., Okpara, E., & Olawoye, J. (2001). *The case of Aba and its region, Southeastern Nigeria:* IIED.

Okoyeh, E. I., Akpan, A. E., Egboka, B., & Okeke, H. (2014). An assessment of the influences of surface and subsurface water level dynamics in the development of gullies in Anambra State, southeastern Nigeria. *Earth Interactions, 18*(4), 1-24.

Oni, P., Jimoh, S., & Adebisi, L. A. (2014). Management of indigenous medicinal plants in Nigeria using phonological information. *Journal of Medicinal Plant Research, 8*, 619-631. doi:10.5897/JMPR2013.5108

Onyekuru, S., Nwankwor, G., & Akaolisa, C. (2010). Chemical characteristics of groundwater systems in the southern Anambra Basin, Nigeria. *Journal of Applied Sciences Research, 6*(12), 2164-2172.

Onyewuchi, R., & Ugwu, S. (2017). Geological interpretation of high resolution aeromagnetic data over Okigwe-Udi area, Anambra Basin, Nigeria, Using 3D Euler Deconvolution and 2D Spectral Inversion Methods. *Journal of Geography, Environment and Earth Science International, 10*(1), 1-22.

Osadebe, C., Abam, T., Obiora, F., & Sani, R. (2014). Evaluating the Stability of Gully Walls in Agulu-Nanka-Oko gully erosion complex area of Anambra State, Nigeria, using empirical approach. *Advancement in scientific and Engineering Research, vol2 (1)*, 35-43.

Razak, K. A., Straatsma, M., Van Westen, C., Malet, J.-P., & De Jong, S. (2011). Airborne laser scanning of forested landslides characterization: Terrain model quality and visualization. *Geomorphology, 126*(1-2), 186-200.

Peltzer, D. A., Wardle, D. A., Allison, V. J., Baisden, W. T., Bardgett, R. D., Chadwick, O. A., . . . Richardson, S. J. (2010). Understanding ecosystem retrogression. *Ecological Monographs, 80*(4), 509-529.

Shahabi, H., & Hashim, M. (2015). Landslide susceptibility mapping using GIS-based statistical models and Remote sensing data in tropical environment. *Scientific reports, 5*(1), 1-15.

Sharma, P. V. (1997). *Environmental and Engineering Geophysics*. Cambridge: Cambridge University Press.

Thomas, M. F. (2001). Landscape sensitivity in time and space—an introduction. *Catena, 42*(2-4), 83-98.

Xu, H., Li, X., & Gong, W. (2017). *Research on Recognition of Landslides with Remote Sensing Images Based on Extreme Learning Machine.* Paper presented at the 2017 IEEE International Conference on Computational Science and Engineering (CSE) and IEEE International Conference on Embedded and Ubiquitous Computing (EUC).

Yalcin, A. (2011). "A geotechnical study on the landslides in the Trabzon Province, NE, Turkey", Applied Clay Science, 52, 11-19, (2011). *Applied Clay Science, 52*, 11-19.

Zainal, M. H., Saad, R., Ahmad, F., Wijeyesekera, D., & Tajul Baharuddin, M. F. (2012). Seismic Refraction Investigation on Near Surface Landslides at the Kundasang Area in Sabah, Malaysia. *Procedia Engineering, 50*, 516 – 531. doi:10.1016/j.proeng.2012.10.057

Zhubayev, A., & Ghose, R. (2011). Physics-based integration of shear wave dispersion properties for soil property estimation. In *SEG Technical Program Expanded Abstracts 2011* (pp. 1343-1347): Society of Exploration Geophysicists.

CHAPTER 2: LITERATURE REVIEW

2.1 Introduction

Landslides are major geohazards, which have been recorded to happen in several places of the world. Their occurrence is not limited to any part of the earth. Hence, no country or region is immune to its devastating impacts (Liao, 2012). Therefore, Igwe (2015) further supports that if left unchecked, they have the capacity to wreak havoc to infrastructure and may lead to huge loss of lives. It is evident that the causes and types of landslides are manifold; one only has to look at the United States Geological Survey's Landslides Hazards Program website to see a regular list of landslide-related fatalities and economic losses.

Landslide is a term that is usually used to describe a set of geological process that involve the downslope flow of debris and ruptured rock under the effect of gravity (Ogunsuyi *et al.,* 2011). In the course of a specific rupture, a landslide could show variable motion type and magnitude of disturbance as shown in Figure 2.1. Furthermore, landslides often occur in areas characterised with high slope gradient such as slopes of mountains, riverbanks, lakes and river valleys (Liao, 2012). Slope stability is influenced by many factors, increasing their potentials for landslides to occur. These factors may be classified into three; geologic, physical and human induced. Examples of geologic factors include strength of rock material, orientation of fractures and structural discontinuities. Volcanic eruptions, earth tremors and high pore pressure resulting from water saturation are examples of the physical class of landslide causative factors. Mining, deforestation, large scale excavations and poor drainage systems are attributed to the human induced factors (Cruden & Varnes, 1996; Hungr *et al.*, 2014a).

Landslides are mainly caused by heavy rainfall especially in West Africa. Characteristic meteorological and geomorphological conditions may cause rainfall to initiate slope failures of varying degrees. The impact of water infiltration on slope stability modelled by Slope Infiltration-Distributed Equilibrium (SLIDE), which is a physical model, used to define correlation between rainfall and factor of safety on an infinite slope (Liao, 2012). Prolonged and high intensity rainfall have been attributed to landslides in Nigeria. This is because, landslides causative factors have been poorly defined in the past (Igwe, 2015).
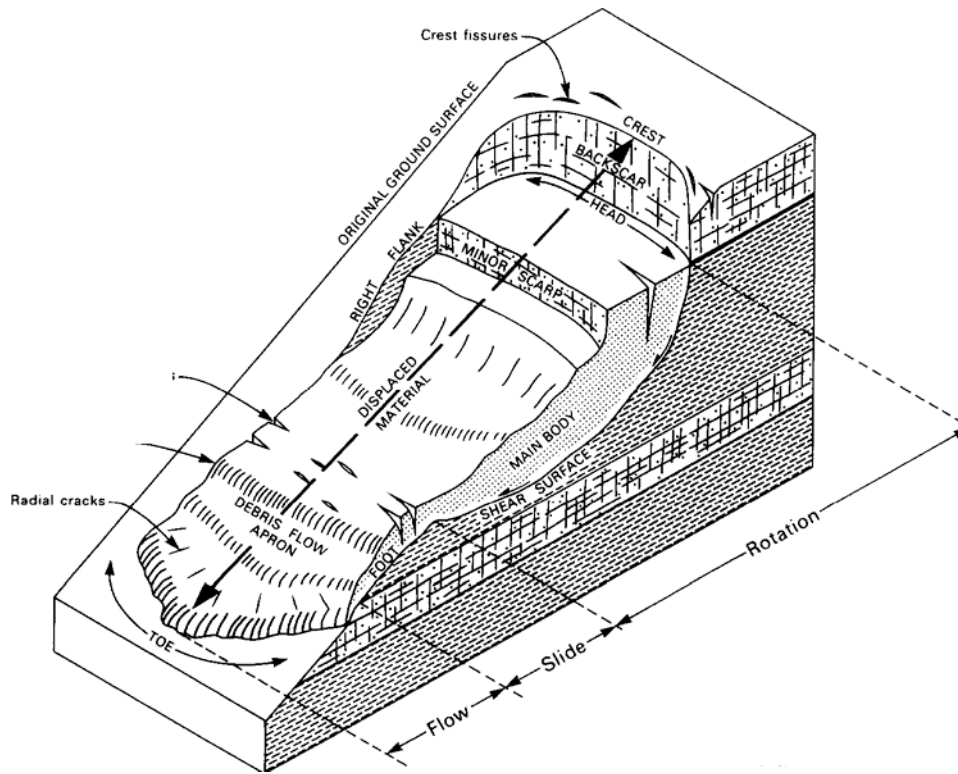
Figure 2.1: Block diagram of a complex landslide with varying movement type downslope (Alexander, 2017).

There have been numerous disastrous landslides that have caused deaths and property damage in the past. Records have revealed that there are usually huge annual financial losses due to landslide (Parise & Iovine, 2009). The number of fatalities and degree of damage depends on the slide size and the proximity to people and facilities. The potential for a rise in future hazards is a result of fast growth in development and urbanisation in areas that are prone to landslides. In order to avoid future occurrences that can result in loss of life and property, features and zones prone to slide must be marked-out, the level of slope instability known, and suitable mitigation measures need to be in place.

While landslides are daily events, as mentioned above, it is still worth listing some notable examples. The mudflow event which happened around 200 km south of Enugu, south-eastern Nigeria, recorded on October 16, 2008, in the early hours of the morning is one of such. Reports indicate that a segment of an unstable hill (< 500 m) collapsed during an intense rainfall session, thereby triggering debris and mudflow in nearby villages, killing a couple of people, and destroying farmlands (Igwe, 2015). Technical description of the landslide event indicate that the landslide was mostly of low volume shallow movements accompanied by material slumps, which were activated on slopes in the direction of the dip of the strata on wavy shear surfaces guided by impermeable bedding planes (Igwe, 2015). According to Wang & Sassa, (2005); Igwe, (2015); Margottini *et al.*, (2013), landslides on a metamorphic terrain are characterised by rotational movements which are complex and translational, while mudslides on steep slopes are sometimes characterised by a slide-flow which is combined with curved head scarps and slicken-sided shear surfaces. However, the dominance of landslides in the sedimentary terrains are chiefly caused by loose slope materials characterised by low resistance parameters.

The report by Glade *et al.*, (2006) describes one of the deadliest landslide events which occurred in Caracas, Venezuela involving a heavy rainfall event between December 14–16, 1999. This storm was responsible for activating several thousands of landslides on steep slopes. The devastation was estimated to be approximately $1.79 billion accompanied by a colossal loss of lives totalling more than 30, 000. Crosta & Frattini (2001) gave credence to past reports which inferred those hydrological incidences were responsible for contributing to repeated floods and landslides in this area. However, those events were not comparable and not as catastrophic as the 1999 event. These previous happenings might be an indication of imminent geohazards. In fact, it is very likely that the devastations caused by these landslides which included damages to lives and properties and social services disruptions, would have been

greatly minimised if these landslides were properly studied and monitored, thereafter, proper hazard mitigation processes were deployed (Crosta & Frattini, 2001).

The research by Cruden (2003) supports that fact that Alberta, Canada is prone to the devasting and destructive effects of landslides. For example, the historic "Frank slide" which occurred in the coal mining town of Frank, southern Alberta on April 29, 1903, at 4:10 am lasted for about 100 seconds. The rockmass was moved from the Turtle Mountain with a great force into the valley beneath, destroying everything in its trajectory. The site of this geohazard zone was characterized by a flat-bottomed river valley at its base and steep slopes of the Turtle Mountain ridges. The account by Lollino *et al.*, 2014, reported that several infrastructure including houses roads and railway tracks coupled with several houses and the landslide destroyd rural homes. This event was not without casualty as more than 70 people were estimated to be killed, while several others were reportedly injured.

The research by Cruden & Martin, (2007); Reid *et al.*, (2008), made inferences alluding those factors, which were responsible for the landslides in Alberta included structure of Turtle Mountain, which has undergone intense tectonic activities as it has been dissected by fractures. This was made worse because of the ongoing coal mining at the foot of the Turtle Mountain. In addition, there were incidences of above-average rainfall in months preceding the slide. Another factor that exacerbated the landslide was the accumulation of ice and water within the fractures at the top of the mountain. Seismic activity before the landslide event and thermal variations with the area were all factors that made the landslide so devastating. It is now very important to note that the risk of more landslides in the future are still certain and hence, selected geophysical landslide monitoring techniques have been deployed and intensive studies of the fracturing mechanisms of the mountain has begun after the occurrence of the landslide (Hungr *et al.*, 2005; Snieder *et al.*, 2007).

As stated earlier, many factors may contribute to making slopes susceptible to failures. However, a landslide is often triggered by external stimuli like an earth tremors, high intensity rainfall and snowmelt, which initiates the actual mass movement by reducing the strength or by increasing the shear stress of the slope materials (Hungr *et al.*, 2014b). Further, landslides can be classified and described by the type of material and the type of movement involved in the slides according to the categorization developed by (Cruden, 1996; Hungr *et al.*, 2014b). The type of material is classified based on the particle size that constitutes the material, for example, rock, debris, or earth materials. On the other hand, the movement is classified based

on the kinematics of the materials such as fall, topple, slide, spread, or flow (Hungr *et al*., 2014b). Using this terminology, the name of any landslide describes the movement system fully. Some historic landslide events, which make good reading, are presented in (Shanmugam & Wang, 2015) and (Evans & DeGraff, 2002). For example, (Hungr *et al*., 2014b) stated that landslides may be described as constituting different types ranging from surficial debris flow to rockfall, and may be triggered by different factors, ranging from earthquakes to human induced activities.

2.2 Review of Related literature

Landslide prone areas have been found to occupy;

 i.   Important transport passage routes such as highways and railways,

 ii. Routes of critical service facilities such as communication cables, power transmission lines and petroleum pipelines,

 iii. Farmlands and residential quarters.

Therefore, efforts to apply methods that may potentially mitigate landslide processes must not be disregarded (Chambers *et al.,* 2011). Consequently, the utilization of geophysical techniques to monitor and study landslides have been deployed in various parts of the world so as to ensure public safety and to safeguard various critical infrastructure (Chambers *et al.,* 2011).

According to Atanackov & Gosar, (2013); Juhlin *et al.,* (2002) suggested the use of reflection seismic profiling as a geophysical tool to be utilized in a wide range of scenarios in order to image the subsurface in areas prone to landslides. They mentioned that it was shocking that the seismic reflection method has not been massively implemented to study landslides. This was a result of the apparent relative-paucity of scientific papers on the subject matter.

However, Chambers *et al.,* (2011), suggest that why the seismic reflection has not gained full adoption was because landslides exhibit structural complexity and the physical property of landslide materials are not a good media for the propagation of seismic waves. This is attributable to dispersion and noise inherent in the recording of the waveforms. Another explanation as given by Bruno & Martillier (2000) may be that the irregular surface topography, which characterises landslides, distinguishable by steep slopes and hummocky features, makes the collection of seismic reflection field data immensely difficult.

However, Bruno & Martillier (2000), suggested that it is possible to employ a high-resolution seismic reflection method to accurately detect the depth of a landslide in the western half of the Swiss Alps. This geophysical technique has also been applied to study a prehistoric slide site in Utah, USA according to (Tingey *et al.,* 2007). (Alves & Cartwright, 2009) equally came up with examples on the utilization of the seismic reflection survey method to the study of submarine landslides. If there is a variation at the underlying stable solid bedrock and the acoustic impedances of the landslide body, strong reflectors are likely to be detected on the surface of the rupture. Pugin *et al* (2009), stress that shallow landslides may just be difficult to image using seismic reflection profiling geophysical technique because the wave signal generated is usually affected by source-generated noise. However, with recent developments in the shallow seismic reflection methods, the use of seismic reflection imaging as applied to shallow landslides could become increasingly successful.

In a research conducted by Stucchi & Mazzotti (2009), they employed onshore and offshore seismic reflection profile survey with the aim of delineating the deepest rupture of a devastating landslide in Italy. The results of the survey revealed a detachment surface, which was based on the boundary demarcated by differences in the seismic velocities of the different profiles. This inferred that there existed chaotic reflection the subsurface area within the landslide and continuous reflections in the subsurface rocks where there was no record of a landslide event. However, the work of Bichler *et al.,* (2004) who used the P- and S-wave seismic reflection geophysical method to investigate the unit boundaries of the Quesnel Forks landslide, Canada was unable to resolve the rupture surface of the landslide.

Seismic refraction survey method is one of the common methods employed in describing landslides. Seismic refraction method uses first arrival time picks to generate compressional or shear wave velocities of the subsurface. According to Palmer, (1981), relatively low compressional and shear wave velocities within landslide bodies are observed when compared to the wave velocities undisturbed rocks. The reason for this is attributable to the fact that landslide masses are often weathered and fractured.

The General Reciprocal Method (GRM) which was proposed by Jongmans *et al.,* (2007) assumes a layered model in order to interpret seismic refraction datasets. This is done by calculating refractor velocities and depths by interpreting overlapping forward and reverse shots' travel times (Grit & Kanli, 2016). Several other authors have reported varying degree of

successes in employing seismic refraction geophysical method in the delineation of landslide depths. (Bekler, *et al.,* 2011; Narwold & Owen, 2002; Sompotan, *et al.,* 2011).

Narwold & Owen, (2002) has described the seismic tomography technique as one, which involves the inversion of first-arrival travel times from many sources and geophones in order to generate a seismic wave velocity circulation of the subsurface. Hence, landslides with complex velocity character can be reliably delineated using seismic refraction imaging. This technique has been used widely to model landslides, (Jongmans *et al.,* 2009; O. Meric *et al.,* 2005; Thiebes, 2011). Seismic tomography has the ability to image lateral velocity change and when integrated with the Surface Wave Method (SWM), it can effectively characterize landslide prone areas (Israil & Pachauri, 2003; Jongmans et al, 2000). SWM utilises Rayleigh-wave data recorded on geophones in order to establish phase-velocity dispersion curve. The dispersion curve and the shear wave velocity ae then subjected to a geophysical inversion process so as to determine the depth of the landslide (Pancha *et al.,* 2008; Xia *et al.,* 2001).

Another geophysical method employed for landslide studies is electrical resistivity method. (Lapenna *et al.,* 2005). This method is based on the response of the subsurface rock materials to current injected into the ground while measuring the potential difference across the electrodes used in delivering the current. The work of Perrone *et al.,* (2014) has successfully outlined the effects of several physical properties in relation to true resistivity of a rock as it concerns landslide investigations. These physical properties include porosity, pore fluid resistivity and water saturation to mention but a few.

Jongmans *et al.,* (2009), reported that there is a variation in the resistivity values of the landslide mass as compared to those from undisturbed body due to the displacement of materials and landslide deformations. The results of Lapenna *et al.,* (2005) showed that lower resistivity values defined within the body of a landslide is characterized by high clay content and increased water saturation when compared with the values of resistivity of the unaffected rock mass. However, the work of Meric *et al.,* (2005) reported higher resistivity values in a landslide body, as compared with the unaffected rock mass. This is due to the degree of fracturing related to air-filled spaces in the deformed rock mass. Therefore, if there is notable resistivity variation between the different rock masses, the slip surface should be readily distinguishable. Electrical resistivity tomography (ERT) shows the electrical resistivity distribution (2D or 3D) of the subsurface.

When combined with seismic refraction data (Moorkamp *et al.,* (2010); Wisén & Christiansen, 2005), the resistivity method can successfully be used to delineate landslides (Drahor, Göktürkler, Berge, & Kurtulmuş, 2006; Gelisli, 2017; Naudet *et al.,* 2008; Yılmaz, 2011). More so, self-potential (SP) measurements may be integrated with resistivity surveys because of the friendly financial budgets of both methods (Hack, 2000). SP geophysical exploration method is based on measurements of natural electrical potentials induced when water flows through a rock (Bogoslovsky & Ogilvy, 2006). Integration of electrical resistivity methods and SP measurements have also been variously employed to study landslides (Lapenna *et al.,* 2003; Naudet *et al.,* 2008).

Ground-penetrating radar (GPR) technique has also been employed in slope stability studies to delineate fractures in rocks (Sajinkumar *et al.,* 2011; Theune *et al.,* 2006). It has also been employed to monitor rockfalls (Talebi *et al.,* 2008) and to calculate the depth of a rupture surface (Surovell *et al.*, 2017). The ground-penetrating radar (GPR) technique utilizes reflected high-frequency electromagnetic (EM) waves to gather information about the subsurface based on contrasts in the dielectric permittivity properties of rock materials. However, there are some disadvantages in using GPR technique to investigate landslides. These disadvantages take the form of signals being heavily attenuated in very conductive formations. In addition, fractures create diffractions thereby reducing signal penetration depths (Jongmans & Garambois, 2007). Finally, in order to properly delineate a target, GPR techniques are often used in conjunction with other geophysical survey methods (Sass *et al.,* 2008).

Another geophysical method employed to study and characterise landslides is the Electromagnetic (EM) (Al-Amoush, 2016). This method uses low-frequency EM waves to determine the conductivity of the subsurface by comparing a transmitted (or primary) field to a secondary field induced in the subsurface materials (Osinowo & Falufosi, 2018). Furthermore, this method yields great results when combined with geophysical methods (Caris & Van Asch, 1991; Giraud *et al.,* 1991; Godio & Bottino, 2001; Jongmans *et al.,* 2009).

Vertical Seismic Profiling (VSP) geophysical technique is another but rarely used method in mapping landslides (Godio *et al.,* 2003). Liu *et al.,* (2003) used VSP to delineate the distribution of sliding surfaces in boreholes of some locality. Godio *et al.,* (2003) adopted horizontal seismic profiling (HSP) in order to conduct a seismic profile geophysical investigation in a horizontal wellbore. HSP technique was effectively utilised in combination with sonic logs to characterize the rock mass based on its presence and characters of fractures

within the rock mass. Other notable geophysical techniques that have been adopted for use in the studies landslides. These include micro seismic monitoring (Tonnellier *et al.,* 2013), seismic noise measurements (Méric *et al.,* 2007), magnetic field observations (Sugmoto, Kawasaki, & Sakai, 2014) and gravimetric measurements (Del Gaudio *et al.,* 2000).

The works of Bichler *et al.,* (2004); Pazzi *et al.,* (2019) and Meric *et al.,* (2005) propose that a better knowledge and understanding could be made of physical properties landslide's materials and its geometry when some of these geophysical techniques are integrated with other methods. This is because different geophysical techniques are sensitive to different physical properties. Hence, it becomes essential to combine a variety of techniques in geohazard investigations to obtain better insights into landslides and their processes (Godio *et al.,* 2003). More in-depth information on the various geophysical methods and their relative suitability for slope stability investigations are discussed in the work of Hack, (2000).

2.3 General geology of Nigeria

The Basement Complex, Young Granites, and Sedimentary Basins are the three primary litho-petrological components of Nigerian geology, as shown in Figure 2.2. The Basement Complex, which is Precambrian in age, consists of the Migmatite - Gneiss Complex, the Schist Belts, and the Older Granites. Younger Granites – the name which is coined to differentiate it from the Older Granites are made up of several Jurassic age magmatic ring complexes within the Jos Plateau and other north-central parts of Nigeria (Mücke, 2003; Obaje, 2009). They are distinct from the Older Granites in structure and petrology. According to Fatoye & Gideon, (2013), the Sedimentary Basins is made up six distinct basins namely: Niger Delta, Benue Trough, Chad Basin and Sokoto Basin. Others include the Mid - Niger Basin (Bida/Nupe) Basin and the Dahomey Basin which contains sediment-fill within the age range of Cretaceous to Tertiary. The Benue Trough is subdivided arbitrarily into three parts: the lower, middle, and upper portions. It is important to note that no exact subdivision can be drawn to demarcate the individual portions. Rather, major localities using topomymns make up the depocenters of the various portions and these have been extensively documented and detailed (Ogungbesan & Akaegbobi, 2011).

Nigeria is endowed with an abundance of solid mineral wealth that are dispersed across all federal states. It is a fact that Nigeria has more than forty-four known major mineral deposits, which are distributed in different locations across the country. This has drawn immense

attractions and offers to both local and foreign investors as reported by the Nigerian Geological Survey Agency (NGSA) (Fatoye & Gideon, 2013).

The Lower Benue Trough (LBT) is documented to contain almost half of the number of reported mineral deposits in the country. These include coal, lead, zinc, barite, calcareous, gypsum, clay, phosphate, glass sand. Others include fluorspar, salt, ironstone, uranium, sulphur, graphite, cassiterite, manganese, mica, and silver (Adekoya *et al.,* 2003; Ananaba & Ajakaiye, 1987; Fatoye *et al.,* 2013). On the other hand, oil and gas are far more abundant in the Niger Delta Basin than in other basin in the country with its attendant huge economic contributions to the assets of the nation (Evamy *et al.,* 1978; Kadafa, 2012).
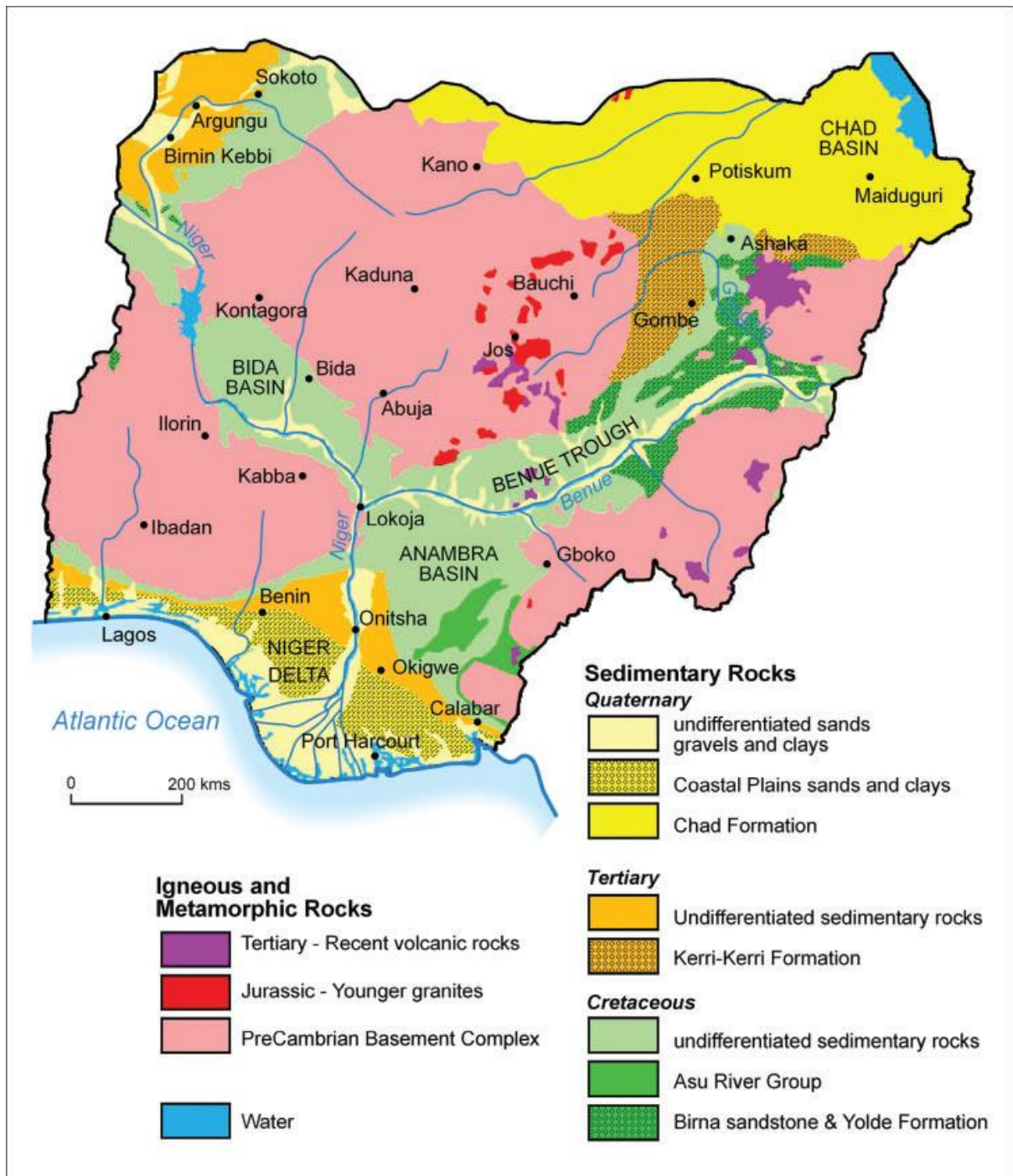
Figure 2.2: Geology Map of Nigeria showing major lithologic components (Adelana *et al.*, 2008).

The research carried out by Ola-Buraimo & Akaegbobi (2013), reported that sedimentation in the Lower Benue Trough began with the marine Neocomian to Albian Asu River Group. Some Groups such as Aptian to Early Albian pyroclastics were scarcely reported. The sediments of the Asu River Group in the Lower Benue Trough consist mainly of shales with localized sandstones, siltstones, and calcareous Limestones. These limestones are characterised as extrusive and intrusive material of the Abakaliki Formation and the Calabar Flank (Nweke, Igwe, & Nnabo, 2015).

The Anambra Basin was formed as a result of intense Middle-Santonian deformation and magmatism in the Benue Trough. This was accompanied by a westward shift of its main depositional axis (Haruna *et al.,* 2012; Obi *et al.,* 2014). Hence, it could be asserted that the post - deformational sedimentation in the Lower Benue Trough makes up the Anambra Basin.

Benkhelil, (1982) & Obaje, (2009) opine that the sedimentation in the Anambra basin is believed to have been initiated after the separation of South American and the African plates in the Aptian/Albian times. This process was documented to have been controlled by three main tectonic events and epeirogenic movements, which resulted in a series of marine transgressions and regressions. During these tectonic processes, the axes of the main basins were shifted giving rise to the formation of three inland basins, which include Abakaliki-Benue Trough, the Anambra Basin, and the Afikpo Sub-Basin (Onu, 2017). Murat (1972) also felt that the changes in the thickness and facies of the sediments throughout these basins would give rise to diverse Member and Formation names (Kelechi, 2017).

The first of the depositional cycles, which was mainly confined to the Benue-Abakaliki Trough occurred in the pre-Albian times and was confined (Hoque, 1977; Odunzeakasiugwu, 2018). This process ended in the Santonian time. The second depositional phase which was initiated in the Campanian marine transgression and terminated in the Palaeocene (Zaborski, 2000), was dominated by the formation of the Anambra basin, as well as the Afikpo Synclinorium (Ao, 2013; Onu, 2017). Furthermore, the third and final depositional phase which produced the Niger Delta basin started in the Eocene time, coinciding with the development of the Niger Delta basin (Bonne, 2014; Reijers, 2011) and it is on account that the deposition is still ongoing. The Southern Benue Trough, Anambra Basin, Afikpo Syncline, Calabar Flank, and Mamfe Embayment are Cretaceous sedimentary basins and sub-basins in south-eastern part Nigeria.

The form in which the sedimentary basins developed on the Basement Complex of Nigeria has been described as an 'X' shaped depression having a NE – SW orientation (Oboh-Ikuenobe *et al.*, 2005; Odigi & Amajor, 2009). The major controls on sedimentation in these basins resulted from eustatic sea-level changes (Ao, 2013), basin tectonics, and local diastrophism. The stratigraphy and paleogeography of the basin have been studied and described by various workers, such as (Murat, 1972; Okeke *et al.*, 2014; Ola-Buraimo & Akaegbobi, 2012) amongst others.

Onu, (2017) further clarified that the Anambra Basin became a significant deposition zone following the Santonian folding in south-eastern Nigeria. The ensuing tectonic inversion and down-warping of the Anambra basin were accompanied by compressional uplift of the Lower Benue Trough sequence (Albian to Coniacian) along the NE-SW axis. The sediment thickness of the Anambra basin has been estimated to range from 1000 m – 4500 m using gravity measurements (Uzoegbu, & Okon, 2017). More than 3000 m of these were deposited in the Late Cretaceous (Upper Campanian - Maastrichtian).

Nwajide, (2013) stated that the sedimentation in the Anambra basin was mainly terrigenous giving rise to up to 3000 m thick shales, sands, and limestones which represents 60%, 39% add about 1% of the various thicknesses respectively. (Uma & Onuoha, 1997) identified three hydrostratigraphic units in the Anambra Basin, which comprise of; the Ameki Formation (sandy horizons and quaternary deposits), Nsukka Formation underlying Ajali Sandstone and sandy horizon, and the Awgu-Nkporo-lower Mamu Formations comprising of sandy beds.

The initial hydro-stratigraphic unit to form a viable reservoir is relatively too shallow having a sediment pile of about 500 m. Onuigbo *et al.,* (2016) confirmed that the Mamu Formation and the Nsukka Formation are likely delta front sand bars. Ajali Sandstone, on the other hand, was linked to fluvial deposition with extensive channels having a lithic fill with a characteristic fining-upward sequence composed of pebbly sandstones. This is also associated with the formation of shallow depth marine subtidal sand bars (Akande & Mücke, 1993; Olabode, 2014). When these are stacked, the potential reservoir sands appear to be generally laterally extensive and can reach local thicknesses of more than 1000 m.

According to Onyeogu *et al.,* (2016) the closing of the Afikpo and Anambra sedimentary basins was initiated during the early Campanian to the early Palaeocene (Danian) under two main eustatic cycles. The area the known Nkporo shale transgression and the less active Nsukka

transgression occupying the most voluminous stratigraphic parts of the Anambra basin (Figure 2.3). Similar cycles are also observed in the Afikpo syncline located South-East of the Abakaliki anticlinorium and the Dahomey embayment west of the Ilesha basement spur, (Obaje, 2009), albeit both are incomplete (Olatunji, 2013). The first cycle, began with the deposition of the Nkporo shale which began in the Maastrichtian and ended in the Lower Campanian, (Ukaonu *et al.,* 2017). It is having same lateral age equivalents with the Enugu shale and Owelli sandstone (Figure 2.3). This represents the Campano-Maastrichtian transgression's base unit, consisting of dark coloured mudstone, grey fissile friable shales with thin layers of marl, sandy shale, and limestone above an angular unconformity (Uzoegbu & Okon, 2017). The regressive phase of this process was effectively discriminated by the formation of a massive off-lap complex, which began with the paralic sequence of the Mamu formation overlying the Nkporo shale (Onyekuru & Iwuagwu, 2010). This has been inferred to be lower Maastrichtian age which is composed of two parts: the basal part which contains thin marine intercalation, and the mineral-bearing part which consists of fresh water and low salinity sandstones, shales, mudstones, and sandy shales with coal seams occurring at several levels (Obaje, 2009).
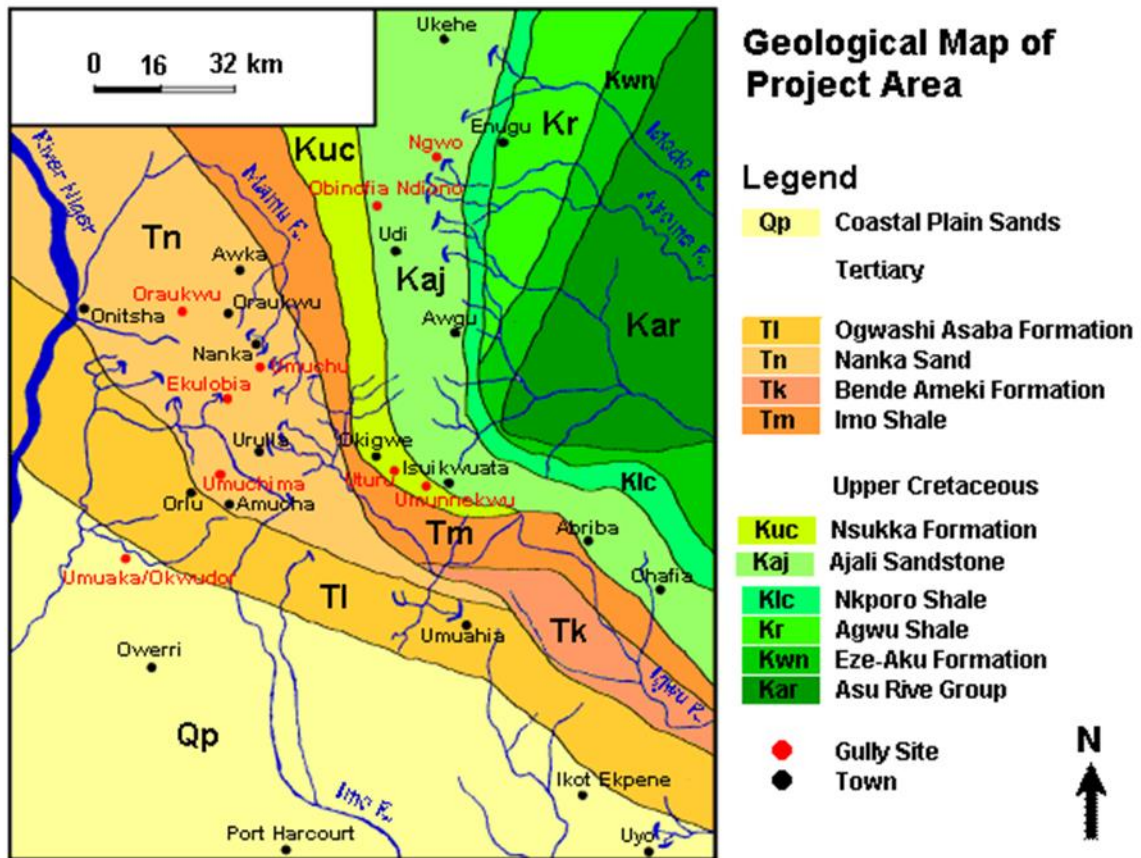
Figure 2.3: Geology Map of the Anambra Basin (Akande *et al*., 2005).

The Ajali sandstone is made up of a continental sequence and is underlain by the Mamu formation. This sandstone unit has been given several names at different times. These include 'false bedded sandstone' (Onyekuru & Iwuagwu, 2010), 'basal sandstone' (Chiaghanam *et al.*, 2012), etc. Its current name was given by (Reyment, 1965), after the establishment of its type locality on the Ajali River. Almost all the exposures of the Ajali sandstone formation are characterized by a lateral profile at the top and this was formed during the regressive phase of the Campano-Maastrichtian transgression dating back to the Maastrichtian age (Uzoegbu & Okon, 2017).

The Nsukka Formation, which overlies the Ajali sandstone, has been described as "an alternating succession of grey sandy shales, sandstones, plant-bearing layers, and thin mineral beds Onyeogu *et al.,* (2016). At the top of the formation, thin marine limestone bands marked the re-initiation of marine sedimentation. Dark coloured shales having highly bioturbated sandstones are well exposed at the Ihube area, along the Enugu-Port Harcourt highway. According to the fossil record, the Nsukka formation age range is of late Maastrichtian to Danian. This formation bears the T-K boundary, which is described by Onyeogu *et al.,* (2016).

Bibliography

Adekoya, J., Kehinde-Philips, O., & Odukoya, A. M. (2003). Geological distribution of mineral resources in southwestern Nigeria. *Journal of Mining and Geology, 47*(1).

Adelana, S. M. A., Olasehinde, P. I., Bale, R. B., Vrbka, P., Edet, A. E., & Goni, I. B. (2008). An overview of the geology and hydrogeology of Nigeria. Applied groundwater studies in Africa, 181-208.

Akande, S., & Mücke, A. (1993). Depositional environment and diagenesis of carbonates at the Mamu/Nkporo formation, anambra basin, Southern Nigeria. *Journal of African Earth Sciences (and the Middle East), 17*(4), 445-456.

Akande, S. O., Ojo, O., Erdtmann, B., & Hetenyi, M. (2005). Paleoenvironments, organic petrology and Rock-Eval studies on source rock facies of the Lower Maastrichtian Patti Formation, southern Bida Basin, Nigeria. *Journal of African Earth Sciences, 41*(5), 394-406.

Al-Amoush, H. (2016). Landslide Investigation Using Transient Electromagnetic Method (TEM): A Case Study on Al-Ja'ydyya-Salhuob Landslide/ Jordan. *Civil and Environmental Research, 8*(12), 1-12. Retrieved from www.iiste.org.

Alexander, D. C. (2017). *Natural disasters*: Routledge.

Alves, T. M., & Cartwright, J. A. (2009). Volume balance of a submarine landslide in the Espírito Santo Basin, offshore Brazil: quantifying seafloor erosion, sediment accumulation and depletion. *Earth and Planetary Science Letters, 288*(3-4), 572-580.

Ananaba, S., & Ajakaiye, D. (1987). Evidence of tectonic control of mineralization in Nigeria from lineament density analysis A Landsat-study. *International Journal of Remote Sensing, 8*(10), 1445-1453.

Ao, O.-B. (2013). Biostratigraphy and paleoenvironment of the Coniacian Awgu Formation in Nzam-1 well, Bornu Basin, Northeastern Nigeria. *International Journal of Scientific & Technology Research, Vol. 2*, 112-122.

Atanackov, J., & Gosar, A. (2013). Field comparison of seismic sources for high resolution shallow seismic reflection profiling on the Ljubljana moor (central Slovenia). *Acta Geodyn et Geomater, 10*(1), 19-40.

Bekler, T., Ekinci, Y. L., Demirci, A., Erginal, A. E., & Ertekin, C. (2011). Characterization of a landslide using seismic refraction, electrical resistivity and hydrometer methods, Adatepe–Çanakkale, NW Turkey. *Journal of Environmental and Engineering Geophysics, 16*(3), 115-126.

Benkhelil, J. (1982). Benue trough and Benue chain. *Geological Magazine, 119*(2), 155-168.

Bichler, A., Bobrowsky, P., Best, M. E., Douma, M., Hunter, J., Calvert, T., & Burns, R. (2004). Three-dimensional mapping of a landslide using a multi-geophysical approach: The Quesnel Forks Landslide. *Landslides, 1*, 29-40. doi:10.1007/s10346-003-0008-7

Bogoslovsky, A. V., & Ogilvy, A. A. (2006). The study of streaming potentials on fissured models. Geophysical Prospecting, 20, 109-117. doi:10.1111/j.1365-2478.1972.tb00624.x

Bonne, K. (2014). Reconstruction of the evolution of the Niger River and implications for sediment supply to the Equatorial Atlantic margin of Africa during the Cretaceous and the Cenozoic. *Geological Society, London, Special Publications, 386*, 327-349. doi:10.1144/SP386.20

Bruno, F., & Martillier, F. (2000). Test of High-Resolution Seismic Reflection and Other Geophysical Techniques on the Boup Landslide in the Swiss Alps. *Surveys in Geophysics, 21*, 335-350. doi:10.1023/A:1006736824075

Caris, J. P. T., & Van Asch, T. W. J. (1991). Geophysical, geotechnical and hydrological investigations of a small landslide in the French Alps. *Engineering Geology, 31*(3), 249-276. Retrieved from http://www.sciencedirect.com/science/article/pii/0013795291900119. doi:https://doi.org/10.1016/0013-7952(1)90011-9

Chambers, J., Wilkinson, P., Kuras, O., Ford, J., Gunn, D., Meldrum, P., & Ogilvy, R. (2011). Three-dimensional geophysical anatomy of an active landslide in Lias Group mud rocks, Cleveland Basin, UK. *Geomorphology, 125*(4), 472-484.

Chiaghanam, O., Ikegwuonu, O., Chiadikobi, K., Nwozor, K., Ofoma, A., & Omoboriowo, A. (2012). Sequence Stratigraphy and Palynological Analysis of late Campanian to Maastrichtian Sediments in the Upper-Cretaceous, Anambra Basin. A Case Study of Okigwe and its Environs, South-Eastern, Nigeria. *A Case Study of Okigwe and its Environs, South-Eastern, Nigeria. Advances in Applied Science Research, 3*(2), 964.

Crosta, G., & Frattini, P. (2001). Rainfall thresholds for triggering soil slips and debris flow. *Proceedings of the 2nd EGS Plinius Conference on Mediterranean Storms*, 463-487.

Cruden, D. M., & Varnes, D. J. (1996). Landslide Types and Processes, Transportation Research Board, U.S. National Academy of Sciences, Special Report, 247: 36-75. *Special Report - National Research Council, Transportation Research Board, 247*, 36-57.

Cruden, D. (2003). *McConnell And Brock's Report on the Great Landslide at Frank, District of Alberta, Northwest Territories*.

Cruden, D., & Martin, D. (2007). Before the Frank Slide. *Canadian geotechnical journal, 44*, 765-780. doi:10.1139/T07-030

Del Gaudio, V., Wasowski, J., Pierri, P., Mascia, U., & Calcagnile, G. (2000). Gravimetric Study of a Retrogressive Landslide in Southern Italy. *Surveys in Geophysics, 21*, 391-406. doi:10.1023/A:1006793009054

Drahor, M., Göktürkler, G., Berge, M., & Kurtulmuş, T. (2006). Application of electrical resistivity tomography technique for investigation of landslides: A case from Turkey. *Environmental Geology, 50*, 147-155. doi:10.1007/s00254-006-0194-4

Evamy, B., Haremboure, J., Kamerling, P., Knaap, W., Molloy, F., & Rowlands, P. (1978). Hydrocarbon habitat of Tertiary Niger delta. *AAPG bulletin, 62*(1), 1-39.

Evans, S. G., & DeGraff, J. V. (2002). *Catastrophic Landslides: Effects, Occurrence, and Mechanisms*: Geological Society of America.

Fatoye, F. B., & Gideon, Y. B. (2013). Geology and mineral resources of the Lower Benue Trough, Nigeria *Pelagia Research Library 4*(6), 21-28. Retrieved from www.pelagiaresearchlibrary.com.

Gelisli, K. (2017). Landslide investigation with the use of geophysical methods: a case study in Eastern Turkey. *Advances in Biology & Earth Sciences, 2*, 52-64.

Giraud, A., Antoine, P., Van Asch, T. W., & Nieuwenhuis, J. (1991). Geotechnical problems caused by glaciolacustrine clays in the French Alps. *Engineering Geology, 31*(2), 185-195.

Glade, T., Anderson, M. G., & Crozier, M. J. (2006). *Landslide Hazard and Risk*: Wiley.

Godio, A., & Bottino, G. (2001). Electrical and electromagnetic investigation for landslide characterization. *Physics and Chemistry of the Earth, Part C: Solar, Terrestrial & Planetary Science, 26*(9), 705-710. Retrieved from http://www.sciencedirect.com/science/article/pii/S1464191701000708. doi:https://doi.org/10.1016/S1464-1917(01)00070-8

Godio, A., de Bacco, G., & Strobbia, C. (2003). Geophysical characterization of a rockslide in an Alpine region. *-1*, 12480.

Grit, M., & Kanli Ali, I. (2016). Integrated Seismic Survey for Detecting Landslide Effects on High Speed Rail Line at Istanbul–Turkey. In *Open Geosciences* (Vol. 8, pp. 161).

Hack, R. (2000). Geophysics for slope stability. *Surveys in Geophysics, 21*(4), 423-448.

Haruna, I., Ahmed, H., & Ahmed, A. (2012). Geology and tectono-sedimentary disposition of the Bima sandstone of the Upper Benue Trough (Nigeria): Implications for sandstone-hosted Uranium deposits. *Journal of geology and mining research, 4*(7), 168-173.

Hoque, M. (1977). Petrographic differentiation of tectonically controlled cretaceous sedimentary cycles, southeastern Nigeria. *Sedimentary Geology, 17*, 235-245. doi:10.1016/0037-0738(77)90047-1

Hungr, O., Fell, R., Couture, R., & Eberhardt, E. (2005). *Landslide Risk Management*: CRC Press.

Hungr, O., Leroueil, S., & Picarelli, L. (2014a). The Varnes classification of landslide types, an update. *Landslides, 11*. doi:10.1007/s10346-013-0436-y

Hungr, O., Leroueil, S., & Picarelli, L. (2014b). The Varnes classification of landslide types, an update. *Landslides, 11*(2), 167-194. Retrieved from https://doi.org/10.1007/s10346-013-0436-y. doi:10.1007/s10346-013-0436-y

Igwe, O. (2015). The geotechnical characteristics of landslides on the sedimentary and metamorphic terrains of South-East Nigeria, West Africa. *Geo-environmental Disasters, 2*. doi:10.1186/s40677-014-0008-z

Israil, M., & Pachauri, A. K. (2003). Geophysical characterization of a landslide site in the Himalayan foothill region. *Journal of Asian Earth Sciences, 22*, 253-263. doi:10.1016/S1367-9120(03)00063-4

Jongmans, D., Bièvre, G., Renalier, F., Schwartz, S., Beaurez, N., & Orengo, Y. (2009). Geophysical investigation of the large Avignonet landslide in glaciolacustrine clays in the Trièves area (French Alps). *Engineering Geology, 109*, 45-56. doi:10.1016/j.enggeo.2008.10.005

Jongmans, D., & Garambois, S. (2007). Geophysical investigation of landslides: A review. *Bulletin de la Societe Geologique de France, 178*. doi:10.2113/gssgfbull.178.2.101

Jongmans, D., Hemroulle, P., Demanet, D., Renardy, F., & Vanbrabant, Y. (2000). Application of 2D electrical and seismic tomography techniques for investigating landslides. *European Journal of Environmental and Engineering Geophysics, 5*, 75-89. doi:10.3997/2214-4609.201406464

Juhlin, C., H. Palm, C. Müllern, & B. Wållberg. (2002). Imaging of groundwater resources in glacial deposits using high-resolution reflection seismic, Sweden. *Journal of Applied Geophysics, 51*, 107-120.

Kadafa, A. A. (2012). Oil exploration and spillage in the Niger Delta of Nigeria. *Civil and Environmental Research, 2*(3), 38-51.

Kelechi, O. F. (2017). The Southern Benue trough and Anambra Basin, Southeastern Nigeria: a stratigraphic review. *Journal of Geography Environment and Earth Science International, 12*, 1-16.

Lapenna, V., Lorenzo, P., Perrone, A., Piscitelli, S., Rizzo, E., & Sdao, F. (2005). 2D electrical resistivity imaging of some complex landslides in the Lucanian Apennine chain, Southern Italy. *Geophysics, 70*, 11-18. doi:10.1190/1.1926571

Lapenna, V., Lorenzo, P., Perrone, A., Piscitelli, S., Sdao, F., & Rizzo, E. (2003). High resolution geoelectrical tomographies in the study of Giarrossa Landslide (Southern Italy). *Bulletin of Engineering Geology and the Environment, 62*, 259-268. doi:10.1007/s10064-002-0184-z

Liao, K. H. (2012). A Theory on Urban Resilience to Floods—A Basis for Alternative Planning Practices. *Ecology and Society, 17*(4). Retrieved from https://www.ecologyandsociety.org/vol17/iss4/art48/. doi:10.5751/ES-05231-170448

Liu, E., h. Queensupbsu, J., Y. Li, X., Chapman, M., Maultzsch, S., B. Lynn, H., & Chesnokov, E. (2003). Observation and analysis of frequency-dependent anisotropy from a multicomponent VSP at Bluebell-Altamont Field, Utah. *Journal of Applied Geophysics - J APPL GEOPHYS, 54*, 319-333. doi:10.1016/j.jappgeo.2003.01.004

Lollino, G., Giordan, D., Crosta, G. B., Corominas, J., Azzam, R., Wasowski, J., & Sciarra, N. (2014). *Engineering Geology for Society and Territory - Volume 2: Landslide Processes*: Springer International Publishing.

Margottini, C., Canuti, P., & Sassa, K. (2013). *Landslide Science and Practice: Volume 6: Risk Assessment, Management and Mitigation*: Springer Berlin Heidelberg.

Meric, O., Garambois, S., Jongmans, D., Wathelet, M., Chatelain, J.-L., & Vengeon, J. M. (2005). Application of geophysical methods for the investigation of the large gravitational mass movement of Schilienne, France. *Canadian Geotechnical Journal, 42*, 1105-1115. doi:10.1139/T05-034

Méric, O., Garambois, S., Malet, J.-P., Cadet, H., Gueguen, P., & Jongmans, D. (2007). Seismic noise-based methods for soft-rock landslide characterization. *Bulletin de la Societe Geologique de France, 178*(2), 137-148.

Moorkamp, M., Jegen, M., Heincke, B., Roberts, A., & W. Hobbs, R. (2010). A framework for 3D joint inversion of MT, gravity and seismic refraction data (Invited). *AGU Fall Meeting Abstracts*.

Mücke, A. (2003). Fayalite, pyroxene, amphibole, annite and their decay products in mafic clots within Younger Granites of Nigeria: Petrography, mineral chemistry and genetic implications. *Journal of African Earth Sciences, 36*(1-2), 55-71.

Murat, R. (1972). Stratigraphy and paleogeography of the Cretaceous and Lower Tertiary in Southern Nigeria. *African Geology*, 251-266.

Narwold, C., & Owen, W. (2002). *Seismic Refraction Analysis of Landslides*.

Naudet, V., Lazzari, M., Perrone, A., Loperte, A., Piscitelli, S., & Lapenna, V. (2008). Integrated geophysical and geomorphological approach to investigate the snowmelt-triggered landslide of Bosco Piccolo village (Basilicata, southern Italy). *Engineering Geology, 98*, 156-167. doi: 10.1016/j.enggeo.2008.02.008

Nwajide, C. (2013). Geology of Nigeria's sedimentary basins. *CSS Bookshops Limited, Lagos, 565*.

Nweke, O., Igwe, E., & Nnabo, P. (2015). Comparative evaluation of clays from Abakaliki Formation with commercial bentonite clays for use as drilling mud. *African Journal of Environmental Science and Technology, 9*(6), 508-518.

Obaje, N. G. (2009). *Geology and mineral resources of Nigeria* (Vol. 120): Springer.

Obi, D., Ekwueme, B. N., & Akpeke, G. B. (2014). Reserve estimation of barite deposits using geological and geophysical investigations in Cross River State, South Eastern Nigerian. *Journal of Environment and Earth Science, 4*(8), 18-38.

Oboh-Ikuenobe, F. E., Obi, C. G., & Jaramillo, C. A. (2005). Lithofacies, palynofacies, and sequence stratigraphy of Palaeogene strata in Southeastern Nigeria. *Journal of African Earth Sciences, 41*(1-2), 79-101.

Odigi, M., & Amajor, L. (2009). Geochemical characterization of cretaceous sandstones from the Southern Benue Trough, Nigeria. *Chinese Journal of Geochemistry, 28*(1), 44-54.

Odunzeakasiugwu, S. (2018). Provenance of the Campanian-Maastrichtian Shales, Anambra Basin: Evidence from Clay Mineralogy.

Ogungbesan, G. O., & Akaegbobi, I. M. (2011). Petrography and Geochemistry of Turonian Eze-Aku Sandstone Ridges, Lower Benue Trough, Nigeria Implication for Provenance and Tectonic Settings. *Ife Journal of Science 13*(2), 263-277.

Ogunsuyi, O. O., Schmitt, D. R., Martin, D., Morgan, J., & Froese, C. (2011). Geophysical Study of the Peace River Landslide. *AAPG Search and Discovery Article, 90173*, 9-11.

Okeke, H., Orajaka, I., Okoro, A., & Onuigbo, E. (2014). Biomarker evaluation of the oil generative potential of organic matter, in the Upper Maastrichtian strata, Anambra Basin, Southeastern Nigeria. *J Sci Red, 2*(1), 016-025.

Ola-Buraimo, A., & Akaegbobi, I. (2012). Neogene dinoflagellate cyst assemblages of the late Miocene-Pliocene Ogwashi-Asaba sediment in umuna-1 well, Anambra basin, Southeastern Nigeria. *Journal of Petroleum and Gas Exploration Research (ISSN 2276-6510), 2*(6), 115-124.

Ola-Buraimo, A., & Akaegbobi, I. (2013). Palynological evidence of the oldest (Albian) sediment in the Anambra Basin, Southeastern Nigeria. *Journal of Biological and Chemical research, 30*(2), 387-408.

Olabode, S. O. (2014). Soft sediment deformation structures in the Maastrichtian Ajali formation western flank of Anambra basin, Southern Nigeria. *Journal of African Earth Sciences, 89*, 16-30.

Olatunji, O. B. A. (2013). Biostratigraphy and Paleoenvironment Of the Coniacian Awgu Formation in Nzam-1 Well, Anambra Basin, Southeastern Nigeria. *International Journal of Scientific & Technology Research, 2*(3), 112-122.

Onu, F. (2017). The Southern Benue trough and Anambra Basin, Southeastern Nigeria: A Stratigraphic Review. *Journal of Geography, Environment and Earth Science International, 12*, 1-16. doi:10.9734/JGEESI/2017/30416

Onuigbo, E., Okoro, A., Obiadi, I., & Okoyeh, E. (2016). Sedimentary facies characterization and depositional settings of the Ajali sandstone, Anambra Basin, southeastern Nigeria. *Archives of Applied Science Research, 8*(10), 10-25.

Onyekuru, S., & Iwuagwu, C. (2010). Depositional Environments and Sequence Stratigraphic Interpretation of the Campano-Maastrichtian Nkporo Shale Group and Mamu-Formation Exposures at Leru-Okigwe axis, Anambra Basin, Southeastern Nigeria. *Aust J Basic Appl Sci, 4*(12), 6623-6640.

Onyeogu, T., Uzoegbu, M., & Ideozu, R. (2016). Clay minerals assessment from Maastichtian Syclinal, Afikpo, Nigeria. *International Journal of Science, 6*(9), 746-747.

Osinowo, O. O., & Falufosi, M. O. (2018). Magnetic and Very Low Frequency Electromagnetic (VLF-EM) investigations for gold exploration around Ihale in Bunnu-Kabba Area of Kogi, north-central Nigeria. *Contributions to Geophysics and Geodesy, 48*, 191-205. doi:10.2478/congeo-2018-0008

Palmer, D. (1981). An introduction to the generalized reciprocal method of seismic refraction interpretation. *Geophysics, 46*(11), 1508-1518.

Pancha, A., Anderson, J. G., Louie, J. N., & Pullammanappallil, S. K. (2008). Measurement of shallow shear wave velocities at a rock site using the ReMi technique. *Soil Dynamics and Earthquake Engineering, 28*(7), 522-535.

Parise, M., & Iovine, G. (2009). Preface to the special issue on «innovative approaches for evaluating landslide hazard and risk». *Geografia Fisica e Dinamicca Quaternaria, 32*, 179-181.

Pazzi, V., Morelli, S., & Fanti, R. (2019). A Review of the Advantages and Limitations of Geophysical Investigations in Landslide Studies. *International Journal of Geophysics, 2019*. Retrieved from <Go to ISI>://WOS:000477835400001. doi:10.1155/2019/2983087

Perrone, A., Lapenna, V., & Piscitelli, S. (2014). Electrical resistivity tomography technique for landslide investigation: A review. *Earth-Science Reviews, 135*. doi:10.1016/j.earscirev.2014.04.002

Pugin, A. J. M., Pullan, S. E., Hunter, J. A., & Oldenborger, G. A. (2009). Hydrogeological prospecting using P-and S-wave land streamer seismic reflection methods. *Near Surface Geophysics, 7*(5-6), 315-328.

Reid, M., Baum, R., LaHusen, R., & Ellis, W. (2008). Capturing landslide dynamics and hydrologic triggers using near-real-time monitoring. *Landslides and engineered slopes, 1*, 179-191.

Reijers, T. (2011). Stratigraphy and sedimentology of the Niger Delta. *Geologos, 17*, 133-162. doi:10.2478/v10118-011-0008-3

Reyment, R. A. (1965). *Aspects of the geology of Nigeria: The stratigraphy of the Cretaceous and Cenozoic deposits*: Ibadan university press.

Sajinkumar, K. S., Anbazhagan, S., A.P, P., & R. Rani, V. (2011). Weathering and landslide occurrences in parts of Western Ghats, Kerala. *Journal of the Geological Society of India, 78*, 249-257. doi:10.1007/s12594-011-0089-1

Sass, O., Bell, R., & Glade, T. (2008). Comparison of GPR, 2D-resistivity and traditional techniques for the subsurface exploration of the Öschingen landslide, Swabian Alb (Germany). *Geomorphology, 93*, 89-103. doi:10.1016/j.geomorph.2006.12.019

Shanmugam, G., & Wang, Y. (2015). The landslide problem. *Journal of Palaeogeography, 4*(2),109-166. Retrieved from http://www.sciencedirect.com/science/article/pii /S209538361530016X. doi:https://doi.org/10.3724/SP.J.1261.2015.00071

Snieder, R., Hubbard, S., Haney, M., Bawden, G., Hatchell, P., Revil, A., & Group, D. G. M. W. (2007). Advanced Noninvasive Geophysical Monitoring Techniques. *Annual Review of Earth and Planetary Sciences, 35*(1), 653-683. Retrieved from https://www.annualreviews.org/doi/abs/10.1146/annurev.earth.35.092006.145050. doi:10.1146/annurev.earth.35.092006.145050

Sompotan, A. F., Pasasa, L. A., & Sule, R. (2011). Comparing models GRM, refraction tomography and neural network to analyze shallow landslide. *Journal of Engineering and Technological Sciences, 43*(3), 161-172.

Stucchi, E., & Mazzotti, A. (2009). 2D seismic exploration of the Ancona landslide (Adriatic Coast, Italy). *Geophysics, 74*. doi:10.1190/1.3157461

Sugmoto, T., Kawasaki, K., & Sakai, H. (2014). Use of magnetic surveying in landslide analysis at the boundary between the granite region and the green tuff region in Southwestern Toyama Prefecture. *Journal of Natural Disaster Science, 35*(2), 55-66.

Surovell, T. A., Toohey, J. L., Myers, A. D., LaBelle, J. M., Ahern, J. C., & Reisig, B. (2017). The end of *archaeological discovery. American Antiquity,* 82(2), 288-300.

Talebi, A., Uijlenhoet, R., & Troch, P. A. (2008). A low-dimensional physically based model of hydrologic control of shallow landsliding on complex hillslopes. *Earth Surface Processes and Landforms: The Journal of the British Geomorphological Research Group, 33*(13), 1964-1976.

Theune, U., Rokosh, D., Sacchi, M. D., & Schmitt, D. R. (2006). Mapping fractures with GPR: A case study from Turtle Mountain. *Geophysics, 71*(5), B139-B150.

Thiebes, B. (2011). *Landslide analysis and early warning - Local and regional case study in the Swabian Alb, Germany*.

Tingey, B. E., McBride, J. H., Thompson, T. J., Stephenson, W. J., South, J. V., & Bushman, M. (2007). Study of a prehistoric landslide using seismic reflection methods integrated with geological data in the Wasatch Mountains, Utah, USA. *Engineering Geology, 95*(1-2), 1-29.

Tonnellier Alice, Agnes Helmstetter, Jean-Philippe Malet, & Jean Schmittbuhl. (2013). Seismic monitoring of soft-rock landslides: The Super-Sauze and Valoria case studies. *Geophysical Journal International, 193*, 1515–1536 doi:10.1093/gji/ggt039

Ukaonu, C. E., Onyekuru, S. O., & Ikoro, D. O. (2017). Facies architecture and reservoir properties of Campanian-Maastrichtian Nkporo Formation in the Anambra Basin, Nigeria. Scientific Research Journal, 5, 1-11.

Uma, O. K., & Onuoha, K. M. (1997). Hydrodynamic flow and formation pressures in the Anambra basin, Southern Nigeria. *Hydrological Sciences Journal, 42*, 141-154. doi:10.1080/02626669709492016

Uzoegbu, M., & Ideozu, D. R. (2016). Clay Minerals Assessment from Maastrichtian Syclinal Afikpo, Nigeria. *International Journal of Scientific Research and Publications, 6*, 746-2250.

Uzoegbu, M. (2013). Lithostratigraphy of the Maastrictian Nsukka Formation in the Anambra Basin, S.E Nigeria. *IOSR Journal of Environmental Science, Toxicology and Food Technology, 5*, 96-102. doi:10.9790/2402-05596102

Uzoegbu, M. U., & Okon, O. S. (2017). Sedimentology and Geochemical Evaluation of Campano-Maastrichtian Sediments, Anambra Basin, Nigeria. *International Journal Geology and Mining, 3*(2), 110-127. Retrieved from www.premierpublishers.org.

Uzoegbu, U., Uchebo, U., & Okafor, I. (2013). Lithostratigraphy of the Maastrictian Nsukka Formation in the Anambra Basin, SE Nigeria. *International Organization of Scientific Research (IOSR): J. Env. Sci., Toxi. Food Tech, 5*(5), 96-102.

Wang, W. H., & Sassa, K. (2005). Comparative evaluation of landslide susceptibility in Minamata area, Japan. *Environmental Geology, 47*, 956-966. doi:10.1007/s00254-005-1225-2

Wisén, R., & Christiansen, A. (2005). Laterally and Mutually Constrained Inversion of Surface Wave Seismic Data and Resistivity Data. *Journal of Environmental and Engineering Geophysics, 10*, 251-262. doi:10.2113/JEEG10.3.251

Xia, J., D. Miller, R., Park, C., Hunter, J., & Harris, J. (2001). Comparing Shear-wave Velocity Profiles from Multi-channel Analysis of Surface Wave with Borehole Measurements.

Yılmaz, S. (2011). A case study of the application of electrical resistivity imaging for investigation of a landslide along highway. *International Journal of Physical Sciences, 6*, 5843-5849. doi:10.5897/IJPS11.564

Zaborski, P. M. (2000). The Cretaceous and Paleocene transgressions in Nigeria and Niger. *Journal of Mining and Geology, 36*, 153-173.

CHAPTER 3: ASSESSMENT OF THE SUBSURFACE CONDITIONS OF A LANDSLIDE IN SOUTH-EASTERN NIGERIA, BY USING GEOTECHNICAL RESULTS FOR A PROPER UNDERSTANDING OF THE GEO-ELECTRICAL SOUNDING FINDINGS.

School of Chemistry and Physics, College of Agriculture, Engineering, and Science, University of KwaZulu-Natal, Pietermaritzburg Campus, Private Bag X01, Scottsville 3209, South Africa.

ASSESSMENT OF THE SUBSURFACE CONDITIONS OF A LANDSLIDE IN SOUTH-EASTERN NIGERIA, BY USING GEOTECHNICAL RESULTS FOR A PROPER UNDERSTANDING OF THE GEO-ELECTRICAL SOUNDING FINDINGS.

Chikwelu Edward Emenike and Naven Chetty

School of Chemistry and Physics, College of Agriculture, Engineering, and Science, University of KwaZulu-Natal, Pietermaritzburg Campus, Private Bag X01, Scottsville 3209, South Africa.

*Corresponding Author: chettyN3@ukzn.ac.za

Abstract

This research studied the surface conditions of a landslide in the Nanka community, South-Eastern, Nigeria, using geoelectrical and geotechnical methods as a tool. Eighteen (18) soil samples for analysis are collected from dug holes at different marked depths and locations. And the samples were analyzed for the following parameters; 'the liquid limit, plastic limit, plasticity index, maximum dry density, and optimum moisture content', and they have the average values of 34.92%, 23.31%, 11.61%, $1.86Mg/m^3$, and 10.18% respectively. The textural characteristics of the analyzed soil samples also proved that the mean value of sand is 77.8%, gravel is approximately 1%, and the silt+clay is 21.3%. The lithologies of the soil in the study area are clays, sandstones, alluvium, gravel, natural water (sediments), which the results from the two methods all agreed. The central parts of the topsoil and subsoil zones constitute the main aquifer unit from the vertical electrical sounding results, that followed in succession by rock fragments, and bedrock with an elevation that could be an up-shouting outcrop resistant to weathering and landslide. The analysis results also showed that the soils in the study areas are friable hence easily washed off when there is any draining away of water from the surface, making the slide active for many years resisting every preventive measure put in place. Preventive measures in more organized ways from institutions will be of great importance in reducing the ugly effect of the slides in the said location.

Keywords: landslide, VES, geotechnical, weathering, lithology.

3.1 Introduction

Permanent forms of erosion are gullies, when rain falls in narrow runoff paths and waterways, cutting through the soil to depths of several feet that cannot be tillage-smoothed over any longer (Boca & Saraçlı, 2019). As a model assumption, this uniform layer of weathered material is without doubt beneficial (Brantley & White, 2009). For some very thick weathered mantles, it's also definitely true, or near enough (Boca & Saraçlı, 2019). And, of course, the mobile motionless difference is self-evident when only a fraction of the regolith thickness moved (Brooks, 2003). Some modern modelling and analytical work on regolith and the so-called critical zone of moveable thickness h and weathered material H that are often removed by erosion (Sommer et al., 2008). As H > h, this implies the existence of an immobile subsurface layer in many cases (Lobkovsky *et al.*, 2004). The regolith zone was the result of a variety of impact, erosion, and weathering processes that resulted in a diverse strange mix of particles, with a variety of forms ranging in size from clay to boulders (Dixon, 2018). The formation of soil regolith profiles and their associated complexity is strongly time-dependent, and the period required for the production-specific soil and weathering characteristics vary (Anderson *et al.*, 2013; Giardino & Houser, 2015). In general, soil characteristics with organic matter build-up progress quickly (Kabala & Zapart, 2012), while soil properties associated with weathering proceed more slowly (Egwuonwu, 2012). Over time, soil and regolith profiles thicken, and horizon complexity rises (Stoops *et al.*, 2018). The gradual build-up of minerals as a result of additions, transformations, and translocations results in increasing soil complexity (Lu *et al.*, 2002).

Bedrock is a solid rock mass physically connected to the deepest Earth (DiPietro, 2018). If the bedrock exposed on the surface of the Earth, it is called an outcrop (Portenga *et al.*, 2013). Landscape formation is the way an outcrop responds to erosion and weathering (Gnyawali *et al.*, 2020; Tian *et al.*, 2020). Rocks particles that withstand weathering and erosion seem to be harder or resistant (DiPietro, 2018). The rocks type at the study area has high erodibility, implying that it is quickly eroded and weathered, also soft, weak, or non-resistant (Otti *et al.*, 2014). The subsurface interlayer of rocks with varying erodibility generates a differential erosion landscape, defined as a region where neighbouring rocks weather and erode differently, with the more resistant rock protruding above and the less resistant rock opposite. (Clark & Burbank, 2011; DiPietro, 2018; Goodfellow *et al.*, 2014; Hayden, 2017; Shobek *et al.*, 2017). With a few exceptions, sedimentary rocks are also soft from the study area, and they do not tend to build towering mountains (Ekwenye *et al.*, 2014). Because crystalline granite (rock)

resists erosion, it produces highland regions with some of the world's most difficult landscapes. (DiPietro, 2012).

Geophysics who gather information on the physical formations of the Earth describes landslides as one type of mass wasting, which is involved in the downward movement of the Earth's surface or unstable slope (Smithson *et al.*, 2013). Igwe (2015) further avow that landslide is a major hazard in Nigeria, where resources worth several million US dollars are lost every year during seasons of heavy rain. The high rainfall intensity period in south-eastern Nigeria has had a notable impact on the climate, the slope stability of the area, and other geomorphological structures of the region (Smithson *et al.*, 2013). The study areas lie in the Anambra Basin with approximately 6,000m of sedimentary rocks (Obaje *et al.*, 2018). Igwe (2015) proved that landslides menace on the sedimentary terrain were mainly shallow, material slumps, low-volume movements, and brief run-out slides, some of which happened on slopes that followed the dip of strata along wavy shear surfaces controlled by water-resistant bedding planes. Many cases of these landslides have resulted due to natural and human causes like landform, deforestation, overgrazing, poor drainage system (Alimohammadlou *et al.*, 2013). Over 6,000 km^2 of land are affected by landslide and about 3,400 km^2 are highly exposed (Sonel, 2009). According to a study conducted by Nkemakonam *et al.*, (2019), that shows that in Anambra State, 37 percent of the total landmass covered severely gullied, 28 percent by moderately gullied, and 35 percent ravage by mildly gullied. These gullies have created many environmental problems including loss of lives and properties (Onweremadu, 2007).

Substantial progress has been achieved in understanding, identifying, and in the processes of landslide control in recent years but still poses some challenges (De Baets *et al.*, 2011). These control phenomena have been one of the many natural processes that reshape the surface of the earth and represent a manifestation of catchment instability and, its initiation and development is an indicator of land degradation (Ionita *et al.*, 2015). Okengwo *et al.*, (2015) investigated the causes and effects of Nanka gully erosion, and there is currently no detailed quantitative information and specific study on the rate of slide expansion and subsurface information, the causative factors, and their significant impact on gullies advancement. Okengwo *et al* (2015) studied the stability of gully walls in the Agulu-Nanka-Oko area using an empirical approach, and he explained that most gullies have deep rotational slumps along the sidewall which is as a result of increased pore pressure from groundwater, he further explained that the rate of this gullies or slumping is widely related to the soil strength hence he analysed the cohesiveness components of the soil and the results proved that for all sites, the top stratum (laterite soil)

shared some cohesion and that the shear resistance increases with depth due to the downward increase in the percentage of sand and decrease in silty-clay content. Amongst other areas covered by the previous researchers, it is evident that none of the studies used combined-geoscientific methods on the study of subsurface conditions of the landslide in the Nanka community, and Figure 3.1 shows the slide site from different views and directions.

Finally, the aims and objectives of this research are to: (1) ascertain the vertical and horizontal subsurface conditions of the area by interpreting the vertical electrical sounding findings using geotechnical properties and results and other geologic information. (2) determine the conditions of groundwater potentials through Vertical Electrical Sounding iso-resistivity contour maps, (3) deduce the lithological component of the slides subsurface.

Figure 3.1: Pictures of Nanka Landslide from four different views.

3.1.1 *Study area and geology setting*

Nigeria is at latitudes 4^0N and 15^0N and Longitudes 3^OE and 14^OE within the Pan African mobile belt of the West African and Congo cratons (Okonkwo & Ganev, 2012). According to Oyinloye, (2011) the geology of Nigeria is characterized by crystalline and sedimentary rocks that occur in almost similar proportion, as presented in Figure 3.2a. The crystalline rocks include the Basement complex and Phanerozoic rock found in the country's eastern and north-central regions (Busato *et al.*, 2016; Oyinloye, 2011). Nigeria's Precambrian basement rocks, predominantly of the migmatite gneissic–quartzite complex from the Archean to the Early Proterozoic (2700-2000 Ma) (Oyinloye, 2011). Other units include NE-SW trending schist belts, found mainly in the western part of the nation, and granitoid plutons from the earlier granite suite, which dated from the Late Proterozoic to the Early Phanerozoic (750-450Ma) (Oyinloye, 2011).

The study area lies between latitudes $N6^0.03^1$-$N6^0.04^1$ and longitudes $E7^0.08^1$- $E7^0.09^1$, as shown in figure 3.2b and 3.2c, within the western flank of the Anambra Basin drawn out in Figure 3.2d as a profile diagram. The Nanka sands, which lay conformably on the Paleocene Imo Shale and overlain by the Ogwashi-Asaba formation, are geological formations (Okengwo *et al.*, 2015). The Basin defines the southern boundary (or portion) of the Benue Trough, created during Santonian tectonics (together with the Afikpo syncline and Abakaliki Ridge) (Patrick *et al.*, 2013). The research area is within the humid tropical zone of the rainforest region, with a mean annual rainfall of 1800 mm (Adelekan, 2011).
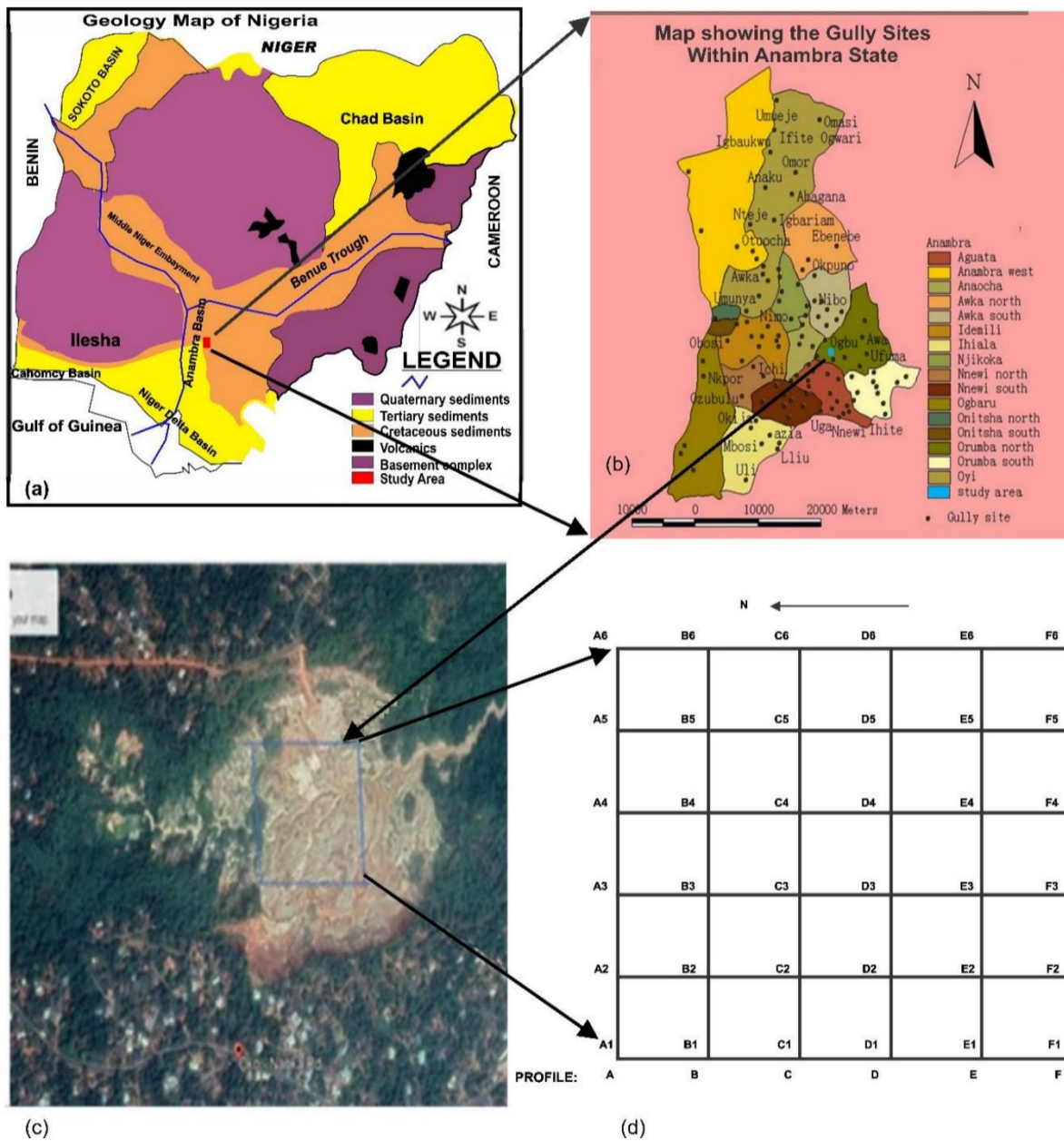
Figure 3.2: Location of the study area showing; (a) Geology Map of Nigeria, (b) Anambra State Map with all the Gullies, (c) Study area from Google Earth 2020, and (d) Profile picture.

3.2 Materials and methods

This research work employed geoelectrical and geotechnical methods in the subsurface investigation.

3.2.1 Geoelectrical Method

In a geoelectrical investigation, Vertical Electrical Sounding was used and mainly applied in the investigation of surfaces that are horizontal or near horizontal (Ehirm *et al.*, 2009). In the field survey, the fraction of the total current that flows in this varies with the electrode's separation in the field procedure, using a fixed centre, and the whole spread progressively expanding around the fixed centre. This allows the current lines to pierce to greater depths depending on the vertical distribution of the conductivity. The aim is to observe the total variation of the resistivity at various depths. This technique is suited for measuring the depth and resistance of a flat-layered rock structure, such as sedimentary layers or water table depths (Layade *et al.*, 2017). It is used in other words to assess the overburden thickness in geotechnical surveys and also to describe horizontal zones of porous strata in hydrogeology (Umar *et al.*, 2020). The VES carried out using the Schlumberger configuration for horizontal spread covering the entire profile. The array for study area investigation consists of four collinear electrodes, as shown in Figure 3.3. The outer two electrodes are current (source; A and B) electrodes, and the inner two electrodes are the potential (receiver; C and D) electrodes (Layade *et al.*, 2017). The Potential electrodes, instilled with separation in the centre of the electrode array, usually less than one-fifth of the space between current electrodes.

During the fieldwork, the current electrodes were moved to a greater spacing, while the potential electrodes were held in place until they were too tiny to measure the observed voltage. The main benefit of the Schlumberger array is the movement of fewer electrodes for each sounding, as well as the shorter length of the wire for potential electrodes (Abdullahi *et al.*, 2015). It has better resolution, greater sampling depth (Aspinall & Gaffney, 2001), and field setup takes less time than the Wenner array (Morrison & Gasperikova, 2012). Long current electrode cables are necessary, the recording device must be sensitive, and the array might be complicated for the field crew to organize (Morrison & Gasperikova, 2012).

AB = Current Electrodes
CD = Voltage Electrodes
L   = Profile Length (m)
I   = Electric Current (Ampere)
V   = Potential Difference (Volt)
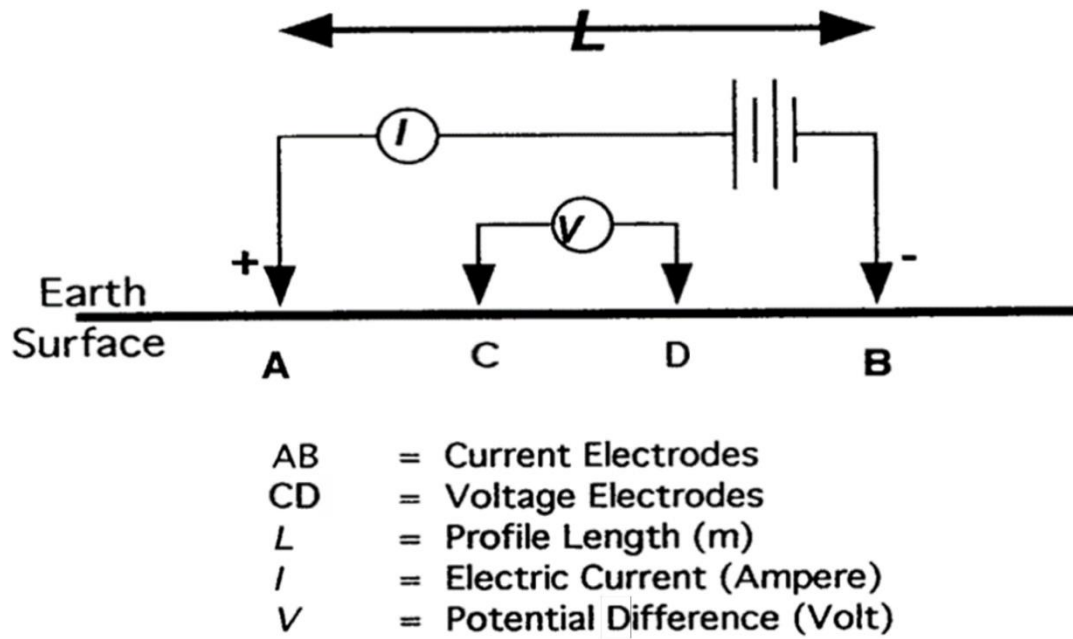
Figure 3.3: Shows the detailed Schlumberger Configuration.

A total of thirty-six (36) VES soundings points carried out in the field, with a spread of 50m (AB/2). The resistivities of the subsurface were recorded using ABEM Terrametre SAS 300c and the Ohmega campus digital resistivity meters, while 'Global Positioning System' (GPS) is also used to get the location coordinates for VES sounding and sample collection points. VES procedures in the field were employed. In Schlumberger configuration, (Aboh & Osazuwa, 2000) shows how to use the Schlumberger array to determine the apparent resistivity using the eq. (3.1) below,

$$\rho = \frac{2\pi \Delta V}{I} \left(\frac{L^2 - a^2}{a} \right) \qquad (3.1)$$

Where:

" ρ " is the Apparent resistivity

"L" is the distance between their mid points

"ΔV" is the Potential difference

"I" is the current

"a" stand for space between two electrodes.

The resistivity curves were then interpreted using a computer interpretation program for Schlumberger sounding data modified after (Zohdy & Jackson, 1989). The VES resistivity curve matching was generated from the partial curve matching technique and was interpreted by computer iteration using Minitab 18 software to generate subsurface contour maps. The subsurface contour maps were interpreted qualitatively with the mapped surface geology and information on existing geologic common rocks shown in Table 3.1 and geotechnical results.

Table 3.1: Resistivity Range for Rock types in Sedimentary Complex (Telford *et al.*, 1990).

Type of Rock	Resistivity Range (Ώ-m)
Clays (Including wet clay)	5 – 100
Gravel	100 – 10,000
Alluvium and sand	10 – 800
Weathered laterite	150 – 900
Surface waters (sediments)	10 – 100
Natural waters (sediments)	1 – 100
Sandstones	$1 - 6.4 \times 10^8$
Shales	5 – 50
Sandstone and Conglomerate	>50 – 10,000

3.2.2 Geotechnical Method

The geotechnical analysis involved the field study, laboratory analyses, and field investigation for soil data collection based on sampling and measuring at the slide site. The sample collection procedures were similar to those used in the previous study (Spangler & Handy, 1973). The points A_1, B_1, C_1, D_1, E_1, and F_1 marks (see Figure 3.2d) the collection points for the sample, and the distance between each point interval is 50m from point A_1 and B_1, point B_1 and C_1, etc. A total of eighteen (18) different soil data samples were collected and packed in polybags from six (6) examined dug holes, three (3) from each one (1). The soil samples were collected at depth ranges of 3m, 6m, and 9m from points A_1, B_1, etc. at the dug holes. Vertical soil sampling in the dug holes was used to determine changes in soil properties, while laboratory tests were used to determine the soil properties index. A chain of geotechnical tests including 'Particle-size analyses, Atterberg limits, Compaction, and Shear strength tests', were carried out on the soil samples by following the procedures specified by the American Society for Testing Materials (ASTM), and the British Standard Methods for testing soils for Civil Engineering purposes (Okengwo *et al.*, 2015).

3.2.2.1 Atterberg or Consistency limit test

The Atterberg or Consistency Limit Test evaluates the moisture content at which the soil will flow below its height (Andrade *et al.*, 2011). Atterberg limit test defines the boundary of several states of plastic soil accuracy (Robertson, 2009), and also used in determining the following: liquid limit, plastic limit, plasticity index, liquidity index, and relative consistency (Huang & Lu, 2014).

3.2.2.2 Liquid Limit Test

The Liquid limit test is the moisture content at which the soil starts to act as fluid under the influence of a standard blow (Dimitrova & Yanful, 2011). According to Öser (2020), the liquid limit of soil can also be the moisture content, expressed as the percentage of the weight of the oven-dried soil, at the boundary between the absolved liquid and plastic states of consistency.

3.2.2.3 Liquidity index (LI)

The Liquidity index is the ratio of the differences between the natural moisture content (Wn) and the plastic limit (PL), (Wn-PL), divide by plasticity index (PI) (Okunlola *et al.*, 2014). Mathematically liquidity index can be represented in eq. (3.2) as;

$$LI = \left(\frac{Wn - PL}{PL}\right), \tag{3.2}$$

3.2.2.4 Plastic Limit

The plasticity index is the range of soil moisture content over which the soil is plastic (Wilson, 2011). Except for the lack of liquid limit apparatus, it has a similar technique as a liquid limit analysis. In general, the arithmetic difference between the Liquid Limit (LL) and the Plastic Limit (PL) is a notably useful indicator of the likely properties of the soil, including its potential for resistance to liquefaction (Adams, 2016), as shown in eq (3.3).

$$PI = LL - PL. \tag{3.3}$$

3.2.2.5 Compaction Test

The purpose of the compaction test was to assess the compaction properties of various soils as moisture content changed. The optimal moisture level at which a soil type is most compacted and achieves its maximum dry density by eliminating air spaces is called soil compaction (Adam & Pistrol, 2016). Dry density and the maximum water content measure the degree of compaction of the soil. A curve is formed between the water content and the dry density to compute the maximum dry density and the optimal water content (Contractor, 2020).

3.2.2.6 Relative consistency (Cr)

The ratio of the differences between liquid limit and natural moisture content (LL-Wn) divided by the plasticity index (PI) (Okunlola *et al.*, 2014). Relative consistency helps to assess whether the soil is mouldable or resistance to deformity and rupture (Penno, 2012). If the Cr is less than zero, any remoulding process will transform the soil into a thick, viscous slurry. As shown in eq. 3.4, if the value of 'Cr' is greater than zero (0), the moulding of soil is not possible.

$$Cr = \left(\frac{LL - Wn}{PL}\right). \tag{3.4}$$

3.2.2.7 Moisture content test

The soil water can be determined by a moisture content test. The percentage of the weight of water of soil to the dry weight will give moisture content (water content).

Thus, moisture content, as shown in eq. (3.5), as:

$$W = \left(\frac{(M_2 - M_3)}{(M_3 - M_1)}\right) x100, \ (Mg/m^3), \tag{3.5}$$

"M_1" stand for the mass of the container, "M_2" is the summation of the mass of wet soil and the mass of the container, "M_3" is the summation of the mass of dry soil and the mass of the container. The moisture content can also be determined from the percentage of the specific gravity test by dividing the density of the material by the density of the water at 4^OC. No dimension for specific gravity. The specific gravity of the water is 1, that of soil ranges from 2.50 to 2.90, while the silt ranges from 2.70 to 2.90 (Okunlola *et al.*, 2014).

Specific gravity,

$$Gs = \frac{(M_2 - M_3)}{(M_4 - M_3)(M_2 - M_1)}, \tag{3.6}$$

"M_1" is the mass of conical flask, "M_2" is the mass of conical and soil, "M_3" is the mass of conical flask, soil and water, "M_4" is the mass of conical flask and water.

3.2.2.8 Permeability Test

Permeability test is also called hydraulic conductivity. It is the measure of the ability of water to flow through the soil (Öser, 2020). It is expressed in units of velocity, which is meter per second (m/s). Thus,

$$K = 2.30 al/A (t_1 - t_o) log10(\frac{h_0}{h_1}), \tag{3.7}$$

"K" is the permeability, "a" is the cross section of standpipe. "L" and "A" are the Length and area of cross section of the soil sample, "t_0" is the initial time, "t_1" is the final time, "h_0" is initial height of water, "h_1" is the final height of water.

3.3   Results and Discussion

3.3.1   *Topsoil, Subsoil, and Rock fragment Contour Map*

The subsoil iso-resistivity contour map and its 3D resistivity contour map are almost identical to the topsoil iso-resistivity contour map due to similarities in both features and lithology, as seen in Figures 3.4a, 3.4b, 3.4c, and 3.4d. The iso-resistivity contour map was plotted from the average values of resistivity produced vertically across the profile. The apparent resistivity value of the topsoil/subsoil was higher at east-west ranging from 160Ωm to > 480Ωm compare to that of north-south values ranging from > 1Ω m to 160 **Ω**m, which showed less effect of weathering. The central parts of the topsoil and subsoil showed severe weathering effects and served as a collection point for groundwater depot (C_4 and D_4). The rock fragments which showed similar apparent resistivity values to the subsoil were due to the impact of water-

bearing materials (weathering) of the rocks at the distance >300 m (E1) downward. The sloping downward at >300m (between D_1 and F_1) may be an aftereffect of a long time of dumping of refuse at the active parts of the slide, which showed very high resistivity values (300Ωm to >600Ωm. This effect is noticeable in both three Iso-resistivity contour maps in Figure 3.4a, 3.4c, and 3.4e. The lithology of the rocks at the low resistivity zones may be clays, alluvium, sand, or natural water (sediments), while lithology of high resistivity zones may be gravel, sandstones, or sandstone and conglomerate (Figures 3.4, compared with Table 3.1). The central parts of the topsoil, subsoil, and rock fragments contour maps also showed the signs of weathering and trap for groundwater potential. The western parts of the three (3) iso-resistivity equally showed a very low resistivity indicating less effect of weathering. The three 3Ds' resistivity contour maps in Figure 3.4b, 3.4d, and 3.4f, showed a clear the interpretation of three (3) iso-resistivity contour maps Figure 3.4a, 3.4c, and 3.4e.

(a)

(b)

Iso-Resistivity Contour Map at Subsoil

(c)

3D Iso-Resistivity Contour Map at Subsoil

(d)

Iso-Resistivity Contour Map at Rock Fragments

(e)

3D Resistivity Contour Map at Rock Fragments

(f)
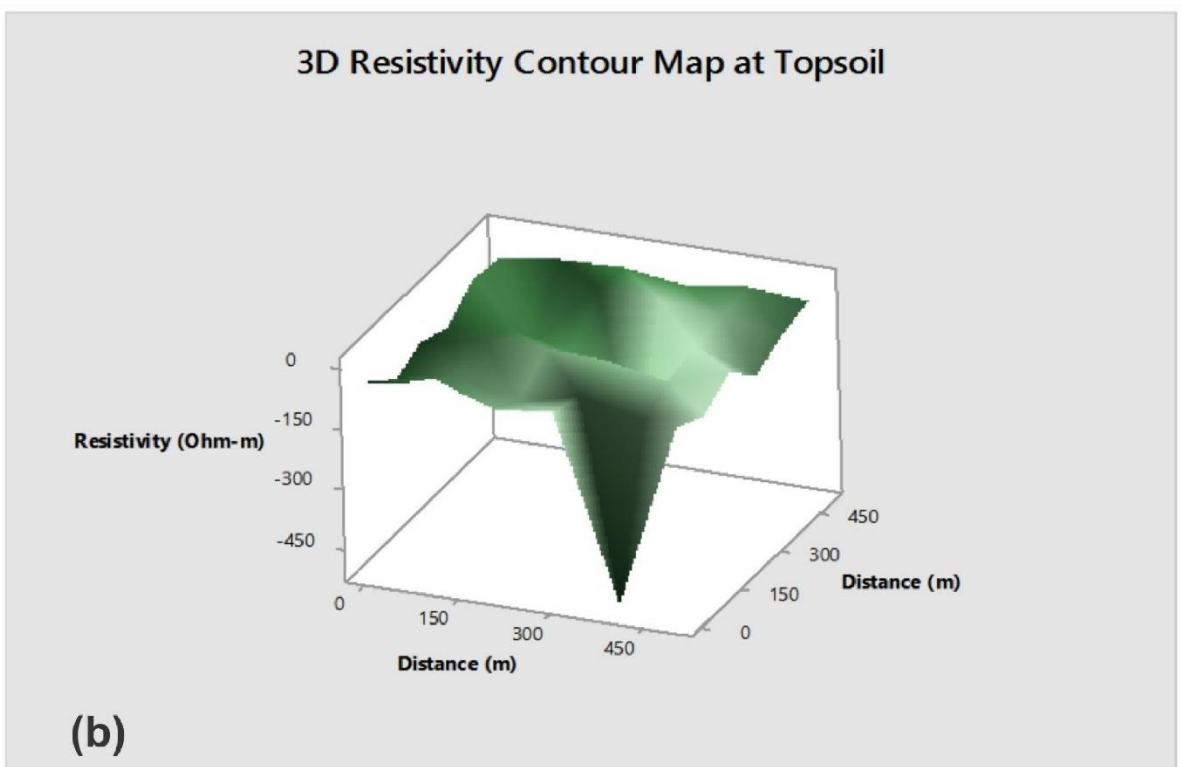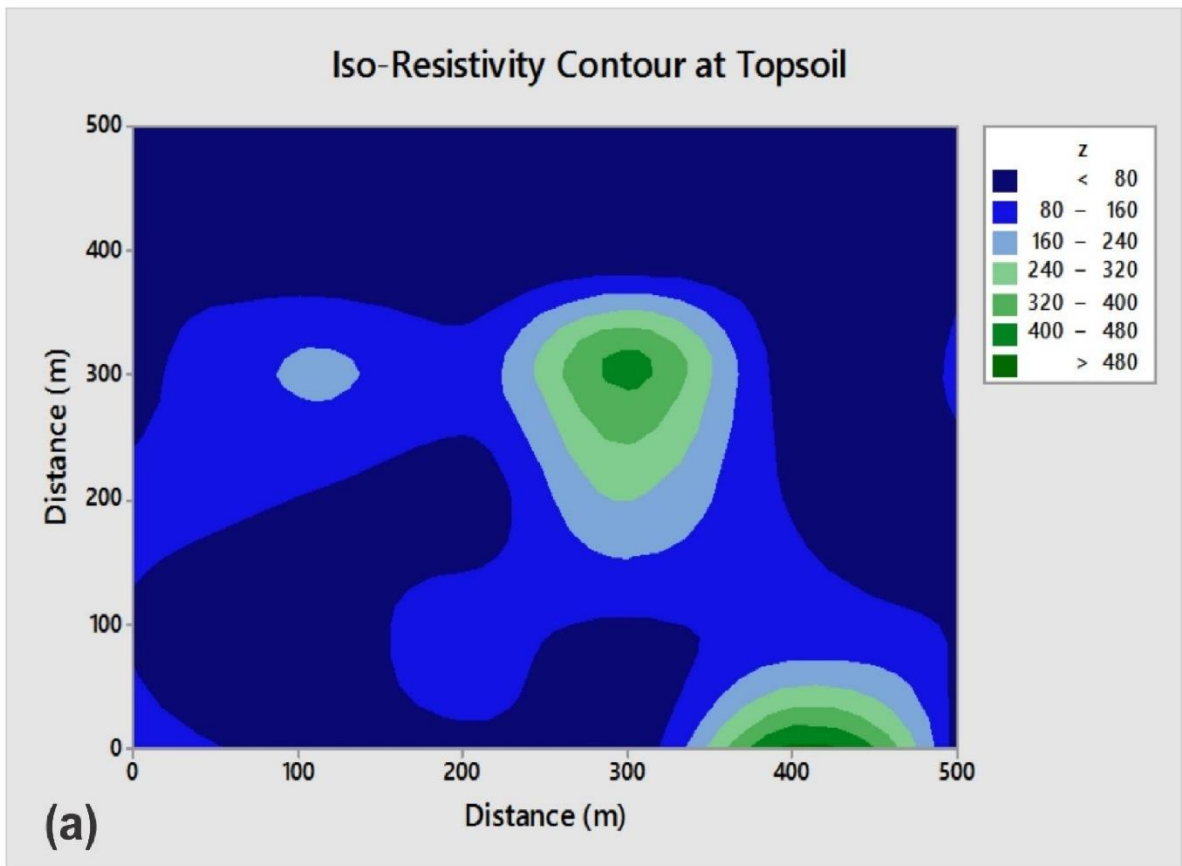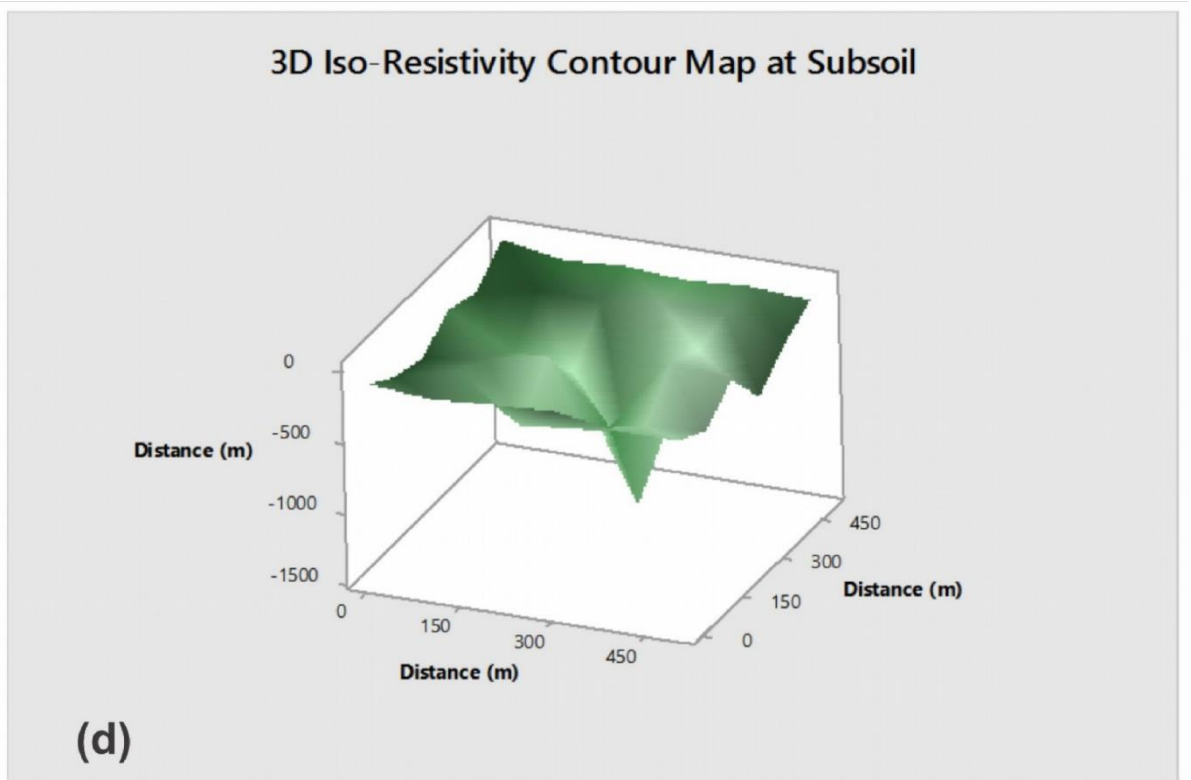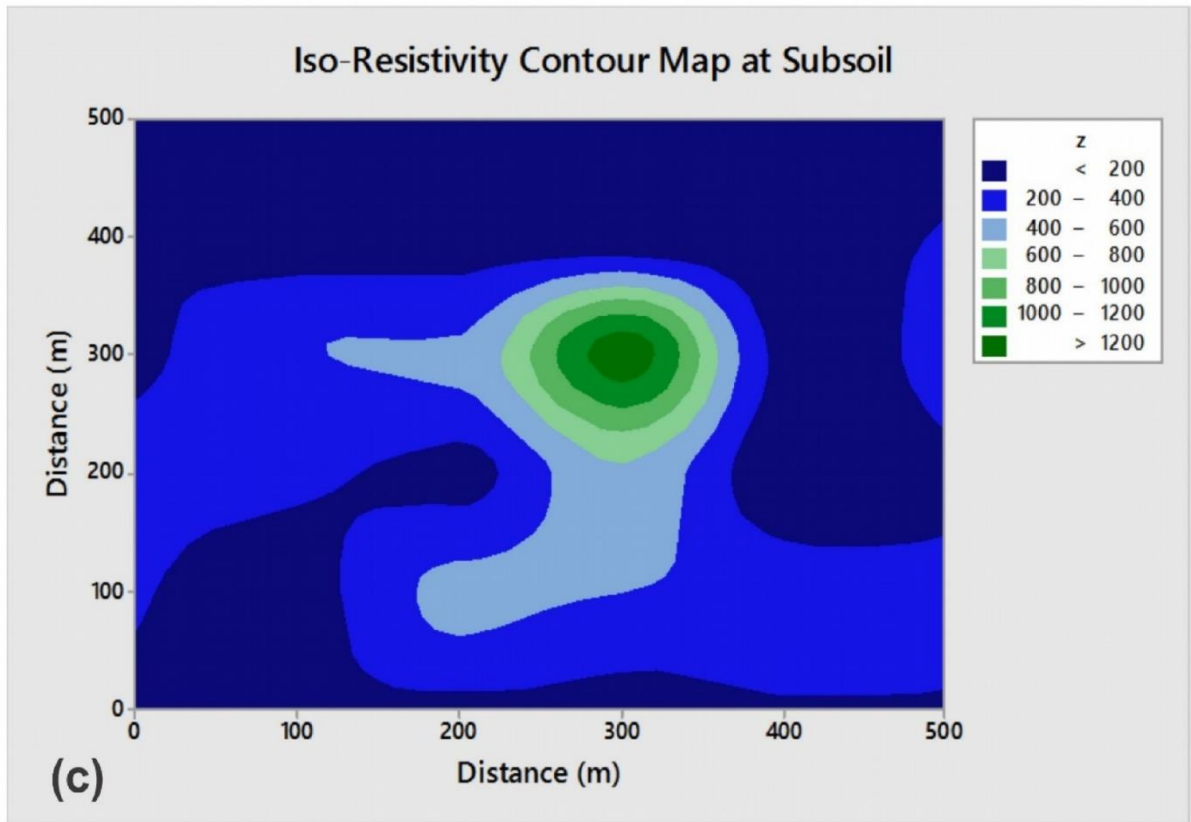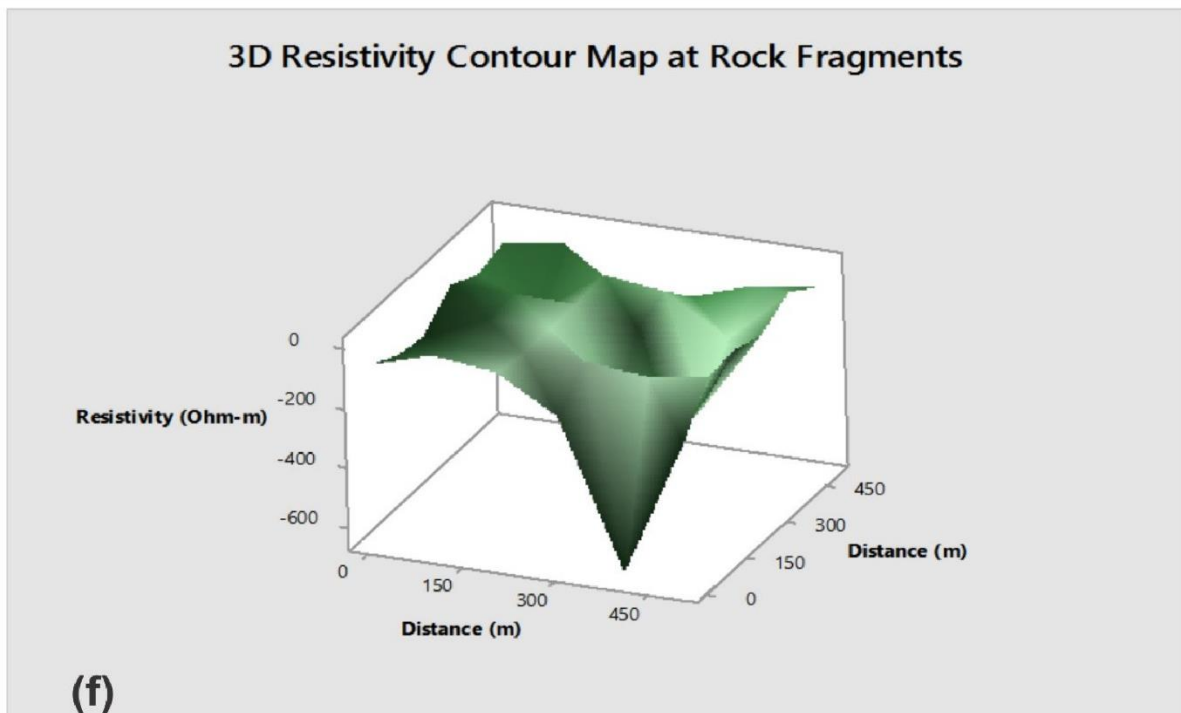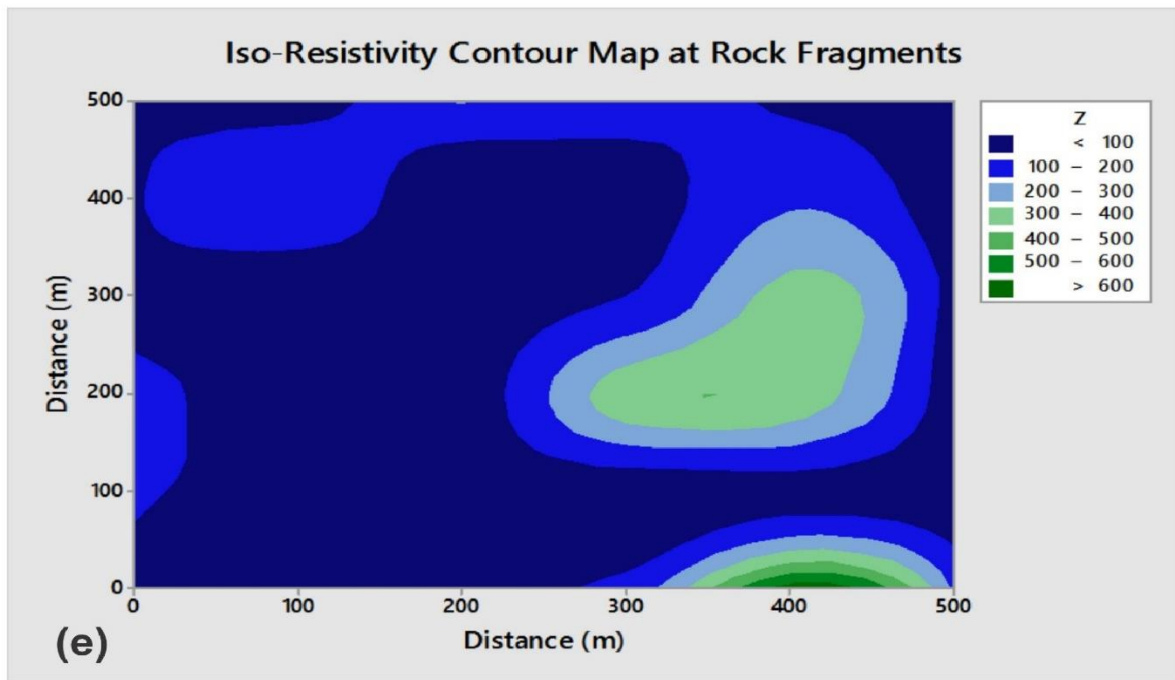
Figure 3.4: (a) Iso-Resistivity Contour Map at topsoil, (b) 3-D Thickness for Topsoil, (c) Iso-Resistivity Contour Map at subsoil, (d) 3-D Thickness for Subsoil, (e) Iso-Resistivity Contour Map at Rock fragments, and (f) 3-D Thickness at Rock fragments.

3.3.2 The vertical geo-electric section

The vertical geo-electric section, as shown in Figure 3.5, proved that the site has four lithological sections, which are topsoil, subsoil, rock fragments, and bedrock. From this, we can conclude that the first and second layers are the hot spot for degradation, weathered topsoil/subsoil (navy blue colour). The formation was followed in succession by rock fragments (weathered in light blue colour) and bedrock (green colour). Qualitative analysis of the vertical geo-electric data collected on the site has revealed that the topsoil, subsoil, and part of rock fragments zones constitute the main aquifer unit from the vertical electrical sounding section. The lithologies of the vertical geo-electric section showed that these layers are sandy, clays, gravel, alluvium, natural water (sediments) confirmed by geotechnical results.
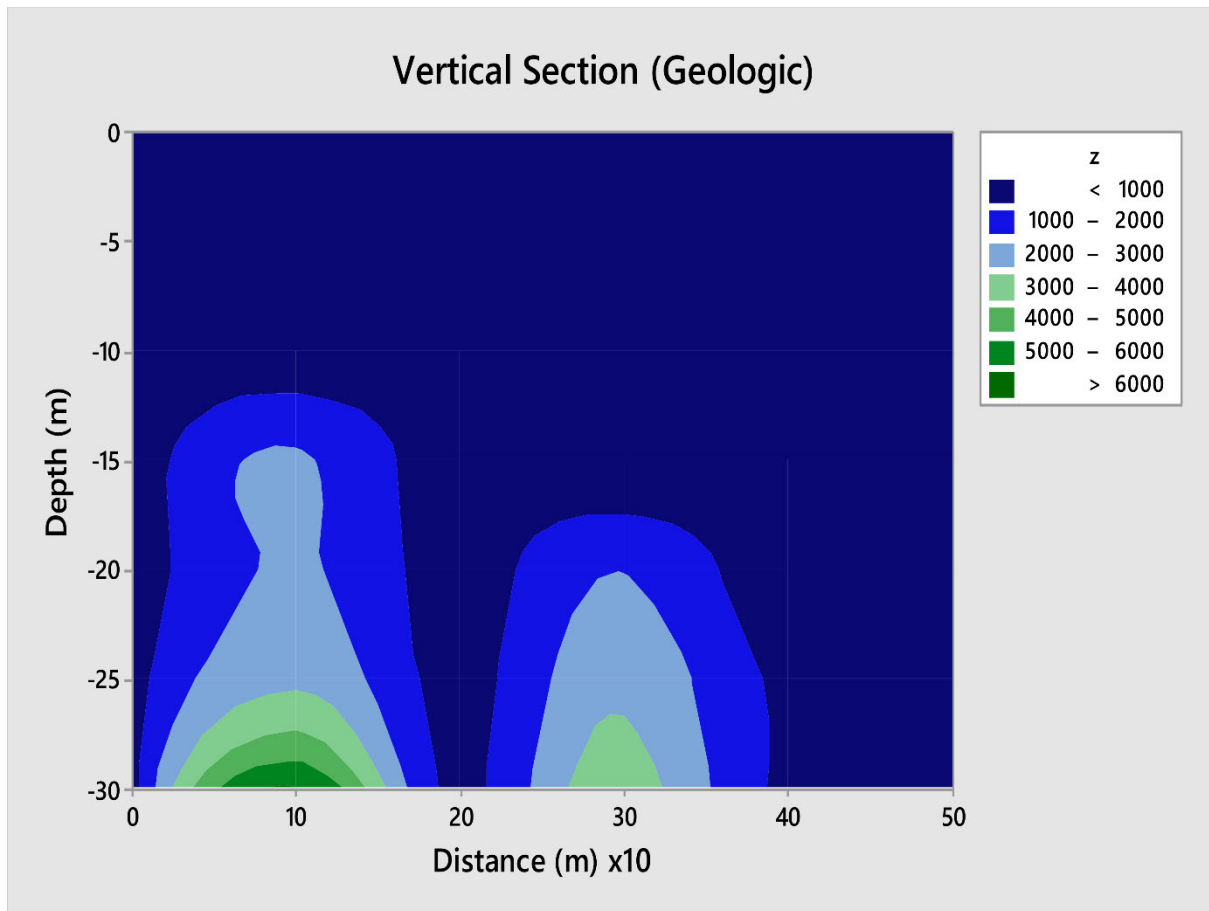
Figure 3.5: The vertical geo-electric section contour map.

3.3.3 *Regolith Contour Map*

The contour plot of regolith thickness shown in Figure 3.6, contoured at a 5m interval. The depth values of the entire thirty-six (36) VES points corresponding to the regolith overburden aquifer layer. The north-eastern parts were on a high plain, and southern-central parts constitute a sizable portion for the groundwater collection. The groundwater flows through all the central parts via profile C_1 of the study site. The western portion along the profile C_3 line was shallow and less contaminated by the agents of weathering, which took place under the influence of the water-bearing capacity.
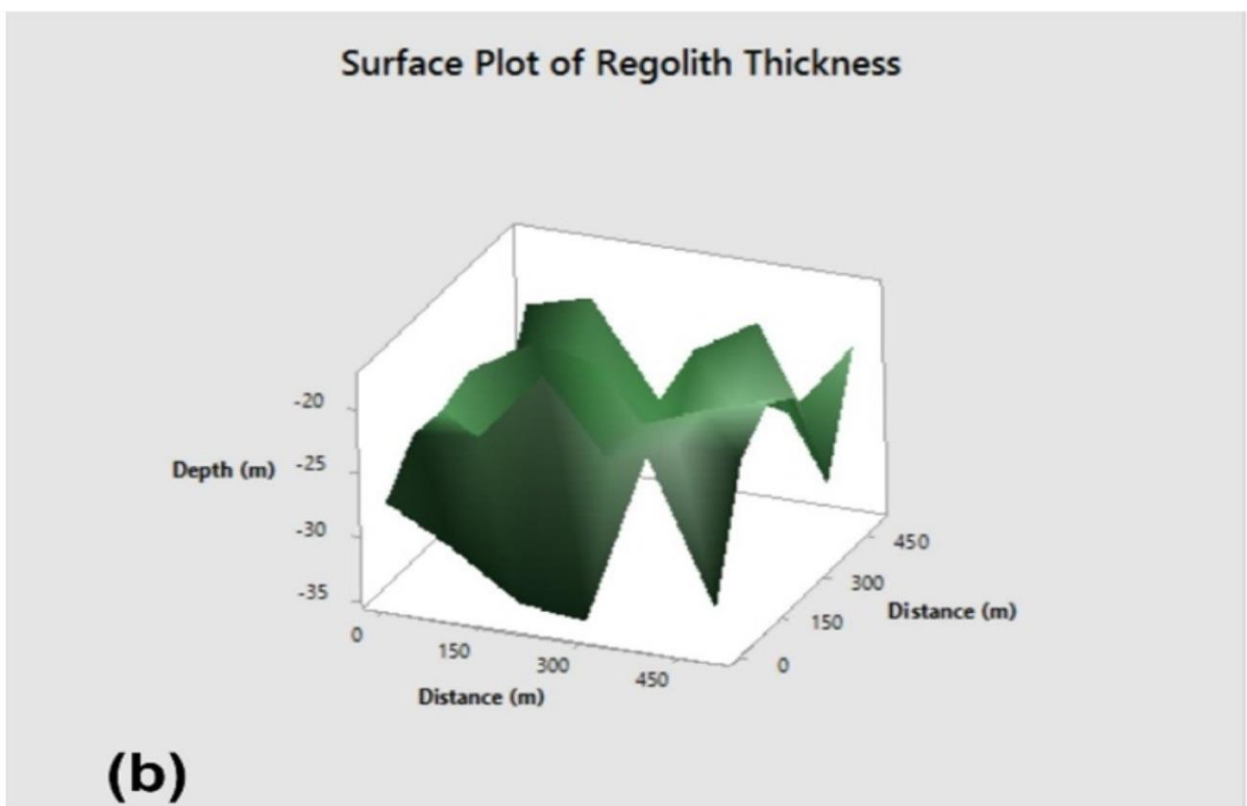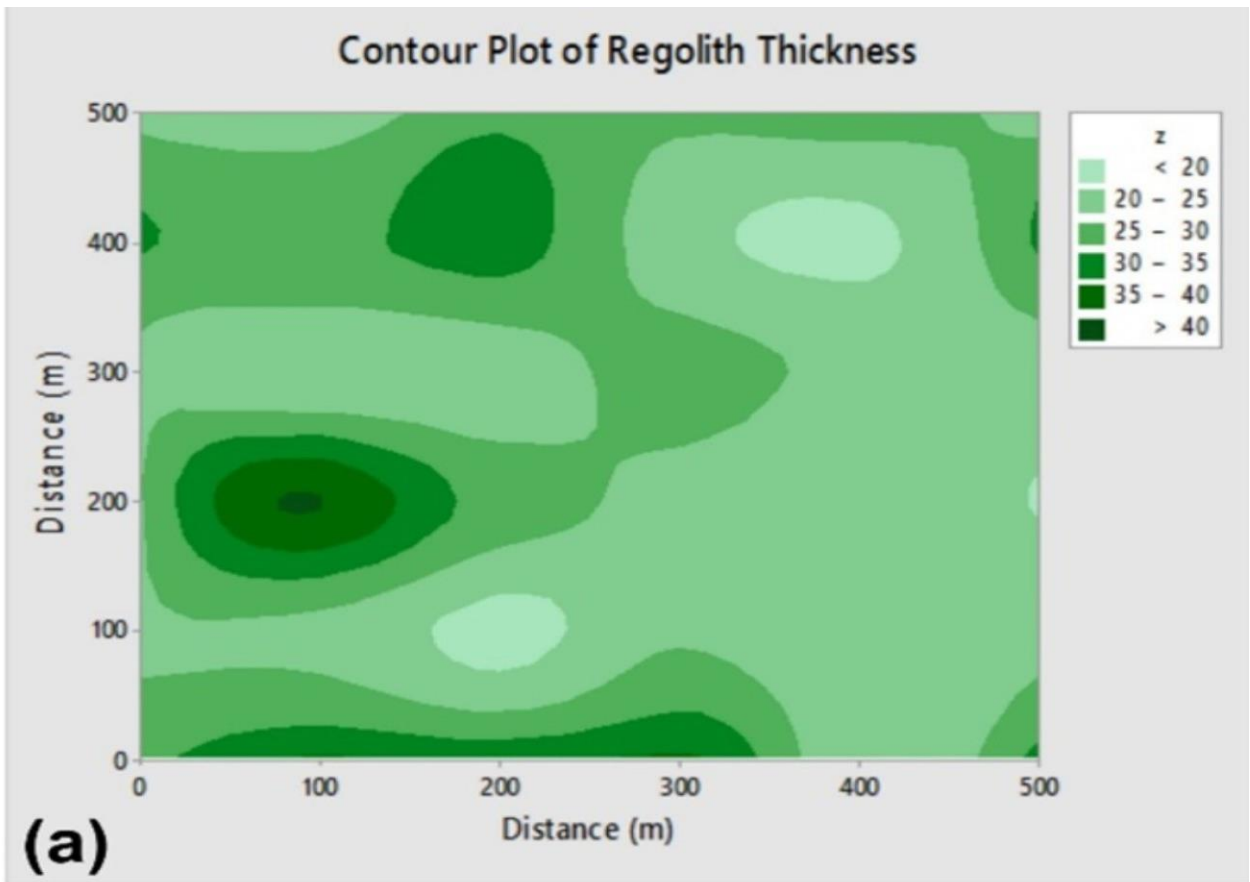
Figure 3.6: (a) Contour Plot of Regolith thickness, and (b) 3D Surface plot of Regolith Thickness.

3.3.4 Bedrock Contour Map

Figure 3.7c shows the bedrock contour map, which was contoured at a 20 m interval for the depth thickness and 500 Ωm interval for the iso-resistivity Figure 3.7a, as mirrored at the ground surface. The depth values linked to the entire (36) VES points. In Figure 3.7b, the 3D wireframe of the bedrock depth structure shows the performances of the aquifer in the weathered bedrock as determined by its bedrock thickness contour map. A_{1-6} profile line was deep from the North to South, while profile line E_{1-6} was shallow from East to West, meaning that the landslide curve is more weathered and severe at the A profile line and mild at the E profile line. However, the areas with depressional features (valleys) are those areas delineated as having good potential for underground water resources (hot-spot for erosion); this correlates with both the vertical section and the iso-resistivity at various zone. Similarly, those areas with elevation could be an up-shouting outcrop resistant to weathering and landslide.

Iso-Resistivity Contoour Map at Bed Rock

(a)

3D Rsistivity Surface Plot at Bed Rock

(b)
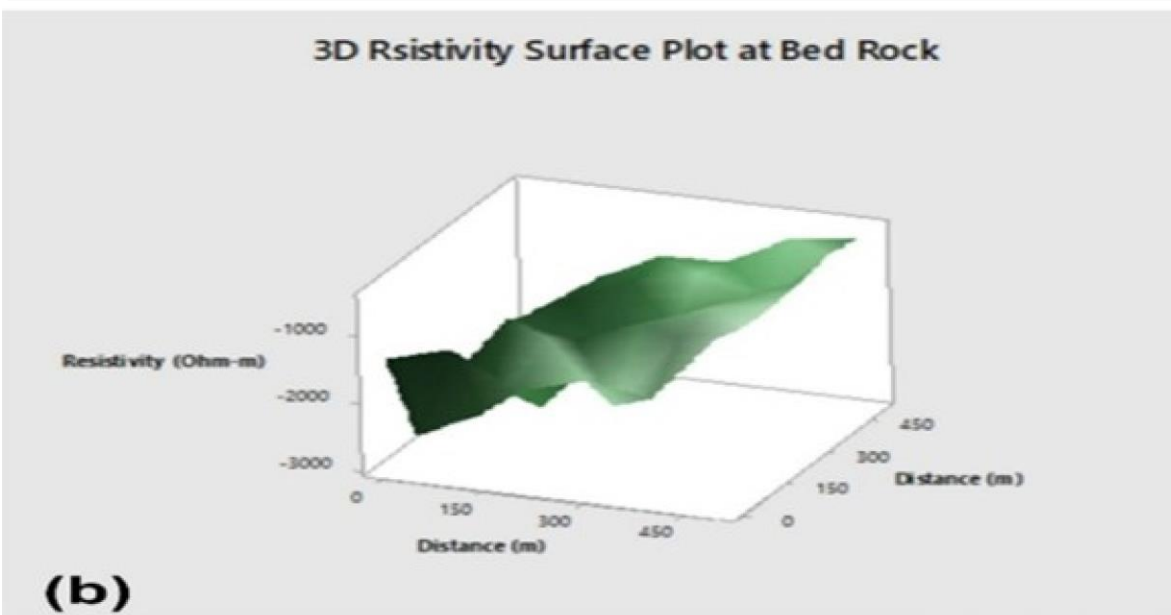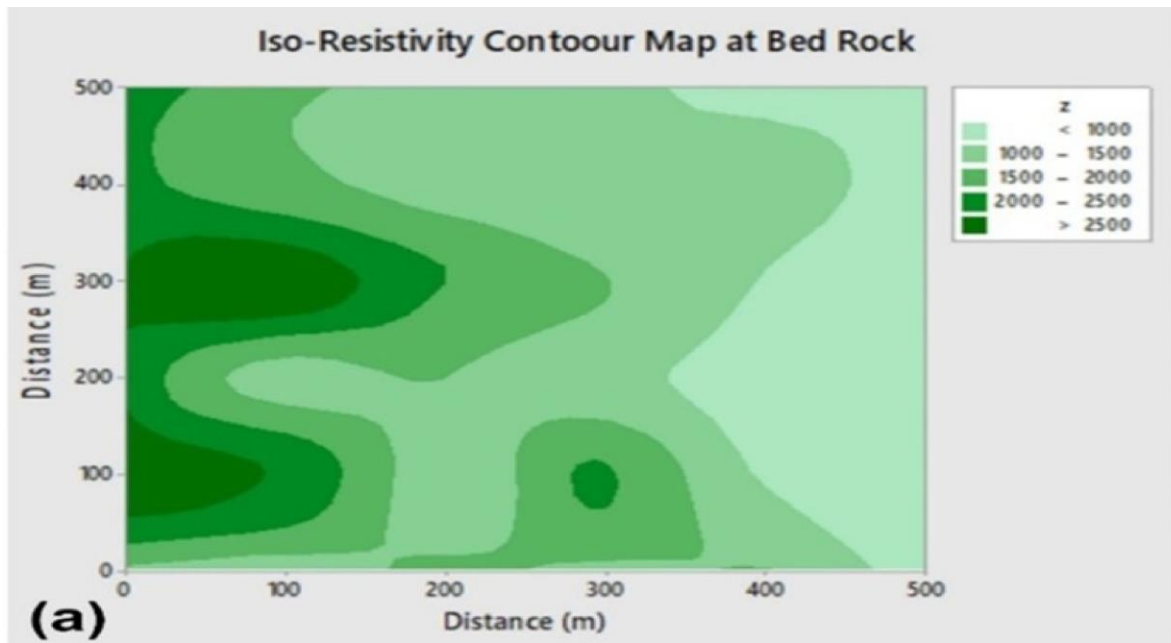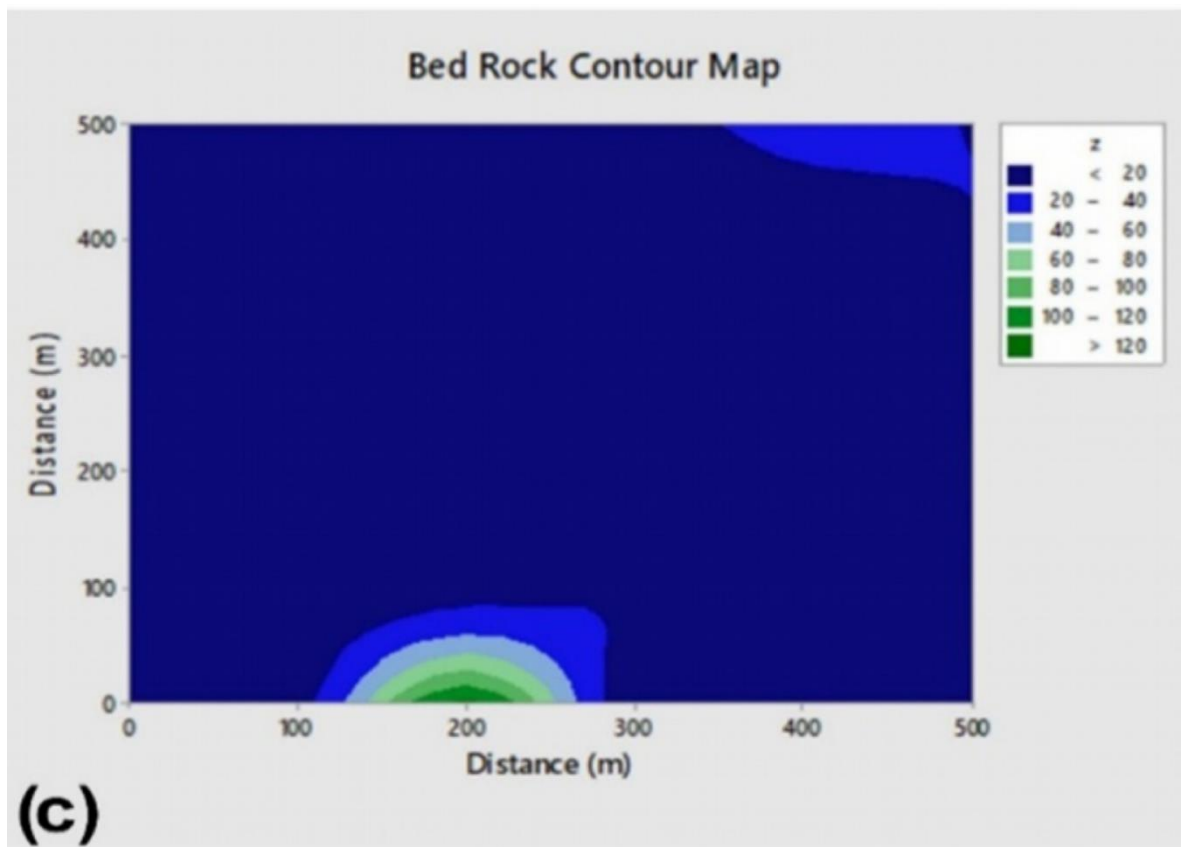
Figure 3.7: Contour map at Bedrock showing; (a) Iso-Resistivity, (b) 3D surface plot at Bedrock, (c) the bedrock depth (thickness).

3.4 Geotechnical Analysis

Table 3.2 shows an overview of the geotechnical properties of soil data samples in the study site, and the results show significant variations in soil properties across the entire sampling depth. The textural characteristics of the analyzed samples proved that the sand fraction ranges from 69% to 81% with a mean-value of 77.8%, gravel ranging from 1% to 2% with approximately 1% mean value, and the silt+clay values also ranging from 18% to 23% with 21.2% mean-value. The percent increase in the sand with depth at topsoil/subsoil soil was generally not well graded with a high content of fine fraction. The relatively high moisture content of 12.3% (A_1, 3m) of the topsoil layer at the same time lower at 9m depth (5.2%, E_1) which are compatible with the high number of fine fractions in the same soil profile. The high moisture absorption at the subsurface leads to a high-water content capacity during the raining season. It ultimately breaks down the grain-to-grain forces that existing in the soil. The site's curvature coefficient (Cc) ranged from 0.198 to 0.243, which resulted in uniformly graded soil. The results also reveal that the underlying strata have low capabilities of shrinkage potential and plasticity that resulted in the highest instability at sub/topsoil. The low number of fine grains in the subsoil layers, which the sand grains would have bonded, indicates a lack of binding materials and, as a result, shows that the underlying soil components are very susceptible to erosion (Öser, 2020). This pattern indicates lowering cohesion and soil cracking resistance. The liquid limit, plastic limit, plasticity index, maximum dry density, and optimum moisture content have average values of 34.92%, 23.31%, 11.61%, 1.86Mg/m^3, and 10.18% respectively. The low value of the liquid limit of the underlying (at E, 9m depth) with strata 32.0% was attributed to low amounts of fine fraction and indicates that the soil can change from one state of consistency to another with minimum change in water content. The low dry density values suggest loose natural deposits and result in a high percentage of voids. The high void ratio of the soils rises with depth and results in high rates of infiltration. High flow velocity, significant seepage pressure, and high inner landslide potential would result from the underlying strata's high void ratio (Okengwo *et al.*, 2015). The attributes support the conclusion of Okengwo *et al.*, (2015) in the creation of a hydraulic gradient that induced water flow through soil strata with a high velocity of the inlet. This implies that soils are not only susceptible to simple dispersal by floodwaters but are also subject to enormous buoyancy. The soil shear strength samples decrease at the various gully locations, with depth, which is why the coherent top/subsoil helps to initiate the gully process by encouraging overland floods that result in the development of rills and landslides (Okengwo *et al.*, 2015).

Table 3.2: The Geotechnical properties of soil types from the study area are summarized.

Parameters	Collection Points																	
Profile	A_1			B_1			C_1			D_1			E_1			F_1		
Depth (m)	50	100	15.0	50	100	15.0	50	100	15.0	50	100	15.0	50	100	150	50	100	150
LL (%)	35.20	35.80	37.00	36.40	33.80	35.20	36.60	34.80	33.50	36.40	34.50	34.50	34.40	35.40	32.00	35.20	34.20	33.70
PL (%)	22.40	23.10	24.40	25.00	23.60	24.20	24.10	23.90	22.30	23.90	21.90	23.50	23.80	24.20	21.80	22.40	21.70	23.40
PI (%)	12.80	12.70	12.60	11.40	10.20	11.00	12.50	10.90	11.20	12.50	12.60	11.00	10.60	11.20	10.20	12.80	12.50	10.30
Gravel (%)	1.00	1.00	1.00	0.00	1.00	1.00	2.00	1.00	0.00	1.00	1.00	1.00	0.00	0.00	2.00	1.00	0.00	1.00
Sand (%)	78.00	79.00	79.00	80.00	76.00	69.00	80.00	76.00	82.0	79.0	78.00	70.00	78.00	81.00	76.00	78.00	80.00	81.00
Silt + Clay (%)	21.0	20.00	20.00	20.00	23.00	20.00	18.00	23.00	18.0	20.0	21.00	19.00	22.00	19.00	22.00	21.00	20.00	18.00
Dry Density (Mg/m^3)	1.82	1.74	1.62	1.72	1.64	1.52	1.54	1.44	1.42	1.82	1.78	1.68	1.78	1.72	1.64	1.56	1.62	1.73
Max. dry density (Mg/m^3)	1.92	1.84	1.84	1.87	1.82	1.87	1.90	1.90	1.87	1.88	1.87	1.85	1.88	1.85	1.78	1.80	1.82	1.92
OMC (%)	11.5	10.4	9.0	15.9	9.0	8.0	11.2	10.0	8.1	11.2	9.8	9.6	11.5	10.0	9.5	10.2	9.8	9.6
MC (%)	12.3	11.8	11.0	12.1	11.0	10.5	10.2	8.2	6.8	8.6	7.2	6.2	8.2	6.0	5.2	9.8	11.1	9.3
CC=. .009(LL-10)	0.227	0.232	0.243	0.238	0.214	0.227	0.239	0.216	0.215	0.238	0.239	0.221	0.220	0.229	0.198	0.227	0.218	0.2138
Shrinkage Potential/ Plasticity	Low	Low	Low	Low	Low	Low	Low	Low	Low	Low	Low	Low	low	low	Low	low	Low	Low

3.5   Conclusion

This study investigated the subsurface situation of the environmental degradation in the Nanka community using soil analyzed results to deduce vertical electrical sounding findings. The geoelectrical results demonstrated that high-resolution VES continuous data is superior to other field methods and traditional surface mapping for complete landslide subsurface monitoring. Volume quantification and differentiation of distinct zones and processes of activity both at the gully rim and within the gully interior are possible with the spatially joined VES survey of the entire form. For this reason, VES is the perfect tool for studying the thickness of the overburden, and it revealed that the western parts of the profile were deeper and influenced by the weathering agents and long-term refuse deposits, which occurred under the influence of water-bearing power.

The eighteen (18) polybag packed samples collected from different marked depths at the dug holes, the liquid limit (LI), plastic limit (PL), plasticity index (PI), maximum dry density, and optimum moisture content have average values of 34.92%, 23.31%, 11.61%, $1.86Mg/m^3$, and 10.18% respectively, while the textural characteristics of the analyzed soil samples proved that the sand mean value is 77.8%, gravel mean value is approximately 1%, and the silt+clay mean value is 21.3%. The lithologies of the soil in the study area are clays, sandstones, alluvium, gravel, natural water (sediments), which the results from the two methods all agreed.

The research area's underlying soil layers are made up of uncompacted sand and a cohesive top/subsoil layer, according to the findings., which was confirmed by Iso-Resistivity Contour Map with 3D thickness for topsoil. The regolith thickness map showed that landslide was active, shallow, material slumps, and runout slides. The cohesiveness of the soil's high void ratio causes high infiltration rates, which leads to high-flow velocity and quickened internal erosion potential. The result also showed that the formation of the landslide into the top red laterite layer of soil tends to be more controlled than a sand cut with no cohesiveness. Landslides are worsened by a variety of variables, including soil properties. A severe landslide is more likely to occur on soil that is dominantly sandy and has a high void-to-density ratio. Once the underlying cohesionless soil with a high void ratio and poor porosity penetrated, the gully formation increases. This is due to the loose soil nature and the inability of the roots of the plant to bind the soil particles together as applicable in the study area.

However, the introduction of protection measures, in particular for humid areas, involves a first understanding of the erosion process and an integrated approach to landscape, among other factors, must be followed in the valley bottoms for integrated subsurface and surface drainage. Enacting essential environmental legislative measures, as well as establishing and empowering an enforcement body, are equally critical.

Bibliography

Abdullahi, M. G., Toriman, M. E., Gasim, M. B. (2015). The application of vertical electrical sounding (VES) for groundwater exploration in Tudun Wada Kano State, Nigeria. *Journal of Geology and Geosciences, 4(*1), 1-3.

Aboh, O. H., Osazuwa, I. D. (2000). Lithological deductions from a regional Geoelectrical Investigations in Kaduna area. *Nigeria Journal of Physics,* 12, 3-4.

Adam, D., Pistrol, J. (2016). Dynamic roller compaction for earthworks and roller-integrated continuous compaction control: State of the art overview and recent developments. *Proceedings, Conferenze di Geotecnica di Torino, XXIV Ciclio,* 1-41.

Adams, M. D. (2016). *Gold ore processing: project development and operations:* Elsevier.

Adelekan, I. O. (2011). Vulnerability assessment of an urban flood in Nigeria: Abeokuta flood 2007. *Natural Hazards, 56*(1), 215-231.

Alimohammadlou, Y., Najafi, A., Yalcin, A. (2013). Landslide process and impacts: A proposed classification method. *Catena, 104*, 219-232.

Anderson, R. S., Anderson, S. P., Tucker, G. E. (2013). Rock damage and regolith transport by frost: An example of climate modulation of the geomorphology of the critical zone. *Earth Surface Processes and Landforms, 38*(3), 299-316.

Andrade, F., Al-Qureshi, H., Hotza, D. (2011). Measuring the plasticity of clays: a review. *Applied Clay Science, 51*(1-2), 1-7.

Aspinall, A., Gaffney, C. (2001). The Schlumberger array—potential and pitfalls in archaeological prospection. *Archaeological Prospection, 8*(3), 199-209.

Boca, G. D., Saraçlı, S. (2019). Environmental education and student's perception, for sustainability. *Sustainability, 11*(6), 1553.

Brantley, S. L., White, A. F. (2009). Approaches to modeling weathered regolith. *Reviews in Mineralogy and Geochemistry, 70*(1), 435-484.

Brooks, A. P. (2003). A conceptual model of geomorphic changes to catchments and river channels in south-eastern Australia since European settlement–causes and implications. *Airs, Waters, Places Transdisciplinary Research in Ecosystem Health*.

Busato, L., Boaga, J., Peruzzo, L., Himi, M., Cola, S., Bersan, S., Cassiani, G. (2016). Combined geophysical surveys for the characterization of a reconstructed river embankment. *Engineering Geology, 211,* 74-84.

Clarke, B. A., Burbank, D. W. (2011). Quantifying bedrock-fracture patterns within the shallow subsurface: Implications for rock mass strength, bedrock landslides, and erodibility. *Journal of Geophysical Research: Earth Surface, 116*(F4).

Contractor, T. (2020). Proctor Soil Compaction Test – Procedures, Tools and Results. Retrieved from https://theconstructor.org/geotechnical/compaction-test-soil-proctors- test.

De Baets, S., Poesen, J., Meersmans, J., Serlet, L. (2011). Cover crops and their erosion-reducing effects during concentrated flow erosion. *Catena, 85*(3), 237-244.

Dimitrova, R. S., Yanful, E. K. (2011). Undrained strength of deposited mine tailings beds: effect of water content, effective stress and time of consolidation. *Geotechnical and Geological Engineering, 29*(5), 935-951.

DiPietro, J. A. (2012). Landscape evolution in the United States: A*n introduction to the geography, geology, and natural history:* Newnes.

DiPietro, J. A. (2018). Geology and Landscape Evolution: *General Principles Applied to the United States:* Elsevier.

Dixon, J. C. (2018). Stone pavements, lag deposits, and contemporary landscape evolution. In *Dynamic Mars* (pp. 387-410): Elsevier.

Egwuonwu, G. N. (2012). Application of Geophysical Imaging in Investigation of Structural Failure of Buildings: Case Study of Three Building Sites in Zaria Area, North-western Nigeria. *Pacific Journal of Science and Technology, 13*(1), 580-589.

Ehirm, C. N., Ebeniro, J. O., Olanegan, O. P. (2009). A combined 2-D resistivity imaging and vertical electrical sounding around solid waste landfill in Port Harcourt municipality. *The pacific journal of science and technology, 10*(2), 604-613.

Ekwenye, O., Nichols, G., Collinson, M., Nwajide, C., Obi, G. (2014). A paleogeographic model for the sandstone members of the Imo Shale, south-eastern Nigeria. *Journal of African Earth Sciences, 96,* 190-211.

Giardino, J. R., Houser, C. (2015). *Principles and dynamics of the critical zone*: Elsevier.

Gnyawali, K. R., Zhang, Y., Wang, G., Miao, L., Pradhan, A. M. S., Adhikari, B. R., Xiao, L. (2020). Mapping the susceptibility of rainfall and earthquake triggered landslides along China–Nepal highways. *Bulletin of Engineering Geology and the Environment, 79*(2), 587-601.

Goodfellow, B. W., Chadwick, O. A., Hilley, G. E. (2014). Depth and character of rock weathering across a basaltic-hosted climosequence on Hawaii. *Earth Surface Processes and Landforms, 39*(3), 381-398.

Hayden, B. (2017). Bedrock features: An overview. *Quaternary International, 439,* 108-111.

Huang, F., Lu, H. (2014). Experiment Study on the Atterberg Limits of Clay Contaminated by Oil. *Electronic Journal of Geotechnical Engineering (EJGE), 19,* 3037-3046.

Igwe, O. (2015). The geotechnical characteristics of landslides on the sedimentary and metamorphic terrains of South-East Nigeria, West Africa. *Geo-environmental Disasters, 2*(1), 1.

Ionita, I., Fullen, M. A., Zgłobicki, W., Poesen, J. (2015). Gully erosion as a natural and human-induced hazard. In: Springer.

Kabala, C., Zapart, J. (2012). Initial soil development and carbon accumulation on moraines of the rapidly retreating Werenskiold Glacier, SW Spitsbergen, Svalbard archipelago. *Geoderma, 175*, 9-20.

Layade, G., Adegoke, J., Oladewa, F. (2017). Hydrogeophysical Investigation for groundwater development at Gbongudu Area, Akobo Ojurin, Ibadan, Southwestern Nigeria. *Journal of Applied Sciences and Environmental Management, 21*(3), 527-535.

Lobkovsky, A. E., Jensen, B., Kudrolli, A., Rothman, D. H. (2004). Threshold phenomena in erosion driven by subsurface flow. *Journal of Geophysical Research: Earth Surface, 109*(F4).

Lu, D., Moran, E., Mausel, P. (2002). Linking Amazonian secondary succession forest growth to soil properties. *Land Degradation & Development, 13*(4), 331-343.

Morrison, H., Gasperikova, E. (2012). DC resistivity and IP field systems, data processing and interpretation. *Berkley course in applied geophysics–online notes.*

Nkemakonam Ukatu, Mozie, A. (2019). *Factors of Gully Expansion in Nanka Gully Site: Orumba-North Local Government Area (L. G. A.) Anambra State. Factors of Gully Expansion in Nanka Gully Site:* Orumba-North. (Bachelor of Science), University of Nigeria, Research gate. Retrieved from www.researchgate.net.

Obaje, N., Amadi, A., Aweda, A., Umar, U., Shuaibu, I. (2018). Processing Nigerian coal deposits for energy source. *Environmental Earth Sciences, 77*(5), 176.

Okengwo, O., Okeke, O., Okereke, C., Paschal, A. (2015). Geological and geotechnical studies of gully erosion at Ekwulobia, Oko and Nanka Towns, South-eastern Nigeria. *Electronic Journal of Geotechnical Engineering (EJGE), 20*(1), 113-122.

Okonkwo, C., Ganev, V. (2012). U-Pb Geochronology of the Jebba granitic gneiss and its implications for the paleoproterozoic evolution of Jebba area, Southwestern Nigeria.

Okunlola, I., Abdulfatai, I., Kolawole, L., Amadi, A. (2014). Geological and geotechnical investigation of gully erosion along River Bosso, Minna, north central Nigeria. *Journal of Geosciences, 2*(2), 50-56.

Onweremadu, E. (2007). Pedology of near gully sites and its implications on the erodibility of soils in central South-Eastern Nigeria. *Res. J. Environ. Sci, 1*(2), 71-76.

Öser, C. (2020). Determining the plasticity properties of high plastic clays: a new empirical approach. *Arabian Journal of Geosciences, 13,* 394.

Otti, V., Aginam, H., Nwolum, F., Ogbuagu, F. (2014). Application of groyne as a sustainable solution to Agulu-Nanka erosion problem. *Civil and Environmental Research, 6*(12), 73-80.

Oyinloye, A. O. (2011). *Geology and Geotectonic setting of the basement complex rocks in Southwestern Nigeria: Implications on provenance and evolution* (Vol. 5): chapter.

Patrick, N., Fadele, S., Adegoke, I. (2013). Stratigraphic report of the Middle Benue trough, Nigeria: Insights from petrographic and structural evaluation of Abuni and environs part of Late Albian–Cenomanian Awe and Keana formations. *The Pacific Journal of Science and Technology, 14*(1), 557-570.

Penno, C. R. D. (2012). How to Assess and Treat Acute-Onset Non–Weight-Bearing Lameness in an Ambulatory Emergency Setting. *AAEP Proceedings, Vol. 58* 201-209.

Peters, D. (1957). Water uptake of corn roots as influenced by soil moisture content and soil moisture tension. *Soil Science Society of America Journal, 21*(5), 481-484.

Portenga, E. W., Bierman, P. R., Rizzo, D. M., Rood, D. H. (2013). Low rates of bedrock outcrop erosion in the central Appalachian Mountains inferred from in situ 10Be. *GSA Bulletin, 125*(1-2), 201-215.

Robertson, P. K. (2009). Interpretation of cone penetration tests—a unified approach. *Canadian geotechnical journal, 46*(11), 1337-1355.

Shobe, C. M., Hancock, G. S., Eppes, M. C., Small, E. E. (2017). Field evidence for the influence of weathering on rock erodibility and channel form in bedrock rivers. *Earth Surface Processes and Landforms, 42*(13), 1997-2012.

Smithson, P., Addison, K., Atkinson, K. (2013). *Fundamentals of the physical environment:* Routledge.

Sommer, M., Gerke, H., Deumlich, D. (2008). Modelling soil landscape genesis a "time split" approach for hummocky agricultural landscapes. *Geoderma, 145*(3-4), 480-493.

Sonel, A. (2009). Environmental and Social Management Plan. *Kribi Power Project. Scott Wilson Ltd. Douala. Cameroon.*

Spangler, M. G., Handy, R. L. (1973). Soil engineering. Retrieved from Sridharan, A., & Sivapullaiah, P. V. (2005). Mini compaction test apparatus for fine grained soils. *Geotechnical Testing Journal, 28*(3), 240-246.

Stoops, G., Marcelino, V., Mees, F. (2018). *Interpretation of micromorphological features of soils and regoliths:* Elsevier.

Telford, W. M., Telford, W., Geldart, L., Sheriff, R. E., Sheriff, R. (1990). *Applied geophysics:* Cambridge university press.

Tian, Y., Owen, L. A., Xu, C., Ma, S., Li, K., Xu, X., . . . Wang, S. (2020). Landslide development within 3 years after the 2015 M w 7.8 Gorkha earthquake, Nepal. *Landslides*, 1-17.

Umar, M., Ahmed, A., Balarabe, B., Adamu, A. (2020). Electrical Resistivity Investigation of Sub-surface Topography of Rafin-Bareda as a tool for groundwater exploration in Dutsen-wai, Nigeria.

Wilson, G. (2011). Understanding soil-pipe flow and its role in ephemeral gully erosion. *Hydrological processes, 25*(15), 2354-2364.

Zohdy, A. A. R., D. B. Jackson. (1989). Schlumberger Sounding data processing and Interpretation (Version 1.88) *U.S. Geological Survey, Denver Co.*

CHAPTER 4: THE APPLICATION OF THE GEOPHYSICAL METHODS IN THE STUDY OF SLOPE INSTABILITY AT FOUR MAJOR LANDSLIDES IN SOUTH-EASTERN NIGERIA

School of Chemistry and Physics, College of Agriculture, Engineering, and Science,
University of KwaZulu-Natal, Pietermaritzburg Campus, Private Bag X01, Scottsville 3209,
South Africa.

THE APPLICATION OF THE GEOPHYSICAL METHODS IN THE STUDY OF SLOPE INSTABILITY AT FOUR MAJOR LANDSLIDES IN SOUTH-EASTERN NIGERIA

Chikwelu Edward Emenike and Naven Chetty

School of Chemistry and Physics, College of Agriculture, Engineering, and Science, University of KwaZulu-Natal, Pietermaritzburg Campus, Private Bag X01, Scottsville 3209, South Africa.

*Corresponding Author: chettyN3@ukzn.ac.za

Abstract

Slope failure is a common incident in South-Eastern Nigeria because it occurs in almost every part of the zone. Despite all the remedial measures in place, it still poses serious challenges, especially during the rainy season. This research studied the slope subsurface in the four high potential areas devastated by a landslide to detect any failure planes using geophysical methods [2D resistivity and induced polarization (IP)]. The results revealed that features that may lead to slope failure are present such as; boulders and weak water-saturation zone. The influence of years of preventative measures at the erosion sites may be responsible for high resistivity values found in some locations and the aquifer system with high-quality clay composition layers. These methods proved successful in slope failure study and for distinguishing the water-bearing unit. For the prevention of further damages, afforestation, and other measures must be in place.

Keywords: 2D-resistivity, slope failure, induced polarization, groundwater, environmental degradation.

4.1 Introduction

Some examples of slope failure include debris and soil flow, block collapse, rockfall, and landslides (MIM *et al.*, 2017). This can be classified as engineering and geo-environmental problems. Slope instability is a multi-faceted phenomenon that encompasses not just landslides but also more subtle processes like soil creep (Glade & Crozier, 2005; Soeters & Van Westen, 1996). For the slope to fail, there is a process involving the deformation of the rock mass, the accumulation of stress, and the changes of mineralogy (Eberhardt et al., 2004). As a result of body movement, the slope failure phenomena only occur at the last stage, where it is directly associated with the mechanical and geological conditions of the rock mass (Agliardi *et al.*, 2001; Gautam & Biswas, 2016). In short, due to complete compliance with the unstable state, the slope becomes unstable as the rock mass loses mechanical stability (Bérest & Brouard, 2003; Tse & Rice, 1986). Apart from that, the increased sensitivity of the rock mass to any external force also triggered the situation of slope failure (Ivars *et al.*, 2011). That may damage or destroy peoples' accommodation and infrastructures such as electric facilities and pipelines situated within the borders of a gully or along a landslide path (Schuster & Highland, 2001). Slope movements must not cover a vast space to be damaging (Wieczorek & Snyder, 2009). Downhill creeps or early-stage debris flows can cause substantial structural damage to critical infrastructures such as dams and buildings, potentially contributing to economic harm and loss of life (Masannat, 2014; Singh, 2013). In comparison, earth movements initially believed to be induced by landslides, may be dictated to be the result of other geotechnical processes such as fill settling, the heaving of expansive soil or rock, or hydro-compaction of collapsible soil after wetting (Bell, 2011; Bell, Cripps, & Culshaw, 1986; Castleton & McKean, 2009).

ERT is a geo-planned field technique that computes the subsurface appropriation of electrical resistivity from a defined number of resistivity measurements produced using electrodes put in a subjective geometric pattern (Salom, 2017). For in-situ applications, ERT utilizes electrodes terminals on the ground surface or in boreholes (Rucker *et al.*, 2014). ERT may likewise be used along these lines for imaging biomedical targets, rock or soil centre, and block structures (Joralemon, 2017). The ERT technique has contributed positively in the areas of hydrogeology, soil science, oil exploration, designed geoengineering survey, and glaciology (Bailey & Stevenson, 2007; Reynolds, 2011). Improvements in instrumentation and data inversion have prompted uses of 2D imaging of time-dependent evaluations and, all the more as of late, expansions to consolidate induced polarization impacts (Capozzoli *et al.*, 2019; Everett, 2012; Gautam & Biswas, 2016; Hahn & Omenetto, 2012; Loke, 2000; M. H. Loke, 2004; MIM *et al.*,

2017). Moreover, ordinary DC resistivity sounding and profiling have effectively promoted resistance re-examination in a weak appreciation of spatial scope (Beckley, 2002; Gautam & Biswas, 2016). The use of microcomputers has made it possible to overcome the deficiency in the multi-electrode resistivity technique (Loke *et al.*, 2013; Perrone *et al.*, 2014).

In general, induced polarization measurements and resistivity measurements are complementary (Doetsh *et al.*, 2015; Schön, 2015). Induced polarization measurements are sensitive to adsorption/desorption processes in the electrical double layer, whereas resistivity measurements are most sensitive to the water phase information (Karaoulis *et al.*, 2011; Revil & Skold, 2011). The resistivity and chargeability data are impacted by geoelectric factors when obtaining subsurface resistivity and chargeability distributions remotely using surface electromagnetic (EM) methods (Ahzegbobor *et al.*, 2014; Zhdanov, 2018). Induced polarization theoretically can be represented in the frequency domain as phase lag measured at a different frequency than the exciting electrical current (I) and realized with the same equipment used for DC resistivity (Schön, 2015; Binley & Kemna, 2005; Taleski & Velevski, 2019). In practice, the impedance (Z) meter requires a high resolution on the phase (0.1 mrad) and few equipment have this phase resolution (Cassiani, 2009; Frangos, 1990; Kemna *et al.*, 2012).

This research aimed to identify lithology, structural deformations, and to differentiate clayey zones from water-saturated zones with almost the same resistivity. The second aim was to obtain a groundwater potential mechanism based on the distribution of resistivities using combined geophysical methods (2D ERT and IP) that leads to the failure of slopes.

4.1.1 Groundwater flow system in South-eastern Nigeria

In south-eastern Nigeria, areas of local, intermediate, and regional groundwater flow systems corresponding to three distinct basin hydraulic systems, i.e., the upper system with hydrostatic forming pressures, the middle system where the pressure is only moderately higher than the hydrostatic, and the relatively deep system of abnormally high forming pressures (Birkholzer *et al.*, 2009; Onyekuru *et al.*, 2010). The regional flow systems empty into the Niger, Anambra, and Cross River rivers, while the intermediate flow systems empty into their minor tributaries (Amangabara, 2015; Onyekuru *et al.*, 2010). Minor and usually seasonal streams are associated with local groundwater flow systems (Alley *et al.*, 2002). Local relief is negligible toward the centre of the basin and coastal areas; thus, regional flow systems dominate these areas (Michael & Voss, 2009; Onyekuru *et al.*, 2010). The fluid potential in the middle and upper hydro-

stratigraphic units circulation shown as the hydraulic heads and fluid energies is at the peak at the eastern edge of the basin where the major aquifers of the unit are exposed (Walvoord *et al.*, 2012), and very low at the centre of the basin to the southwestern parts where the confined aquifer is present (Goutaland *et al.*, 2008).

According to Ao *et al.*, (2015), Anambra Basin is one of the most economically strategic watersheds in South-Eastern Nigeria and occupies an area of about 95,000km^2. Not only does it have abundant water resources, but it also has oil and gas deposits potential (Abubakar, 2014; Ogala, 2011).

4.1.2 The geographical location and geology of the study area

The study areas are located geographically at latitudes 6º 10^1 to 6º 05^{1}N and longitudes 7º 00^1 to 7º 10^{1}E, in South-Eastern Nigeria. The western flank of the Anambra Basin covers the study areas as shown in Figure 4.1. The Eocene Nanka, Oligocene-Miocene Ogwashi, and Oligocene Benin formations are the three formations that underlain the geology of the areas (Egbueri & Igwe, 2020). The three formations are lithologically composed of sands interbedded with thin layers of mud-rocks and ironstones (Egbueri & Igwe, 2020; Nwajide, 2013). The formations are generally widespread in Southern Nigeria and are extremely weak and movable, according to researches (Chikwelu & Ogbuagu, 2014; Egbueri et al., 2017). Regardless of age, all of the soils under the research area are mainly composed of loose and weakly consolidated fine-grained sand components with minimal clay content and little or no coarse-grained aggregates (Egbueri & Igwe, 2020; Igwe, 2012; Igwe & Egbueri, 2018). The humid tropical rainforest belt of Nigeria housed the study area, with an average annual rainfall of 1800mm (Okengwo *et al.*, 2015). It also had an uneven topography, several surface water networks, and a humid tropical rainforest belt, despite the loss of the primary forest due to forest fires, urban growth, roadway renovation, indiscriminate farming practices, and other forms of man-induced activities (Egbueri & Igwe, 2020; Nnadi *et al.*, 2019).
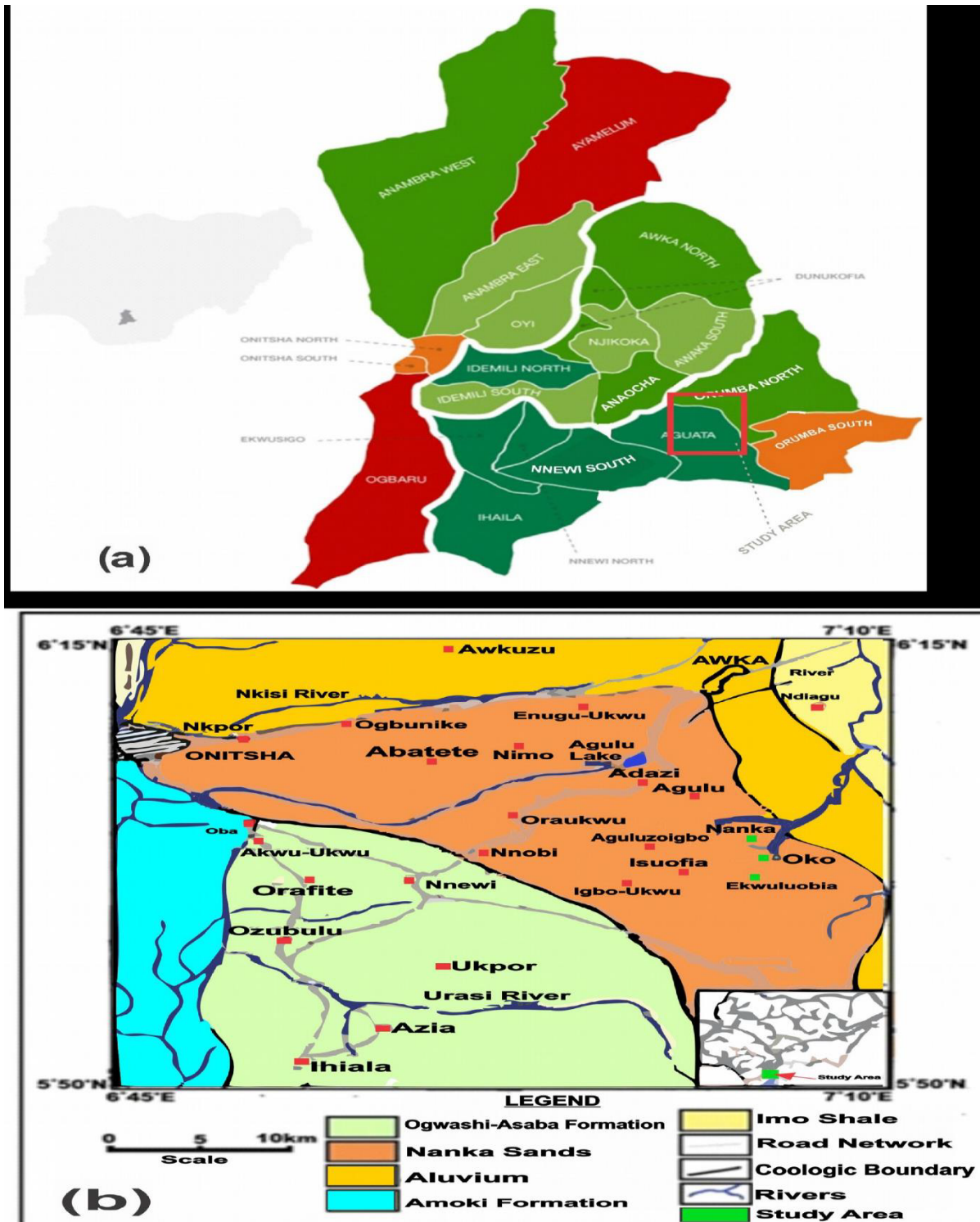
Figure 4.1: (a) Anambra State map showing study area, (b) Geological map of the study area.

4.2 Methodology

4.2.1 Theory electrical resistivity method.

Resistance (in Ohm) is a resistance measurement of a given size of a specific material to electrical conductivity (Binley & Kemna, 2005; Doetsch *et al.*, 2015; Zhdanov, 2018). In a resistance conducting cylinder '∂R', length '∂L', and cross-sectional area '∂A' as shown in Figure 4.2, the resistivity 'ρ' is given as the most variable physical properties. Most minerals-forming rocks are insulators, and electrical current 'I' is carried through them mostly by ions in pore fluids. Thus, the majority of rocks carry electricity by electrolytic rather than electrical processes (Kearey *et al.*, 2002).

As in Figure 4.2, a current 'I' was passed through the cylinder, resulting in a potential drop '$-\delta V$' between the ends of the element.

Ohm's law state that;

$$\rho = \frac{\partial R \partial A}{\partial L} \qquad\qquad 4.1$$

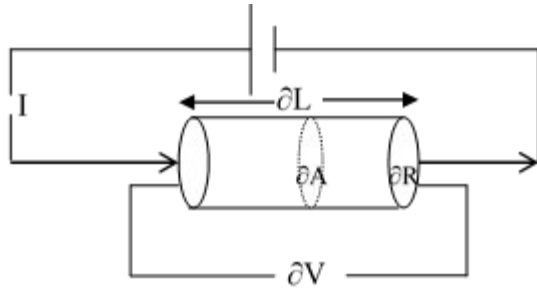Ohm-meter (Ω-m) is the SI unit of Resistivity.

Figure 4.2: Conducting a cylinder of resistance ∂R, length ∂L, and cross-sectional area ∂A

$$\partial V = \partial R I \qquad\qquad 4.2$$

From equation (4.1), we have that

$$\frac{\partial V}{\partial L} = \frac{\rho I}{\partial A} \qquad\qquad 4.3$$

Consider a single current I electrode on the surface of a medium of uniform resistivity ρ as shown in Figure 4.3 below.
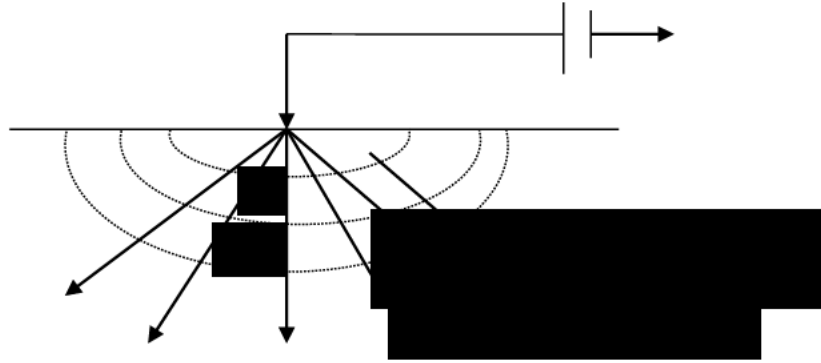

Figure 4.3: Current flow through a single surface electrode

The Figure 4.3 shows the current flows away radially from the main electrode so that the current circulation is uniform over the source-centric hemispheric shells. Current density i, from the source with distance r, is given as:

$$i = \frac{I}{2\pi r^2} \qquad\qquad 4.4$$

From eq. (4.3), the potential gradient associated with this current density is:

$$\frac{\partial V}{\partial r} = -\rho i = -\frac{\rho I}{2\pi r^2} \qquad\qquad 4.5$$

Therefore, V at distance r is given by

$$V_r = \int \partial V = -\int \frac{\rho I \delta r}{2\pi r^2} = \frac{\rho I}{2\pi r} \qquad\qquad 4.6$$

The constant of integration is zero, since $V_r = 0$ when r→∞. The calculation of the potential at any location or below the surface of a homogeneous half-space using Eq. (4.6).

Similarly, consider the following scenario, the current drain is a fixed distance from the source, as illustrated in Figure 4.4. $V_C = V_A + V_B$ gives the potential V_C at an internal electrode C.

From equation 4.6

$$V_c = \frac{\rho I}{2\pi}\left(\frac{1}{r_A} - \frac{1}{r_B}\right),$$ 4.7

Similarly

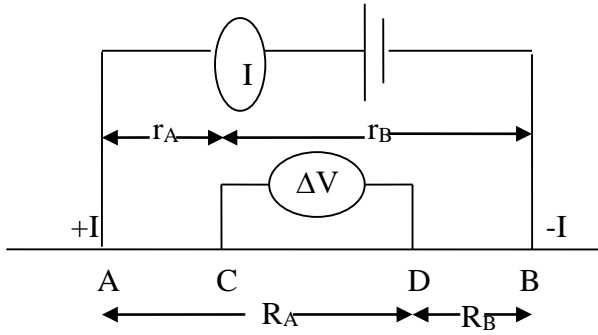$$V_D = \frac{\rho I}{2\pi}\left(\frac{1}{R_A} - \frac{1}{R_B}\right),$$ 4.8

Figure 4.4: Generalized form of the electrode configuration used in resistivity measurements

Because absolute potentials are difficult to measure, the potential difference ΔV across electrodes C and D is calculated as follows:

$$\Delta V = V_c - V_D = \frac{\rho I}{2\pi}\left\{\left(\frac{1}{r_A} - \frac{1}{r_B}\right) - \left(\frac{1}{R_A} - \frac{1}{R_B}\right)\right\},$$

Therefore:

$$\rho = \frac{2\pi \Delta V}{I\left\{\left(\frac{1}{r_A} - \frac{1}{r_B}\right) - \left(\frac{1}{R_A} - \frac{1}{R_B}\right)\right\}}$$ 4.9

When the field of study is homogeneous, the resistivity ρ calculated by eq. (4.9) is constant and not depending on the electrode spacing and surface position. The resistivity will change with the relative positions of the electrodes if the subsurface is uniformly maintained regardless of the variables (Philip *et al.*, 2014; Onugba & Yaya, 2008). The calculated value is called apparent resistivity 'ρa' and is a function of inhomogeneity body. Eq. (4.9) is the basic equation for calculating 'ρa' for any electrode array. Assuming that the constant term in bracket is K, eq. (4.9) becomes:

$$\rho = \frac{2\pi \Delta V}{I} K.$$ 4.10

The geometric factor is free of the field electrode arrangement used in the study. The change in the value of resistivity 'ρ' with electrode spacing makes it possible to determine the variation of resistivity with depth (Campos & Pérez, 1989; Onugba & Yaya, 2008). As a result, apparent resistivity is the resistivity that the earth would have if it was homogenous (Samouëlian *et al.*, 2005). Because it does not measure average resistivity, it might be lower than the lowest and higher than the highest within the subsurface to which it relates (Besson *et al.*, 2004).

4.2.2 Electrode configuration and choice of field procedure

The general resistivity formula, measured by four electrodes, is simple for some geometry of current and potential electrodes. The most commonly used configurations are Wenner array, Schlumberger array, and dipole-dipole array, but dipole-dipole used for this research due to its relatively high lateral and vertical resolution (Coşkun, 2012). Employ mostly in the electrical survey method for landslide investigation and slope failure remedially (Friedel *et al.*, 2006; Rezaei *et al.*, 2019). This array also has been, and is still, widely used in resistivity and IP surveys because of the low electromagnetic (EM) coupling between the current and potential circuits (Schmutz., 2014; Van Schoor, 2002; Ward, 1988). With proper geophysical equipment and survey techniques, this array has been successfully used in many areas to determine the cause of the structural failures, such as cavities, and the horizontal resolution of this array is advantageous.

In the dipole-dipole configuration as shown in Figure 4.5, the spacing of the electrodes in each pair is a, while the distance between their midpoints is L. This implies that: $r_1 = r_4 = L$, $r_3 = L-a$ and $r_2 = L+a$.

The measured resistivity is

$$\rho = \frac{\pi \Delta V}{I}\left(\frac{L(L^2-a^2)}{a^2}\right), \qquad\qquad 4.11$$

We have from (4.11)

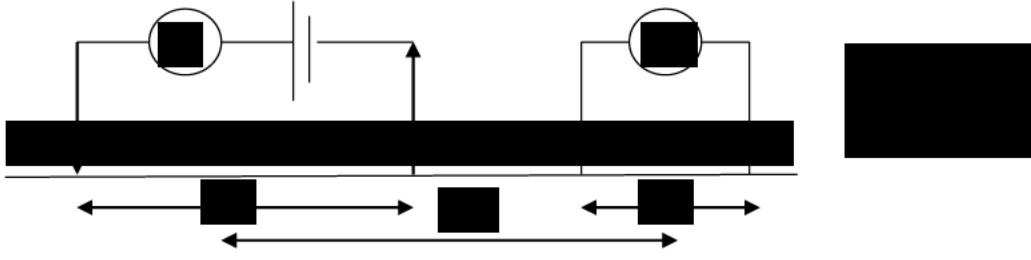$$\rho = \pi R \left(\frac{L(L^2-a^2)}{a^2}\right). \qquad\qquad 4.12$$

Figure 4.5: Dipole-dipole configuration of current and potential electrodes (Ph Kearey et al., 2002; Telford et al., 1990).

4.2.3 The Mathematical Symbols of the Induced polarization (IP)

The value of a residual voltage amplitude divided by the direct current potential value immediately after the current cut-off will give you the chargeability in milliseconds (mV / V) (Gautam & Biswas, 2016). The chargeability can be defined in the time domain as

$$m_t = 1870 \left(\frac{\int_{0.15}^{1.1} Vsdt}{V_{DC}} \right). \qquad\qquad 4.13$$

The original and perturbed conductivities are the models using in calculating the apparent IP, and they are as follows:

$$m_t = [\phi(\sigma_{IP}) - \phi(\sigma_{DC})]/\phi(\sigma_{DC}), \qquad\qquad 4.14$$

$$\sigma_{IP} = (1 - m)\sigma_{DC}, \qquad\qquad 4.15$$

where σDC is the conductivity measured through the normal resistivity survey, and the effect of the chargeability is to decrease the effective conductivity to σIP and ϕ is the calculated potential. It depends on electrical ground charging to detect materials that have been able to store electrical charges for some time. The chargeability is the ability of the field material (measured in mV/V) and, estimated by measuring the voltage decay at a point when the current is off, divided by the measured potential (Vo), measured during the current injection (Martínez *et al.*, 2019; Zhdanov, 2017).

4.3 Data Collection

The 2D Geoelectric Resistivity Imaging used was similar to combining vertical electrical sounding technique with electrical profiling (Ahzegbobor, 2010; Andrews *et al.*, 2013). It

involves the resistivity computation from electrodes placed along a line using dipole-dipole array separations. This field survey configuration procedure is repeated many times by combinations of current and potential electrode profile positions. In this research, a 2D resistivity survey was carried out using 42 electrodes connected to multi-core cables, and the area covered was extended along the survey line using the roll-along technique (Bernstone *et al.*, 2000; Dahlin *et al.*, 2002).

We collected resistivity-IP data at four landslide sites in a straight profile through a Multi-electrode resistivity imaging system using ABEM Terrameter SAS 4000 and ABEM LUND ES464 electrode selector system.

4.4 Data Interpretation

The 2D resistivity and IP chargeability data collected from the survey field were in the file format of .s4k. Using the Terrameter utility software, the data were converted to interpretable format (.dat). Then, using the RES2DINV inversion algorithm, data sets for each traversal were inverted simultaneously (Aizebeokhai *et al.*, 2016; Loke & Barker, 1996). The RES2DINV program applies a non-linear optimization technique that automatically calculates the inverse model of the 2D resistivity and chargeability distribution of the subsurface for the apparent resistivity and chargeability (Loke, 2004; Loke & Barker, 1996). The software subdivides the subsurface layers into several quadrilateral blocks based on the distribution and density of the observed data as well as the parameters of the survey (electrode arrangement, electrode spacing and position, and data level) (Loke *et al.*, 2013).

4.5 Results and Discussion

For this study, eight profiles were acquired, two profiles each for a study site, one for 2D resistivity, and the other for IP-chargeability as shown in Table 4.1. Each profile consisted of 48 electrodes, forming a mesh, with an electrodes' spacing of 5.0 m, and 31.1 m as the maximum investigation depth for all profiles. The chosen electrode separation is a compromise between resolution and depth of investigation.

Table 4.1: Characteristics of the acquired ERT and IP profiles.

Site Name and Number	Profile Number	Coordinates		Location	Profile length (m)	Electrode Spacing (m)	Number of Electrodes	Survey Method	Direction
Ekwulobia (Site 1)	ER Line 1	$06^0 05^1$N	$07^0 03^1$E	Km 12, Aguata-Ekwulobia Road	295	5	48	Dipole-dipole	NW-SE
	IP line 1				295	5	48		
Oko (Site 2)	ER line 2	$06^0 04^1$N	$07^0 09^1$E	Km 10, Ekwulobia-Oko Road	178	5	48	Dipole-dipole	NW-SE
	IP line 2				178	5	48		
Ezioko (Site 3)	ER line 3	$06^0 05^1$N	$07^0 10^1$E	Km 10, Ekwulobia-Nanka Road	156	5	48	Dipole-dipole	E-W
	IP line 3				156	5	48		
Ubahu Nanka (Site 4)	ER line 4	$06^0 05^1$N	$07^0 08^1$E	Km 16, Ekwulobia-Nanka Road	195	5	48	Dipole-dipole	E-W
	IP line 4				195	5	48		

4.5.1 Ekwulobia Site 1 (ER and IP) line 1:

First, the analysed resistivity and chargeability values measured in the field have calculated RMS errors of 41.4%, acquired in NW-SE direction, Km 12, Aguata-Ekwulobia Road.

The analysis of the ERT profile (ER line 1 in Figure 4.6a) makes it possible to deduce the geological model of the basin in Figure 4.6b. The values close to the surface generally present lower resistivities, ranging from 5.71 to 85.5 ohm-m. This group interpreted as the detrital sedimentary weathered zone, made up of clayey conglomerates or silty clay deposit, immersed in clay facies (Quaternary colluvium). After this structure comes geological structure with an intermediate resistivity between 287 to 1282 ohm-m. It could be interpreted as clastic fine to medium sand and alluvium (see Figure 4.6b). The highly clayed content and aquifer salinization might lead to low resistivity in the centre of the ER line 1 section, 10 m depth. However, this contrast in resistivity values at the surface and the bedrock is abrupt. The Palaeozoic bedrock is composed of coarse sand plus gravel in this sector, which present very high resistivities, over 6494 ohm-m. These high resistivities formed a gravel boulder at the topsoil. Important variations in thickness (40 to 90m) of this sedimentary cover in adjacent sectors reveal the complex shape of the basin and the presence of fractures.

In IP line 1 shown in Figure 4.6c, it can be observed that chargeability values increased with clay/ water content making the salinity composition of the electrolyte influence the occurrence of maximum chargeability values. In this research work, the results from the Induced polarization (chargeability) did not contribute so much to the interpretation of the geologic/ lithology features. However, when the normalized chargeability results were analysed, there is a difference between the layers with high clay content and the coarse material, which showed that the normalized chargeability is dependent on the mineralogy of clay and its contents. IP line 1 model indicates two major chargeability range, the most obvious one was the low chargeability value between 4.01 to 13.6 mV/V, located at the saturated zone based on the resistivity values at depth 3.88 to 13.4 m, interpreted as the clayey water-saturated zone due to low resistivity and chargeability value. At a depth of 14.8 to 22.1 m, the saturated zone has a high chargeability value of 48.9 to 176mV/V. Thus, this area was identified as the bedrock.
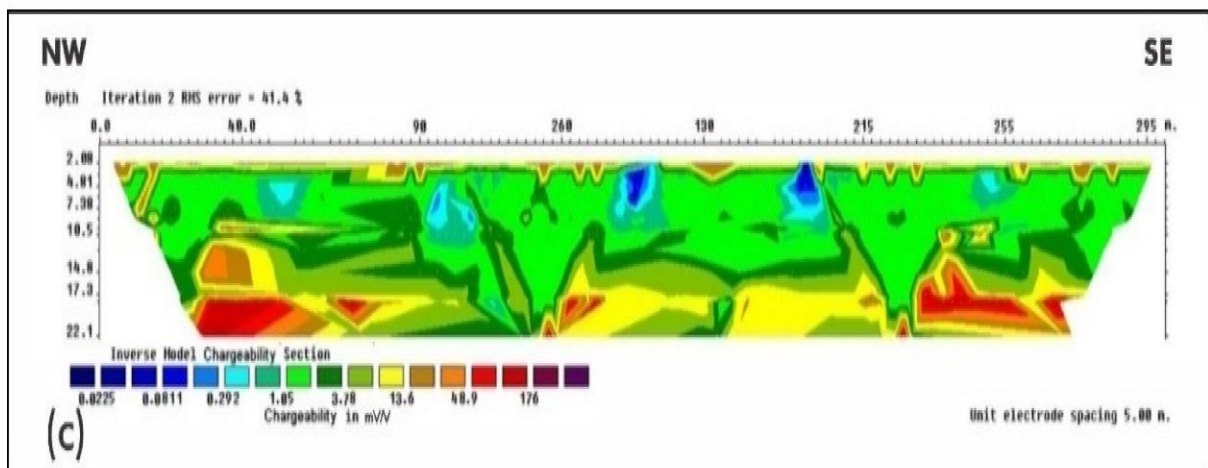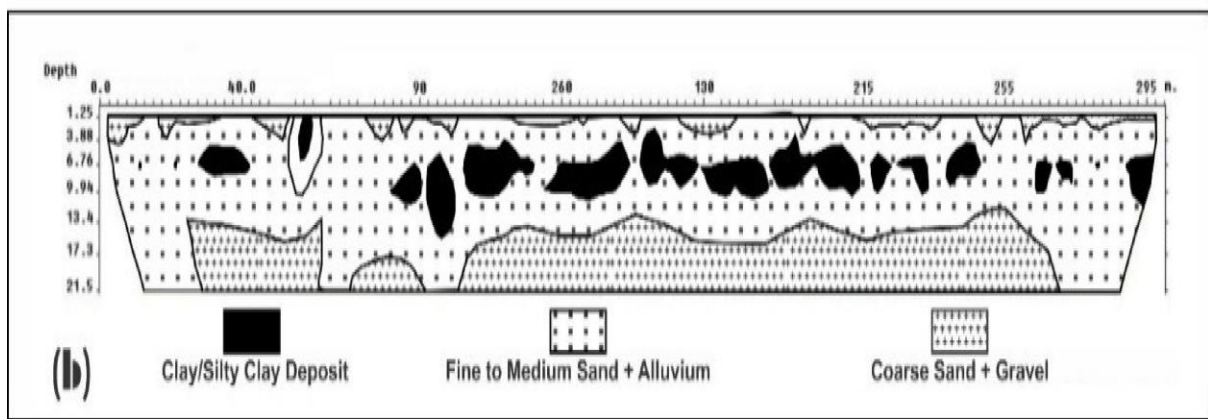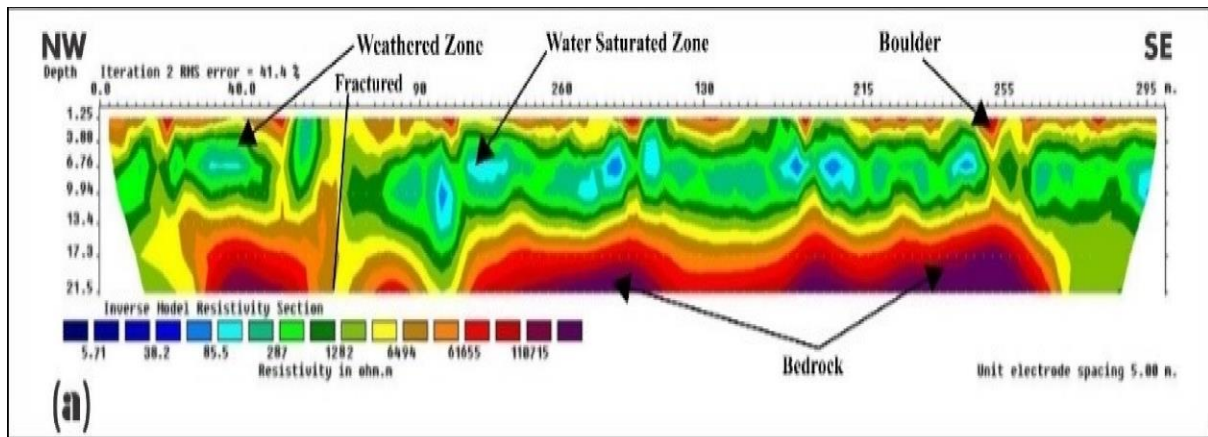
Figure 4.6: (a) 2D inverse model resistivity, (b) Geologic cross-section interpreted from the resistivity model, and (c) IP-chargeability for Ekwulobia (site 1).

4.5.2 Oko Site 2 (ER and IP) line 2:

From line 2, the analysed field values of the resistivity and chargeability measured in the field have calculated RMS errors is 50.8 %, acquired in the direction of NW-SE, Km 10, Ekwulobia-Oko Road.

This line has analysed resistivity reading ranging from 2.67 ohm-m to more than 22925 ohm-m (see Figure 4.7a) with the extracted geological model of the basin in Figure 4.7b. The highest range of resistivity values is between 7329 ohm-m to more than 22925 ohm-m. These are colours represented from yellow to dark purple, distributed from the left side of the image to the central part and the central part towards the right side of the inverse model resistivity image. The geologic interpretation of the highest resistivities is coarse sand with the gravel which formed the bedrock. The medium resistivity values are about 422 ohm-m to 1605 ohm-m, which are showed by the three colours of green and are mostly located at topsoil and subsoil. These are interpreted geologically as the alluvium and weathered fine to medium sand. Besides, the lower resistivity values are between 2.67 to 166 ohm-m, seen in the middle of the left side of the profile represented by the blue colour. The zone holds the potential groundwater with silty clay deposits as the lithological interpretation (see Figure 4.7b).

Based on the IP line 2 in Figure 4.7c, two main chargeability ranges can be detected. Intermediate chargeability values range from 3.51mV/V to more than 7.89 mV/V was interpreted as the coarse sand basement. The anomalies obtained from this Induced Polarization (IP line 2) section and represented by the red colour on the profile corresponds to the sand-filled unit having cracks or fractures. Lower range chargeability values from 0.462 to 2.34 mV/V was interpreted as the clayey water-saturated zone. The erosional channels in the topsoil helped to weaken the subsurface and aid slope failure.
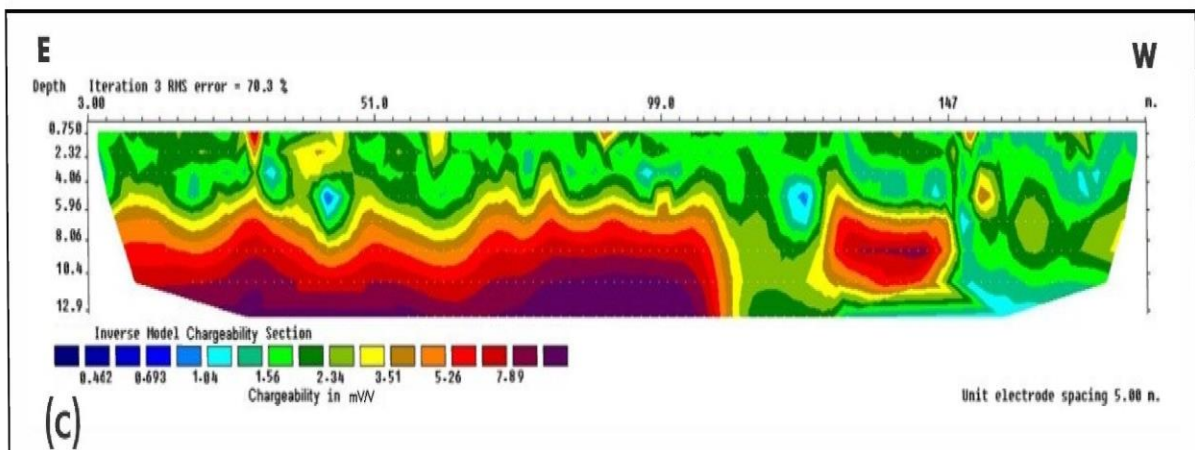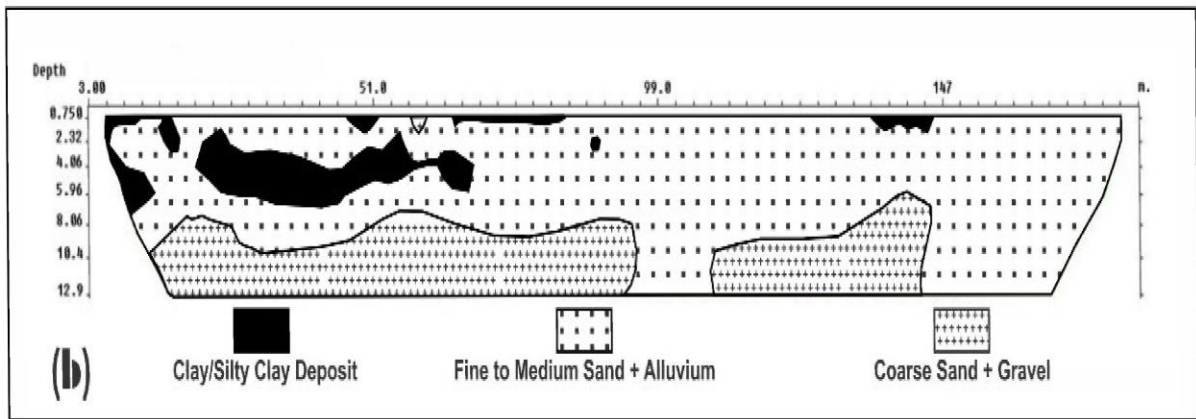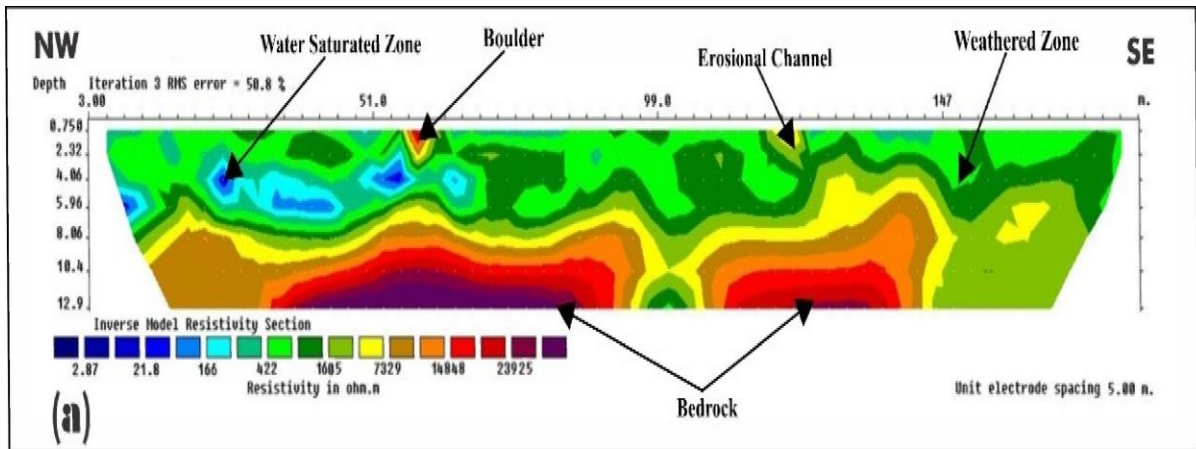
Figure 4.7: (a) 2D inverse model resistivity, (b) Geologic cross-section interpreted from the resistivity model, and (c) IP-chargeability for Oko (site 2).

4.5.3 Ezioko Site 3 (ER and IP) line 3:

The analysed values of resistivity and chargeability measured in this site have calculated RMS errors as 14.3 % and 12.2%, acquired in the direction of E-W, Km 10, Ekwulobia-Nanka Road.

From the 2D resistivity image of Line 3, the resistivity values are from 48.3 ohm-m to more than 9553 ohm-m (i.e. dark blue to dark purple colour as shown in Figure 4.8a). The higher resistivities are around 2311 ohm-m to the values greater than 15000 ohm-m at the bottom part of the image section with light red to dark purple colours, interpreted as the gravelled coarse sand that aids slope failure shown in Figure 4.8b. Meanwhile, the medium resistivities values is between 260 ohm-to 1130 ohm-m, distributed dominantly at topsoil and rock fragments in the image, and indicated by different colours of green. This can lithologically be interpreted as weathered fine to medium sand plus alluvium deposits. The zones of lower values (48.3 ohm-m to 260 ohm-m) settled at the bedrock and can be interpreted as the silty clay deposits. This bedrock has low resistivity values due to its increased ability to conduct electricity and water-saturated capability.

The IP inversion line 3 in Figure 4.8c, showed that there were two main chargeability ranges. First, the intermediate chargeability values from 5.89 to >20.1 mV/V was interpreted as the coarse sand gravel deposits found at the profile depth 17.0 to 25.0 m. At the profile length 46 m, the coarse sand deposit projected to the topsoil forming an erosional channel that weakens the bedrock and the slope failure at that point is imminent. Next, the low chargeability range was 0 .0381to 1.73 mV/V. At the profile length, approximately 54 to 104 m, this low chargeability was lithologically interpreted as the clayey (barren) due to high water-bearing capability and weathered characteristics. The low chargeability value also observed at a profile distance of 10 m, and this occurred because of the fractured impact.
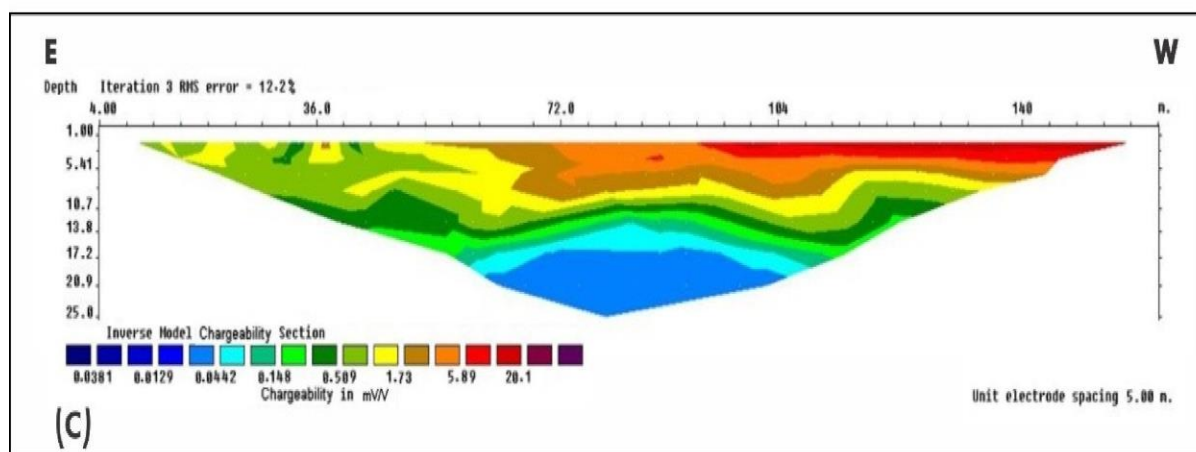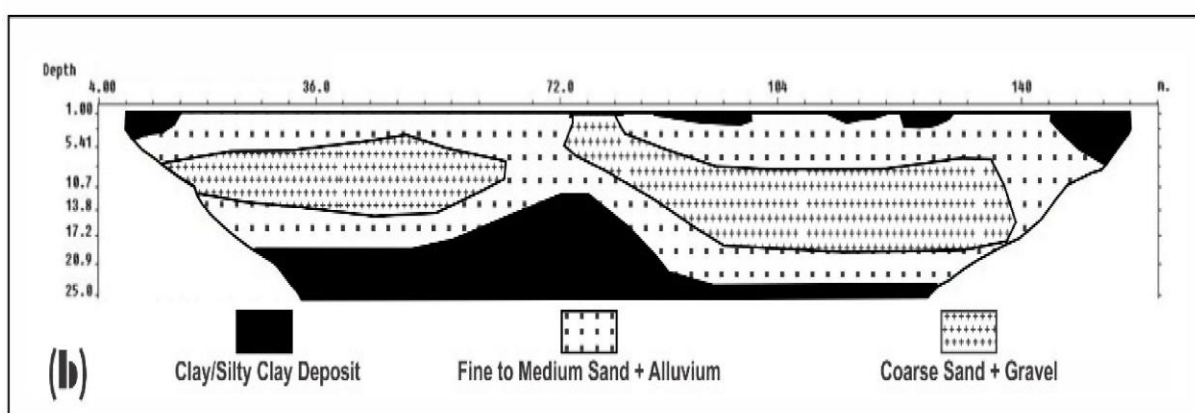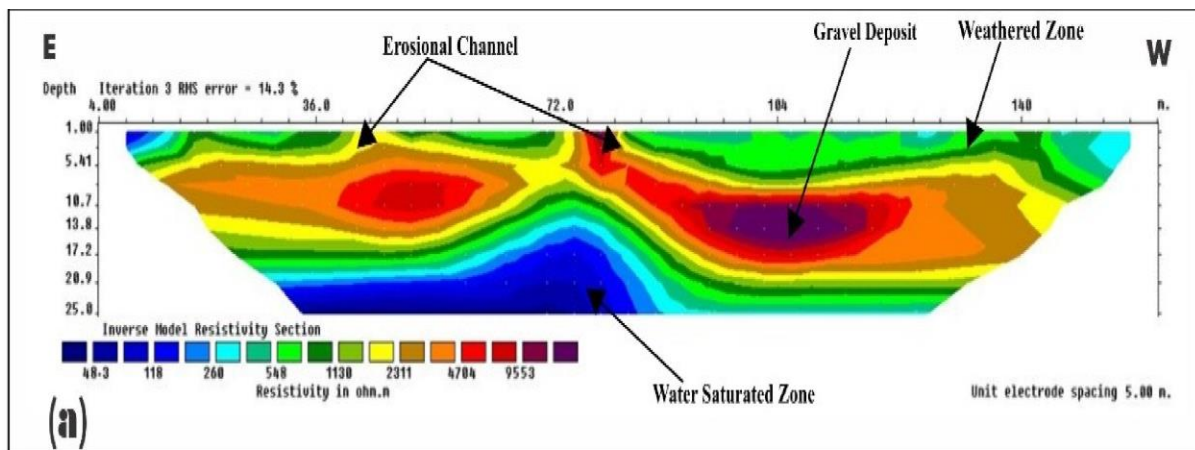
Figure 4.8: (a) 2D inverse model resistivity, (b) Geologic cross-section interpreted from the resistivity model, and (c) IP-chargeability for Ezioko (site 3).

4.5.4 Ubahu Nanka Site 4 (ER and IP) line 4:

The analysed values of resistivity and chargeability measured in this site have calculated RMS errors as 24.2 %, acquired in the direction of E-W, Km 16, Ekwulobia-Nanka Road.

The analysis of the ERT profile (see ER line 4 in Figure 4.9a) makes it possible to deduce the geological model of the basin showed in Figure 4.9b. The values close to the surface generally present lower resistivities, ranging from 95.3 to 381 ohm-m. This group interpreted as the detrital sedimentary weathered zone, made up of clayey conglomerates or silty clay deposit, immersed in clay facies (Quaternary colluvium). The lithological composition of this zone houses the aquifer formation and depot for groundwater. After this structure comes geological structure with an intermediate resistivity between 761 to 1523 ohm-m. It could be interpreted as clastic fine to medium sand and alluvium (see Figure 4.9b). The Palaeozoic bedrock is composed of coarse sand plus gravel in this sector, which present very high resistivities, over 3844 ohm-m. These high resistivities formed a gravel boulder at the bedrock. At the topsoil, a boulder of rock fragment with different sizes that weathered into sediments of rocks and easily collapsed in slides plate.

Based on the IP line 4 in Figure 4.9c, two main chargeability ranges can be detected. Low chargeability values range from 0.0043 to 0.118 mV/V interpreted as the clayey deposits. It was also demarcated as the clayey water-saturated zone. However, the anomalies obtained from this Induced Polarization section and represented by the yellow colour on the profile corresponds to the sand-filled unit having cracks. The second range of intermediated chargeability values are 1.63 to 5.98 mV/V.
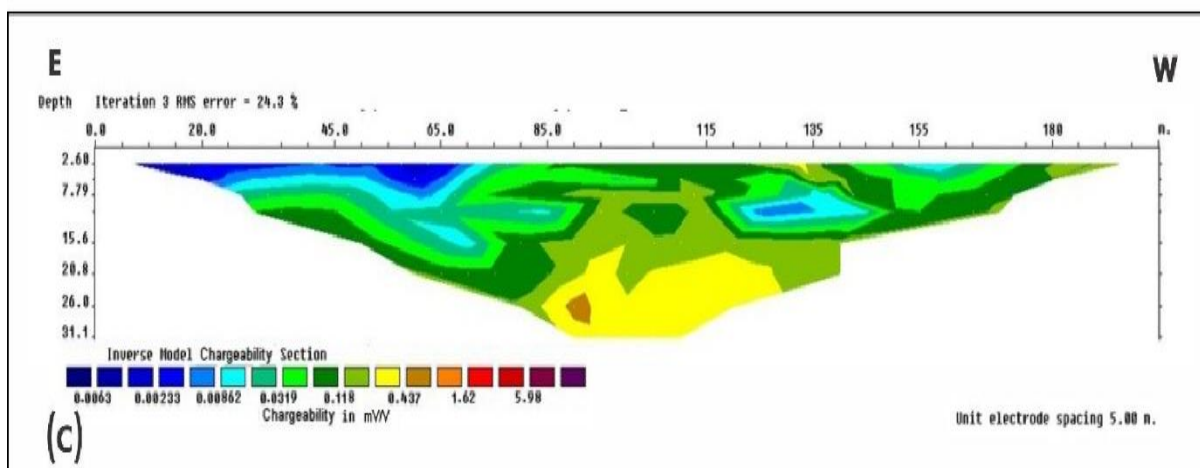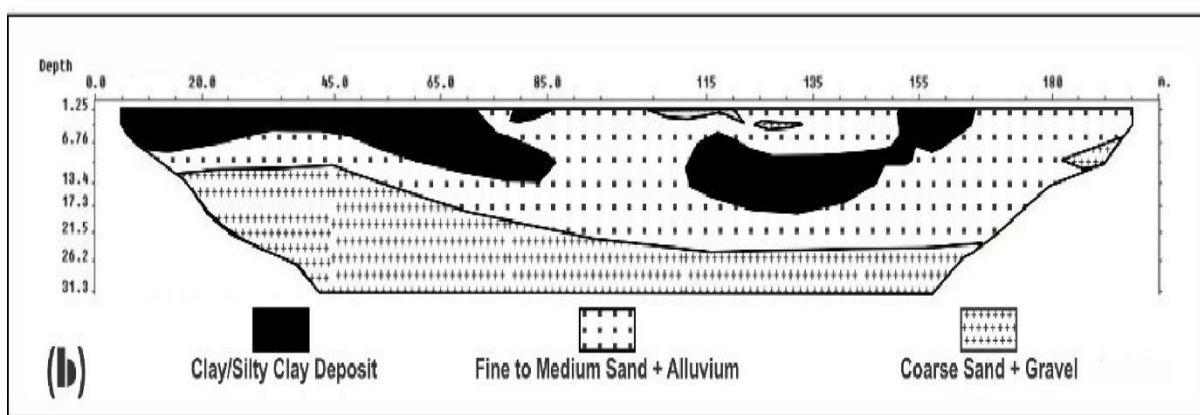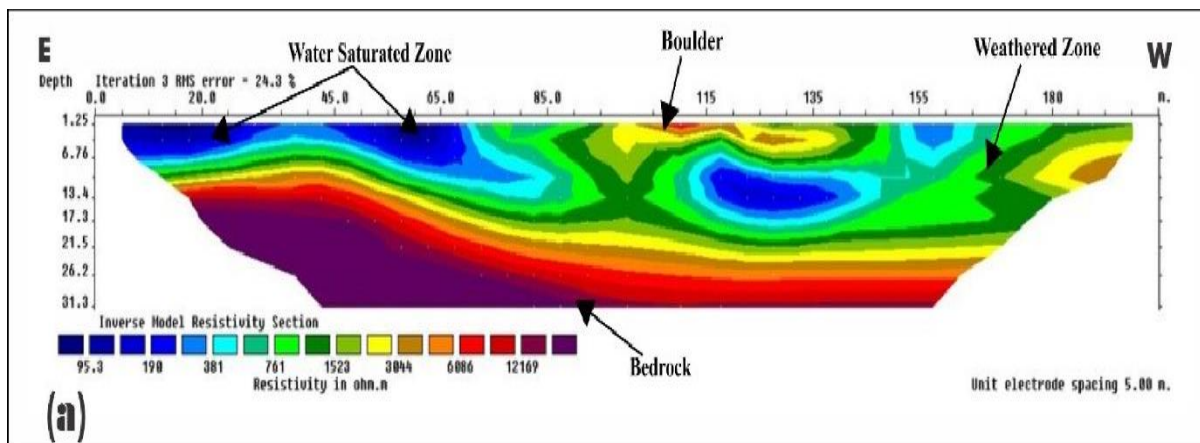
Figure 4.9: (a) 2D inverse model resistivity, (b) Geologic cross-section interpreted from the resistivity model, and (c) IP-chargeability for Ubahu Nanka (site 4).

4.6 Conclusions

The correlation between 2D, IP, and geologic lithology was very helpful as they provide complementary results. They provided valuable information as data for understanding the hydrogeological model of these landslide terrains. The groundwater formation in the study areas was tampered with by the creep's events of the landslide. The geophysical survey performed in the research has proved to be the most suitable tool for understanding the subsurface situation of slope failure. The resolution of ERT interpretation ambiguity was possible by the normalized chargeability. This survey showed high values of measured chargeability at different parts of the profiles because of the large and chargeable surface of the sandy particles with the clay composition. In general, for resistivity values below 100 ohm-m, the material is expected to have a high content of clay. Values of electric resistivity greater than 150 ohm-m were connected to fine to medium sand deposits. High resistivity values above 1000 ohm-m were lithologically interpreted as coarse tills materials. This high resistivity values were obtained mostly at the bedrock decreases in value with depth and also, a boulder of rock fragments with different sizes that weathered into sediments of rocks easily collapsed as the slides plate found at the topsoil. The electric resistivity shrivelled with depth as the coarse soil materials ranged from boulders to sand, and the aquifer system was composed of layers of the high content of clay. Based on the findings, it proved that the study areas have the potential for slope failure due to the existence of features such as weathered zones and boulders and that the soil properties and compositions contribute immensely to this geo-environmental hazard. By having this, the remedial steps taken in the event of a slope failure control should also be taken differently and more efficiently.

In conclusion, further geophysical surveys, such as well-logging, seismic, Transient Electromagnetic (EM), and Magnetic Resonance Sounding to determine the mineralogy of the clay in the study areas, should be encouraged. Other areas for further studied include assessing both the overburden thickness of the bottom layers with high clay content and the boundary conditions of the groundwater.

Bibliography

Abubakar, M. (2014). Petroleum potentials of the Nigerian Benue Trough and Anambra Basin: a regional synthesis. *Natural Resources, 2014*.

Agliardi, F., Crosta, G., and Zanchi, A. (2001). Structural constraints on deep-seated slope deformation kinematics. *Engineering Geology, 59*(1-2), 83-102.

Aizebeokhai, A., Oyeyemi, K., and Joel, E. (2016). *Electrical resistivity and induced-polarization imaging for groundwater exploration.* Paper presented at the 2016 SEG International Exposition and Annual Meeting.

Aizebeokhai, A. P. (2010). 2D and 3D geoelectrical resistivity imaging: Theory and field design. *Scientific Research and Essays, 5*(23), 3592-3605.

Aizebeokhai, A. P., and Oyeyemi, K. D. (2014). The use of the multiple-gradient array for geoelectrical resistivity and induced polarization imaging. *Journal of Applied Geophysics, 111,* 364-376.

Alley, W. M., Healy, R. W., LaBaugh, J. W., and Reilly, T. E. (2002). Flow and storage in groundwater systems. *Science, 296*(5575), 1985-1990.

Amangabara, G. (2015). Drainage morphology of Imo basin in the Anambra–Imo river basin area, of Imo state, southern Nigeria. *Journal of Geography, Environment and Earth Science International, 3*(1), 1-11.

Andrews, N., Aning, A., Danuor, S., and Noye, R. (2013). Geophysical investigations at the proposed site of the KNUST teaching hospital building using the 2D and 3D resistivity imaging techniques. *Int. Res. Jour. Geol. Min, 3*(3), 113-123.

Ao, O.-B., Adebayo, O., Madukwe, H., and Aturamu, A. (2015). Palynological and Sequence Stratigraphy Characterization of the Early-Late Campanian Nkporo Shale, Orekpekpe-Imiegba Area, Anambra Basin, Nigeria. *European Journal of Basic and Sciences, Vol. 2,* 1-15.

Bailey, D., and Stevenson, J. (2007). British Geological Survey Annual Report 2006-07. In: British Geological Survey.

Beckley, P. (2002). *Electrical steels for rotating machines:* IET.

Bell, F. (2011). Natural hazards and the environment. *Environmental and Engineering Geology- Volume I,* 75.

Bell, F., Cripps, J., and Culshaw, M. (1986). A review of the engineering behaviour of soils and rocks with respect to groundwater. *Geological Society, London, Engineering Geology Special Publications, 3*(1), 1-23.

Bérest, P., and Brouard, B. (2003). Safety of salt caverns used for underground storage blow out; mechanical instability; seepage; cavern abandonment. *Oil & Gas Science and Technology, 58*(3), 361-384.

Bernstone, C., Dahlin, T., Ohlsson, T., and Hogland, H. (2000). DC-resistivity mapping of internal landfill structures: two pre-excavation surveys. *Environmental Geology, 39*(3-4), 360-371.

Besson, A., Cousin, I., Samouëlian, A., Boizard, H., and Richard, G. (2004). Structural heterogeneity of the soil tilled layer as characterized by 2D electrical resistivity surveying. *Soil and Tillage research, 79*(2), 239-249.

Binley, A., & Kemna, A. (2005). DC resistivity and induced polarization methods. In *Hydro-geophysics* (pp. 129-156): Springer.

Birkholzer, J. T., Zhou, Q., and Tsang, C.-F. (2009). Large-scale impact of CO_2 storage in deep saline aquifers: A sensitivity study on pressure response in stratified systems. *International Journal of Greenhouse Gas Control, 3*(2), 181-194.

Campos, A., & Pérez, M. J. (1989). High and low imagers and their scores on creativity. *Perceptual and Motor Skills, 68*(2), 403-406.

Capozzoli, L., De Martino, G., Polemio, M., and Rizzo, E. (2019). Geophysical Techniques for Monitoring Settlement Phenomena Occurring in Reinforced Concrete Buildings. *Surveys in Geophysics,* 1-30.

Cassiani, G., Kemna, A., Villa, A., and Zimmermann, E. (2009). Spectral induced polarization for the characterization of free-phase hydrocarbon contamination of sediments with low clay content. *Near Surface Geophysics, 7*(5-6), 547-562.

Castleton, J. J., and McKean, A. P. (2009). *The Utah Geological Survey Geologic Hazards Mapping Initiative.* Paper presented at the Geological Society of America Abstracts with Programs.

Chikwelu, E., and Ogbuagu, F. (2014). Geotechnical Investigation of Soil around Mbaukwu Gully Erosion Sites, South-Eastern Part of Nigeria. *Jour. Appld. Geol. Geophys, 2*(4), 6-17.

COŞKUN, N. (2012). The effectiveness of electrical resistivity imaging in sinkhole investigations. *International Journal of Physical Sciences, 7*(15).

Dahlin, T., Bernstone, C., and Loke, M. H. (2002). A 3-D resistivity investigation of a contaminated site at Lernacken, Sweden. *Geophysics, 67*(6), 1692-1700.

Doetsch, J., Ingeman-Nielsen, T., Christiansen, A. V., Fiandaca, G., Auken, E., and Elberling, B. (2015). Direct current (DC) resistivity and induced polarization (IP) monitoring of active layer dynamics at high temporal resolution. *Cold Regions Science and Technology, 119,* 16-28.

Eberhardt, E., Stead, D., and Coggan, J. (2004). Numerical analysis of initiation and progressive failure in natural rock slopes—the 1991 Randa rockslide. *International Journal of Rock Mechanics and Mining Sciences, 41*(1), 69-87.

Egbueri, J., Igwe, O., and Nnamani, C. (2017). Assessment of the engineering properties and suitability of some tropical soils as backfill materials. *International Journal of Trends in Scientific Research and Development, 2*(1), 590-605.

Egbueri, J. C., and Igwe, O. (2020). The impact of hydro-geomorphological characteristics on gullying processes in erosion-prone geological units in parts of Southeast Nigeria. *Geology, Ecology, and Landscapes,* 1-14.

Everett, M. E. (2012). Theoretical developments in electromagnetic induction geophysics with selected applications in the near surface. *Surveys in Geophysics, 33*(1), 29-63.

Frangos, W. (1990). Stable-oscillator phase IP systems. *Induced Polarization: applications and case histories: Soc. Expl. Geophys., Invest. Geophys, 4,* 79-90.

Friedel, S., Thielen, A., and Springman, S. M. (2006). Investigation of a slope endangered by rainfall-induced landslides using 3D resistivity tomography and geotechnical testing. *Journal of Applied Geophysics, 60*(2), 100-114.

Gautam, P. K., and Biswas, A. (2016). 2D Geo-electrical imaging for shallow depth investigation in Doon Valley Sub-Himalaya, Uttarakhand, India. *Modeling Earth Systems and Environment, 2*(4), 1-9.

Glade, T., and Crozier, M. J. (2005). The nature of landslide hazard impact. *Landslide hazard and risk. Wiley, Chichester,* 43-74.

Goutaland, D., Winiarski, T., Dubé, J.-S., Bièvre, G., Buoncristiani, J.-F., Chouteau, M., and Giroux, B. (2008). Hydrostratigraphic Characterization of Glaciofluvial Deposits Underlying an Infiltration Basin Using Ground Penetrating Radar All rights reserved.

No part of this periodical may be reproduced or transmitted in any form or by any means, electronic or mechanical, including photocopying, recording, or any information storage and retrieval system, without permission in writing from the publisher. *Vadose zone journal, 7*(1), 194-207.

Hahn, D. W., and Omenetto, N. (2012). Laser-induced breakdown spectroscopy (LIBS), part II: review of instrumental and methodological approaches to material analysis and applications to different fields. *Applied spectroscopy, 66*(4), 347-419.

Igwe, C. (2012). Gully erosion in South-eastern Nigeria: role of soil properties and environmental factors. *In-Tech Open Science Publishers,* 157-171.

Igwe, O., and Egbueri, J. C. (2018). The characteristics and the erodibility potentials of soils from different geologic formations in Anambra State, South-eastern Nigeria. *Journal of the Geological Society of India, 92*(4), 471-478.

Ivars, D. M., Pierce, M. E., Darcel, C., Reyes-Montes, J., Potyondy, D. O., Young, R. P., and Cundall, P. A. (2011). The synthetic rock mass approach for jointed rock mass modelling. *International Journal of Rock Mechanics and Mining Sciences, 48*(2), 219-244.

Joralemon, D. (2017). *Exploring medical anthropology:* Taylor & Francis.

Karaoulis, M., Revil, A., Werkema, D., Minsley, B., Woodruff, W., and Kemna, A. (2011). Time-lapse three-dimensional inversion of complex conductivity data using an active time constrained (ATC) approach. *Geophysical Journal International, 187*(1), 237-251.

Kearey, P., Brooks, M., and Hill, I. (2002). An Introduction to Geophysical Exploration, ix 262 pp. In: Oxford: Blackwell Science. Price.

Kearey, P., Klepeis, K. A., and Vine, F. J. (2014). *Tectônica Global*: Bookman Editora.

Kemna, A., Binley, A., Cassiani, G., Niederleithinger, E., Revil, A., Slater, L., . . . Hördt, A. (2012). An overview of the spectral induced polarization method for near-surface applications. *Near Surface Geophysics, 10*(6), 453-468.

Loke, M. (2000). Electrical imaging surveys for environmental and engineering studies: A practical guide to 2-D and 3-D surveys. *Electronic version available from http://www.terraplus.com.*

Loke, M., Chambers, J., Rucker, D., Kuras, O., and Wilkinson, P. (2013). Recent developments in the direct-current geoelectrical imaging method. *Journal of Applied Geophysics, 95,* 135-156.

Loke, M. H. (2004). Tutorial: 2D and 3D electrical Imaging Surveys *(Copyright 1996-2004)*, 136.

Loke, M. H., and Barker, R. D. (1996). Rapid least-squares inversion of apparent resistivity pseudo-sections by a quasi-Newton method 1. *Geophysical prospecting, 44*(1), 131-152.

Martínez, J., Rey, J., Sandoval, S., Hidalgo, M., and Mendoza, R. (2019). Geophysical Prospecting Using ERT and IP Techniques to Locate Galena Veins. *Remote Sensing, 11*(24), 2923.

Masannat, Y. M. (2014). Landslide hazards: geotechnical aspects and management policies. *Jordan Journal of Civil Engineering, 159*(3175), 1-22.

Michael, H. A., and Voss, C. I. (2009). Controls on groundwater flow in the Bengal Basin of India and Bangladesh: regional modeling analysis. *Hydrogeology Journal, 17*(7), 1561.

MIM, F. A., AH, M. Y., Ismail, N., and Muztaza, N. (2017). The Application of 2D Resistivity and Induced Polarization Methods for Slope Study at Penang Island, Malaysia.

Nnadi, O., Liwenga, E., Lyimo, J., and Madukwe, M. (2019). Impacts of variability and change in rainfall on gender of farmers in Anambra, Southeast Nigeria. *Heliyon, 5*(7), e02085.

Nwajide, C. (2013). Geology of Nigeria's sedimentary basins. *CSS Bookshops Limited, Lagos*, 565.

Ogala, J. E. (2011). Hydrocarbon potential of the Upper Cretaceous coal and shale units in the Anambra Basin, South-eastern Nigeria. *Petroleum & Coal, 53*(1), 35-44.

Okengwo, O., Okeke, O., Okereke, C., and Paschal, A. (2015). Geological and geotechnical studies of gully erosion at Ekwulobia, Oko and Nanka Towns, South-eastern Nigeria. *Electronic Journal of Geotechnical Engineering (EJGE), 20*(1), 113-122.

Onugba, A., & Yaya, O. (2008). Sustainable groundwater development in Nigeria. In *Applied Groundwater Studies in Africa* (pp. 113-124): CRC Press.

Onyekuru, S., Nwankwor, G., and Akaolisa, C. (2010). Chemical characteristics of groundwater systems in the southern Anambra Basin, Nigeria. *Journal of Applied Sciences Research, 6*(12), 2164-2172.

Perrone, A., Lapenna, V., and Piscitelli, S. (2014). Electrical resistivity tomography technique for landslide investigation: a review. *Earth-Science Reviews, 135*, 65-82.

Revil, A., & Skold, M. (2011). Salinity dependence of spectral induced polarization in sands and sandstones. *Geophysical Journal International, 187*(2), 813-824.

Reynolds, J. M. (2011). *An introduction to applied and environmental geophysics:* John Wiley & Sons.

Rezaei, S., Shooshpasha, I., and Rezaei, H. (2019). Reconstruction of landslide model from ERT, geotechnical, and field data, Nargeschal landslide, Iran. *Bulletin of Engineering Geology and the Environment, 78*(5), 3223-3237.

Rucker, D. F., Crook, N., Winterton, J., McNeill, M., Baldyga, C. A., Noonan, G., and Fink, J. B. (2014). Real-time electrical monitoring of reagent delivery during a subsurface amendment experiment. *Near Surface Geophysics, 12*(1), 151-163.

Salom, A. T. (2017). Remining And Restructure of a Tailing Deposit-Technical Feasibility.

Samouëlian, A., Cousin, I., Tabbagh, A., Bruand, A., and Richard, G. (2005). Electrical resistivity survey in soil science: a review. *Soil and Tillage research, 83*(2), 173-193.

Schmutz, M., Ghorbani, A., Vaudelet, P., and Blondel, A. (2014). Cable arrangement to reduce electromagnetic coupling effects in spectral-induced polarization studies Reducing EM coupling effects for SIP. *Geophysics, 79*(2), A1-A5.

Schön, J. H. (2015). Electrical Properties. In *Developments in Petroleum Science* (Vol. 65, pp. 301-367): Elsevier.

Schuster, R. L., and Highland, L. (2001). S*ocioeconomic and environmental impacts of landslides in the western hemisphere:* Citeseer.

Singh, V. P. (2013). *Dam breach modeling technology* (Vol. 17): Springer Science & Business Media.

Soeters, R., and Van Westen, C. (1996). Slope instability recognition, analysis and zonation. *Landslides: investigation and mitigation,* 247, 129-177.

Taleski, I., and Velevski, A. (2019). *Application of Electrical Resistivity Tomography and Induced Polarization for Identification of Underground Reinforced Concrete Structures.* Paper presented at the 10th Congress of the Balkan Geophysical Society.

Telford, W. M., Geldart, L., Sheriff, R. E., and Sheriff, R. (1990). *Applied geophysics* (Vol. 1): Cambridge university press.

Tse, S. T., and Rice, J. R. (1986). Crustal earthquake instability in relation to the depth variation of frictional slip properties. *Journal of Geophysical Research: Solid Earth, 91*(B9), 9452-9472.

Van Schoor, M. (2002). Detection of sinkholes using 2D electrical resistivity imaging. *Journal of Applied Geophysics, 50*(4), 393-399.

Walvoord, M. A., Voss, C. I., and Wellman, T. P. (2012). Influence of permafrost distribution on groundwater flow in the context of climate-driven permafrost thaw: Example from Yukon Flats Basin, Alaska, United States. *Water Resources Research, 48*(7).

Ward, S. H. (1988). The resistivity and induced polarization methods. Paper presented at the 1st EEGS Symposium on the Application of Geophysics to Engineering and Environmental Problems.

Wieczorek, G. F., and Snyder, J. B. (2009). Monitoring slope movements. *Geol. Monit,* 245-271.

Zhdanov, M. S. (2018). *Foundations of geophysical electromagnetic theory and methods:* Elsevier.

CHAPTER 5: ELECTRICAL RESISTIVITY TOMOGRAPHY FOR INTERNAL STRUCTURE INVESTIGATION AND GROUNDWATER CHARACTERIZATION OF THE NANKA LANDSLIDE IN ANAMBRA STATE, NIGERIA

School of Chemistry and Physics, College of Agriculture, Engineering, and Science, University of KwaZulu-Natal, Pietermaritzburg Campus, Private Bag X01, Scottsville 3209, South Africa.

ELECTRICAL RESISTIVITY TOMOGRAPHY FOR INTERNAL STRUCTURE INVESTIGATION AND GROUNDWATER CHARACTERIZATION OF THE NANKA LANDSLIDE IN ANAMBRA STATE, NIGERIA

Chikwelu Edward Emenike and Naven Chetty

School of Chemistry and Physics, College of Agriculture, Engineering, and Science, University of KwaZulu-Natal, Pietermaritzburg Campus, Private Bag X01, Scottsville 3209, South Africa.

*Corresponding Author: chettyN3@ukzn.ac.za

Abstract

Over two decades, incidences of landslides in Nanka Community, Anambra State, Nigeria, in the eastern phase of Awka-Orlu upland, has been active and persistent, defying many control measures that have been put in place and causing the loss of property, lives, and assets to increase. As a result, this research work involves the study of geo-engineering and geophysical measurements of the slide site to delineate the aerial scale and direction of movement of the landslide zone, determine the lithological portion, estimate the thickness of the sliding sheet, and delineate the water-saturated areas. The data was collected using ABEM Terrameter SAS 4000 and ABEM LUND ES464 electrode selector system and processed using RES2DINV software for a 2D subsurface image. During data acquisition, a Wenner array was set-up as this array is capable of imaging deeper profile data, and apparent resistivity is easily calculated in the field. The results of the models indicate that the study area consists mainly clayey and sandstone formations, which exhibited low resistivity values correspond to the shale layers and groundwater zones. However, gravel deposit was also present in some areas, as indicated by both the imaging and geological measurements.

Keywords: landslide, 2D resistivity, geophysics, lithology

5.1 Introduction

The use of geophysical methods for landslide studies has increased considerably in recent years. Geophysical methods are known as indirect methods, and they include non-destructive, compact approaches that are utilized to cover large regions at a minimal cost (Bichler *et al.*, 2004; Lapenna *et al.*, 2003). A landslide is a complex geological entity composed of strata with opposing and gradational physical characteristics (Jongmans & Garambois, 2007). The increasing complexity of many landslides necessitates the need to investigate their features as thoroughly as possible (Bichler *et al.*, 2004). Sequel to this, it is paramount to determine the substructure information of the landslide and its surrounding environment to facilitate reliable stability assessments and control (Bruno & Marillier, 2000). The main challenges in the landslide characterization are related to the internal properties and hydrological changes; in many cases, the boreholes and geological evidence cannot provide accurate information on the depth and lateral continuity of the failing surface (Sastry *et al.*, 2006). Moreover, geophysical investigations can provide in situ subsurface conditions (Gowen *et al.*, 2011; Oyedele *et al.*, 2012), which may, in turn, be converted into geotechnical knowledge on subsoil parameters towards a full understanding of a slope's physical characteristics (Sastry *et al.*, 2006). The viability of different direct and indirect geophysical techniques addresses sliding mass details, such as downward slope movement, thickness, bedrock relief, water table depth, and inner sliding mass structure (Bichler *et al.*, 2004; Israil & Pachauri, 2003; Sastry & Mondal, 2013; Sastry *et al.*, 2006).

ERT survey is one of the geophysical tools used to obtain the internal resistivity distribution by measuring with the survey equipment on the ground surface (Andrade, 2011; Riwayat *et al*, 2018b; Saad *et al.*, 2012). This technique, known as a non-destructive tool, will minimize the damage to the site by virtue of its surface methods of measurement (Asry *et al.*, 2012; Samsudin *et al.*, 2000). Due to its non-invasive to the environment during data gathering, it may be called a sustainable approach. This ERT method also offers a chance to overcome some of the difficulties that most traditional ground investigative procedures face (Azhar *et al.*, 2016; Riwayat *et al.*, 2018b). Furthermore, this technique is known for being less time-consuming and low-cost while yet offering higher physical property characteristics in undisturbed environment (Meng *et al.*, 2003; Sass *et al.*, 2008; Sastry *et al.*, 2006). The conventional approach has numerous flaws, including the fact that it only offers information at the actual drilling location, requiring interpolation between borings to establish conditions, which might introduce some uncertainty (Hazreek, 2010; Riwayat *et al.*, 2018a). However, the traditional

technique is now utilized as a reference and comparison to the ERT results to interpret the images from the study area (Riwayat *et al.*, 2018b). Overlapping resistance values of different rock and soil classes relied heavily on many factors, such as porosity, level of water content, and dissolved salt concentration (Chambers *et al.*, 2006). Electrical imaging has become one of the effective techniques for infrastructure projects and environmental engineering studies in recent years. It has high resolution at shallow depths with a superior area coverage of at least two-dimensional information with automated data acquisition for cost-effectiveness, and the output presented in an easily interpretable form. Resistivity imaging is a reliable technique that produces good results (Kaufmann, Deceuster, & Quinif, 2012; Leontarakis & Apostolopoulos, 2013), unlike Electromagnetic methods, which are now ineffective, difficult to mount, and sometimes affect by disturbances arising from the ground anomalies (Binley & Kemna, 2005; Coggon, 1971).

Many scholars have worked on landslide menace in South-Eastern Nigeria with different approaches and methods without a permanent solution to the devastating nature of the slides. Obiadi *et al* (2011) studied the primary causes of landslide risk in Anambra State using the geological assessment method; his findings proved that the expansion and growth of the slides complex increased due to the nature of the geological formation and seasonal variability of the groundwater table in the region. Egbueri & Igwe, (2020) in his extensive work on slope failure in the eastern region of Nigeria using a similar technique, he observed the susceptibility of the landslide as a function of the topography of the area as well as the stability of the soil, climate, and degree of afforestation. Among other methods used by the previous researchers, it is evident that none of the studies carried out a quantitative assessment using the ERT technique to investigate the rate of gully expansion in the Ekwulobia-Nanka communities in Anambra, Nigeria.

The following objectives must be achieved for the landslide expansion to be evaluated:

a) to identify the formation of lithology (i.e. the composition of the rock, minerals, and clay content), and the stratigraphic/structural deformation (i.e. detection of permeable pathways, fracture zones, and faults).

b) to identify the hydrological zones and temperature-influenced resistivity.

c) to delineate the aerial movement of the landslide zone, calculate the depth/thickness of the sliding layer and mark out the water-saturated zones.

5.1.1 General description of the study area

The study area is located in the Nanka, Orumba-North Local Government Area of Anambra State, Nigeria as shown in Figure 5.1. It lies between latitudes $6^03^126.65^{11}$N-$6^025.36^{11}$N and longitudes $7^02^153.41^{11}$E-$7^051.84^{11}$E. Its neighboring communities are Oko, Agulu, Ekwulọbia, Aguluz-Ọigbo, Isuọfia, Umuọna, and Awgbụ. Nanka community comprises of seven villages including, Agbiligba, Enugwu, Ifite, Amakor, Umudala, Ubahu, and Etti, starting from the elderly to the younger one. There are two (2) main landslide sites at the Nanka community; the first landslide site is located in Amakor village and has its geographical coordinates between latitude 6°2′28.75″ N and 7°4′57.2″ E; the second site is located in Ubahu village and has its geographical coordinates as 6°3′13.22″ N and 7°4′33.84″ E.

Nanka gully is an ecological disaster, as the erosion induces landslides regularly (Oyedele *et al.*, 2012). Eke-Ntai in Amako Village, popularized by Ezenwenwe, was said to have been a bustling slave market during the heyday of human cargo trafficking in the community. The current issue of erosion in Nanka has its origins in the infamous slave market (Oyedele *et al.*, 2012). The highly profitable and disguised business of the slave trade conducted within these two sites led to the development of hidden bush footpaths that have been flooded heavenly by uncontrolled running water during heavy rain from neighbouring communities that have precipitated gully erosion (Kern-Simirenko, & Wawro, 1990; Oyedele *et al.*, 2012).

The landslide occurrence is peculiar to the tropical rain forests with half of Southern Nigeria coverage and is known for its evergreen vegetation and diverse plant species (Ogbuefi & Ijeomah, 2019). Several areas have been severely deforested due to anthropogenic activity, reducing the land to savannah vegetation in many places (Ukatu, 2019). Geological factors, such as relief and lithology, and other human activities affect the vegetation in the studied area (Obiadi *et al.*, 2011). Rainy and dry seasons are the two weather-influenced conditions in the tropical environment of the Nanka community.
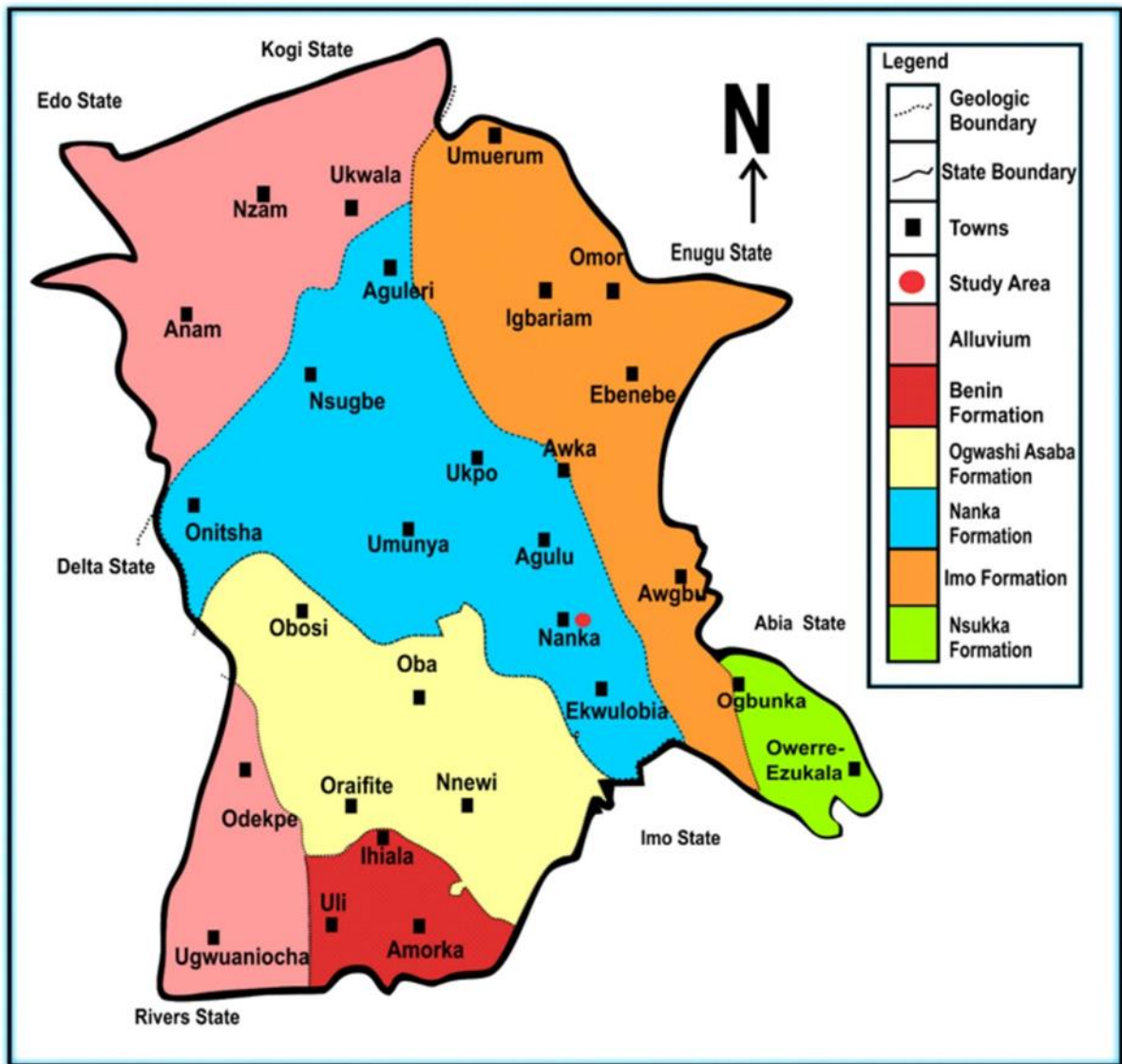
Figure 5.1: Geologic map of Anambra State showing study areas (Ukatu, 2019).

5.1.2 Climate, Rainfall, and the Vegetation of Anambra State, Nigeria.

Anambra State is within the wet tropical climate in South-Eastern Nigeria with a mean annual temperature range of 27°C to 34°C, respectively (Obiadi *et al.*, 2011). The temperature is highest around March–April, as observed by Obiadi *et al.*, (2011) and Chinweze, (2017), when the Sun moved through the latitude of Nigeria. The rain forest zone of Nigeria has high rainfall between May-August, and this has a lowering effect on the temperature condition of the study area. The climate variability has increased rainfall intensity resulting in massive flooding and storms that aggravated environmental and land degradation issues in Anambra State, Nigeria. The wind system often comes into the nation around September and progressively spreads throughout the country until March of the following year, when the sun repeats the cycle (Obiadi *et al.*, 2011). The rainy season is characterized mostly by flash floods, thunder-storm and lasts between April to October, while the dry season lasts with high temperature and dusty atmosphere between November and March. The rainy season also goes with relatively high temperatures (330) and high relative humidity (85%) (Chinweze, 2017). The vegetation of the study area is part of the West-African rainforest belt, which has been severely deforested as a result of anthropogenetic practices, reducing it to savannah vegetation, and the heavy rainforest has also made light rainforest possible as man's invasion of the ecosystem continues. The study area has long steep slopes that enhance the speed of runoff that gather momentum to produce the force that quickly detaches and transports soil particles, resulting in gullies.

5.2 Materials and methods

As shown in Figure 5.2a, the ERT data was gathered in the research region utilizing an SAS 4000 ABEM Lund Imaging System, a relay switching unit (Electrode Selector ES 464+5m spacing of electrode takeout), five 100-m multiconductor cables, and steel rod electrodes.
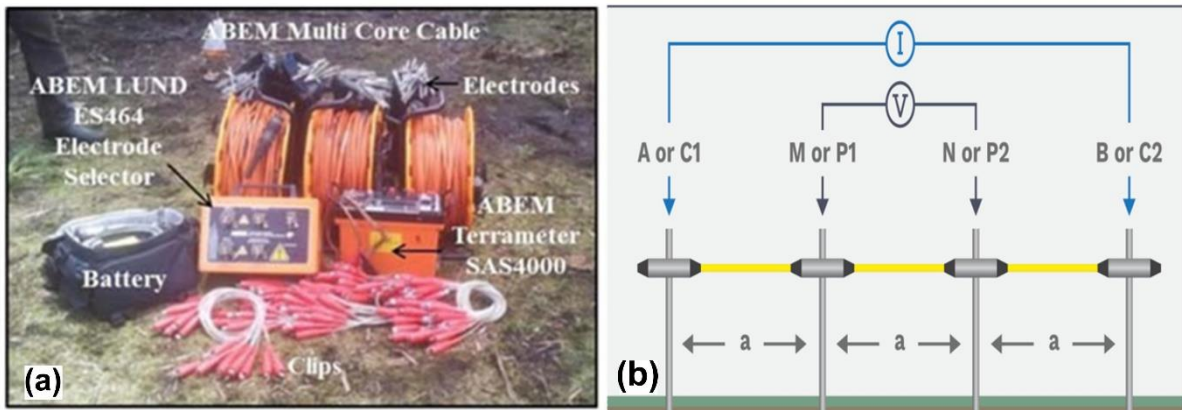
Figure 5.2: (a) The ABEM Terrameter SAS4000 resistivity meter and ABEM LUND ES464 electrode selector system (Nazaruddin *et al.*, 2016), (b) Wenner array (Batayneh, 2006; Dahlin & Loke, 1998).

The electrodes spacing was 5 m, and the profile maximum line was 300 m. The 'ABEM Terrameter SAS 4000 and ABEM LUND ES464 electrode selector' device was designed to take measurements of resistivity during the data acquisition. In the collection of data, we used Wenner protocol with a remote cable setup about perpendicular form spread line with a distance of about 400 m. The field work array spacing expands around the midpoint array while maintaining an equivalent spacing between each electrode as shown in Figure 5.2b. The Wenner array is the most beneficial field arrangement for calculating apparent resistivity, especially in the field with the computer, and the instrument's sensitivity is not as critical as other array designs (Cubbage *et al.*, 2017). The following configuration equation 5.1 was used to determine the apparent resistivity;

$$\rho = 2\pi a \frac{V}{I}, \qquad\qquad\qquad 5.1$$

Where:

$'\rho'$ stands for Apparent resistivity

'V' stands for Potential difference

'I' stands for current

'α' stands for the spacing of the electrodes in each pair

5.3 Data Interpretation

First, the resistivity data collected from the study areas were all in the .s4k file format. Using the Terrameter utility software, the data were converted to interpretable format (.dat). The converted data were then imported into the RES2DInv Software package for iterative inversion modeling after adjustments were made to the inversion settings. For processing the apparent resistivity data, RES2DINV software was also applied (ver.3.42d) (Loke, 2004).

This iterative program, RES2DINV, employs an inversion method based on the smoothness restricted least-squares technique (MacInnes & Raymond, 2001; Sasaki, 1994). The program automatically generates a 2D model by dividing the subsurface into rectangular blocks and chooses the appropriate inversion variables for the data, including the damping factor, vertical to horizontal flatness filter ratio, convergence limit, and iterations number (Muchingami *et al.*, 2012). Different data formats can be accommodated by adjusting the inversion parameters. With the help of a finite-difference approach or infinite-element approach, the RES2DINV

software estimates the apparent resistivity values of the model blocks and compares them to observed data. The resistivity of the model blocks were altered continuously until the model's calculated apparent resistivity values match the actual measurement on the ground (Loke & Barker, 1996; Muchingami *et al.*, 2013). The program generates a pseudo-section for the eleven survey lines, which is the qualitative means of showing the spatial variability of observed or computed apparent resistivity (Muchingami *et al.*, 2012; Ramazi & Jalali, 2015). The 2D tomograms obtained from the ERT geophysical techniques of the survey are shown in Figures 5.4 to 5.10 for the six survey lines, respectively.
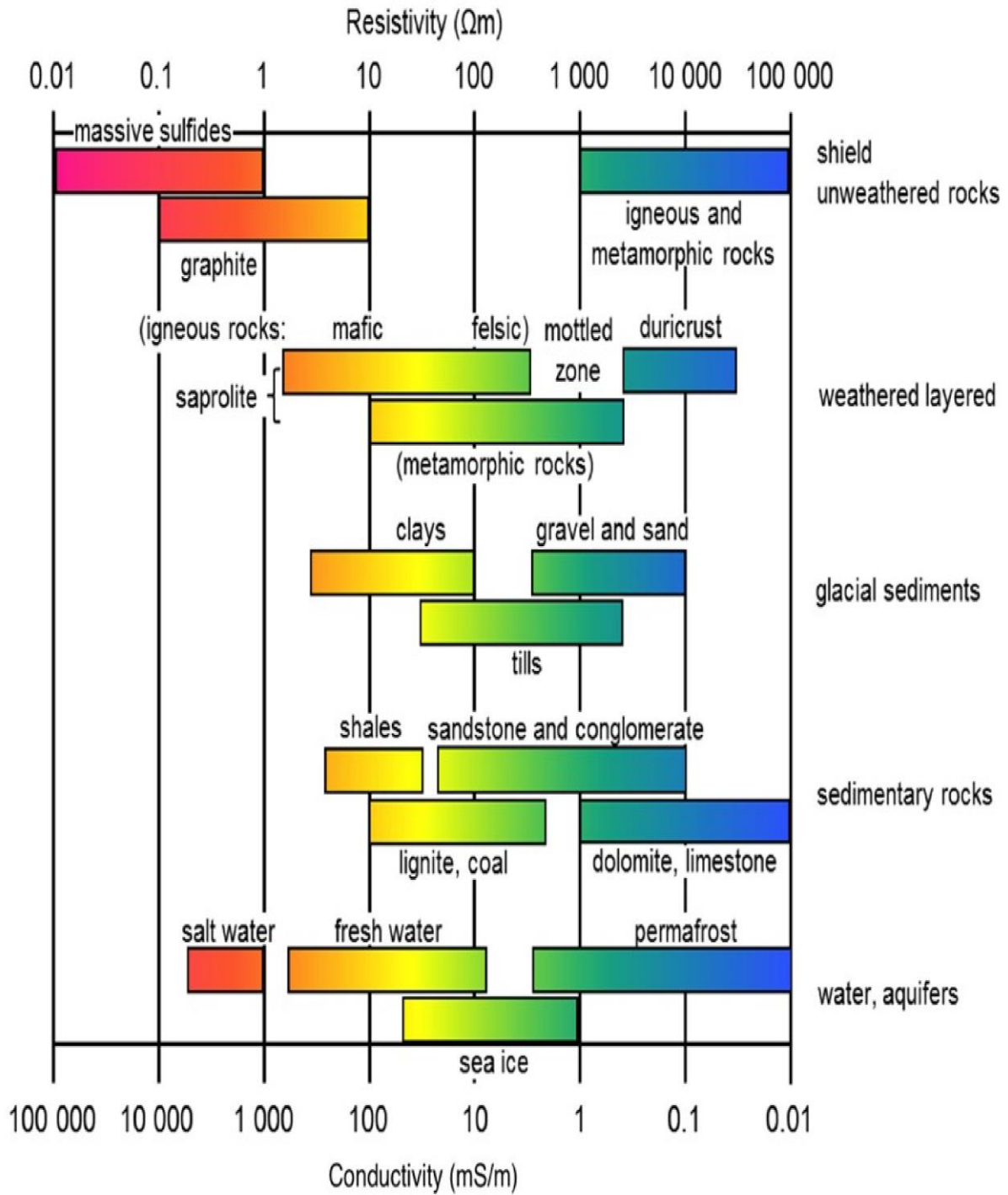
Figure 5.3: Electrical conductivity and resistivity of common rocks (Gercek, 2007; Nicollin *et al.*, 2010).

5.4 Results and Discussion

The profiles cross-section runs parallel to the NS trending segment along a dirt road (see Figure 5.1). This landslide is one of the largest in Nigeria, with 66 meters deep, 2,900 meters long, and 349 meters wide (Unah, 2020; Wallace-Wells, 2019). The earth subsurface resistivity images obtained at the study site were shown in Figure 5.4 to 5.10 (as inverse resistivity models) with its geologic cross-section interpreted from the resistivity model within a sequence of the horizontal sedimentary sequence. The inverted geo-electrical sections of the study area were obtained through the optimization technique of RES2DINV software by reducing the difference between the calculated and measured apparent resistivity values.

5.4.1 Profile 1

The inverted resistivity section can be characterized lithologically based on different resistivity values distribution as shown in Figure 5.4a. This profile is mostly sandy-clay deposit, which showed non-consolidated minerals such as shale materials, as shown in Figure 5.4b. The low resistivity value was between 14.3 – 101 Ωm, which interpreted as the clayed water saturation zone located at different zones from topsoil to bedrock. The intermediate resistivity range with resistivity value 222 Ωm to 415 Ωm that formed the part of the topsoil, subsoil, rock fragments, and bedrock, can also be interpreted from the inverted section. This was also interpreted as fine to medium sandstone plus alluvium. However, the zone of high resistivity value (i.e. 761Ωm and above) can be detected at distance from 40.0 to 150m, depth 9.94m to 17.3m. Coarse sandstone plus gravel is the lithological interpretation. The presence of sandstone boulders of various sizes in this profile 1 is an evidence that the soil unconsolidation, leading to landslide. This profile is within the Benin formation (see Figure 5.1). The sediments in this basin, which was deposited by fluvial processes has been adjudged to be the most recent sediment in the Anambra Basin. It belongs to Pliocene – Recent age.
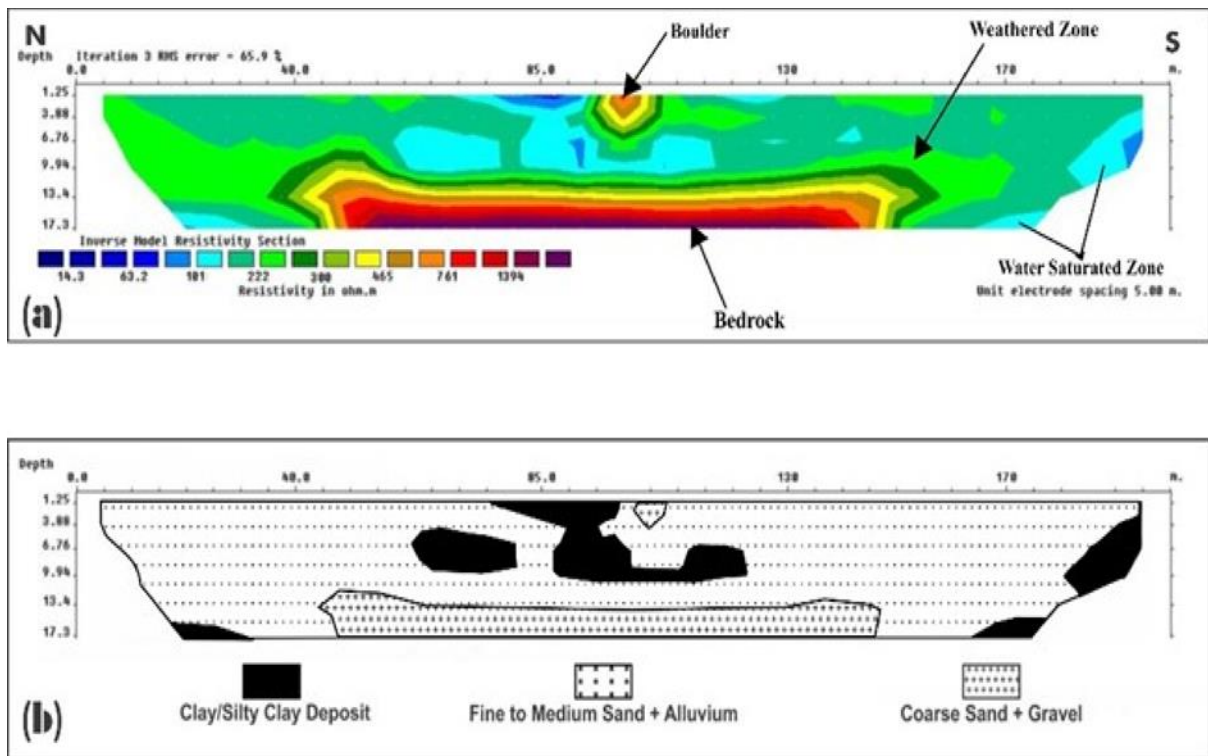
Figure 5.4: (a) Profile 1 electrical resistivity tomography, (b) Geologic cross-section interpreted from the resistivity model within a sequence of horizontal sedimentary sequence (see figure 5.3).

5.4.2 Profile 2

The electrical resistivity tomography section, as shown in Figure 5.5a, was lithologically interpreted in the geologic section (see Figure 5.5b), showed that wet silty-clay material spread across all the zones in the profile from topsoil to bedrock. Clay is a softer rock than sandstone, so it eroded more quickly, and in this context, it makes all zones prone to environmental degradation. So, it is weathered and probably a clear erosional channel in the zones with resistivity values ranging from 57.5 to 157Ωm. This zone is also a possible source of groundwater. Another range was the intermediate resistivity value ranging from 246 to 401Ωm. It can also be interpreted as the sandstone plus alluvium material that formed parts of the bedrock and topsoil, scattered at different depths. However, high resistivity values were also detected at the distance of 0 - 40m, depth 6.76 - 9.94m with the resistivity values above 649Ωm. Thus, this can be defined as the gravel boulder due to its high resistivity value. The values of the resistivities correlate with the lithofacies in the Ogwasi-Asaba Formation (Figure 5.1). This formation consists of dark grey shale and sandy shale and has been characterized using evidences of sediment reworking. The age has been postulated to be in the range of Late Miocene–Pliocene (Ola-Buraimo, & Akaegbobi, 2012).
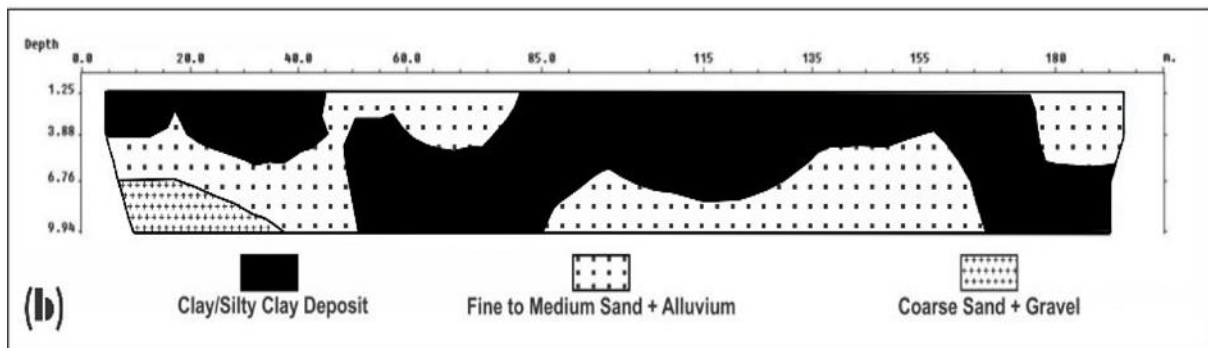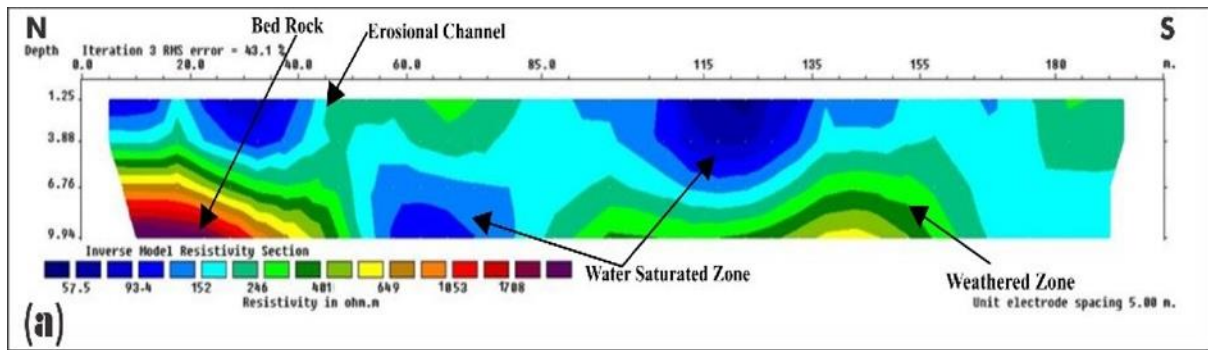
Figure 5.5: (a) Profile 2 electrical resistivity tomography, (b) Geologic cross-section interpreted from the resistivity model within a sequence of horizontal sedimentary sequence (see figure 5.3).

5.4.3 Profile 3

Based on the resistivity model inversion as shown in Figure 5.6a and geologic cross-section interpreted as also shown in Figure 5.6b, three resistivity ranges with outstanding demarcation are found. Low resistivity zone with resistivity values between 0 - 22.7Ωm, which was found at distance 0.0 - 190m interpreted as the weak zone (i.e. clayey topsoil). Next, the intermediate resistivity range which was between 44.8 – 153Ωm. At depth 10.08 – 17.30m with depth thickness of 7.22m, the intermediate zone was interpreted as the weathered zone (i.e. fine to medium sandy plus alluvium subsoil). Relatively high resistivity zone was ranged 299 ->597Ωm which dominated from 17.3m and deeper. This zone was interpreted as the coarse sand plus gravel bedrock. However, the mixed lithological bedrock with resistivity value >299Ωm was found separated by a distance 17.3m. Thus, an unconsolidated weathered zone based on the degree of oxidation or colour was identified at this horizon. This is a phenomenon normally associated with the Nanka formation of the Anambra Basin. Profile 4 was omitted because of its geological similarities with profile 3.
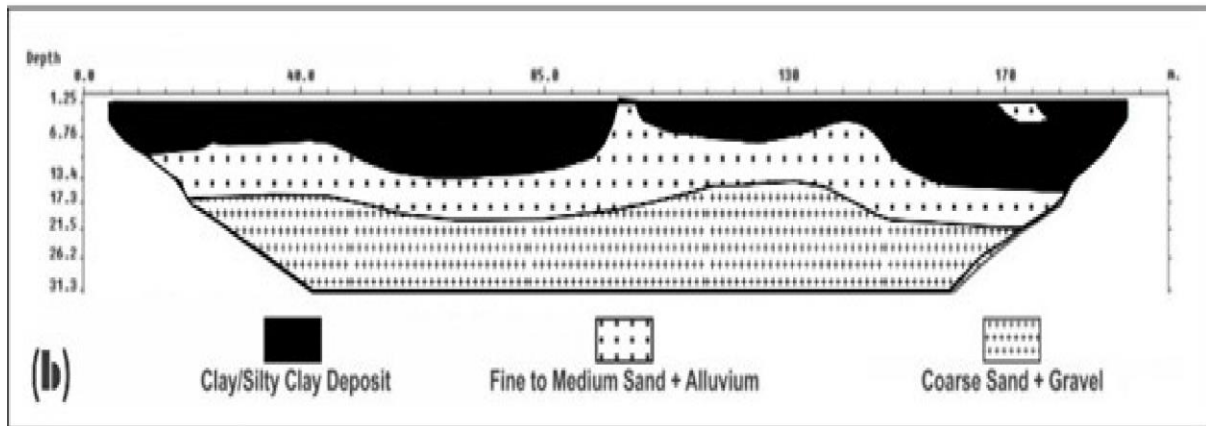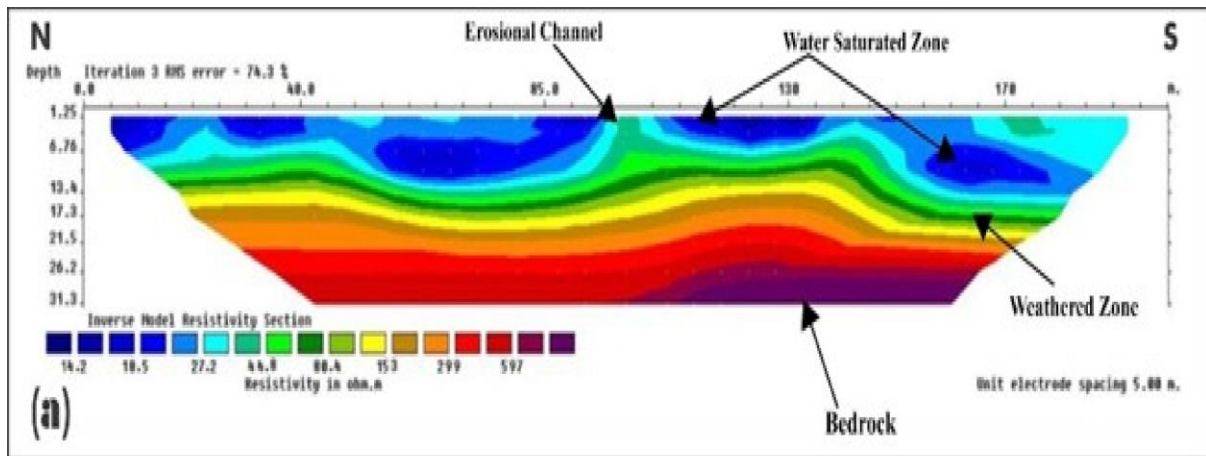
Figure 5.6: (a) Profile 3 electrical resistivity tomography, (b) Geologic cross-section interpreted from the resistivity model within a sequence of horizontal sedimentary sequence (see figure 5.3).

5.4.4 Profile 5

The electrical resistivity tomography section, as shown in Figure 5.7a, was characterized lithologically based on different resistivity values distributed across the profile, and was interpreted in the geologic section in Figure 5.7b. We observed wet silty-clay material up-to-the bedrock 21.5 m depth on the right side and 17.3m on the other side of the profile under the electrodes from -80 to -60 and 60 m respectively, and the resistivity range of this material is 45 to 145Ωm. Likewise, the second zone showed intermediate resistivity values (212 to 445Ωm) with high chargeability to the groundwater. This layer was probably a clear demarcation of the erosional channels in the other zones that formed the sandstone-alluvium bedrock. The near-surface materials under the electrode distance from -5 to 10m up to a depth of about 9.94m, have resistivity value of 642Ωm are observed to be alluvium and fine to medium sand deposits, while the distance from -40 to 25m from the depth of 17.3m to the bedrock shows moderately high resistivity value greater than or equal to 833Ωm, which lithologically interpreted as a deposit of gravel and coarse sand. This interpretation has been inferred from the fact that the profile crosses both the Nanka formation and the Imo formation of the Anambra Basin.
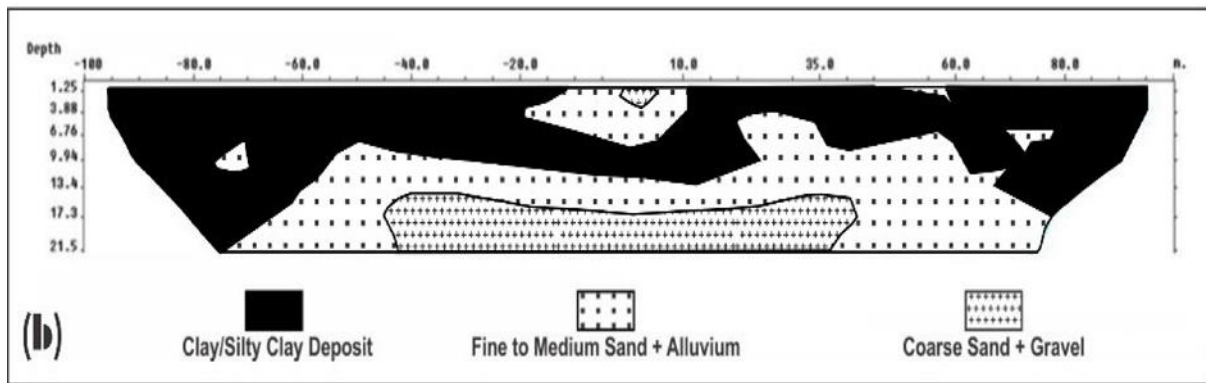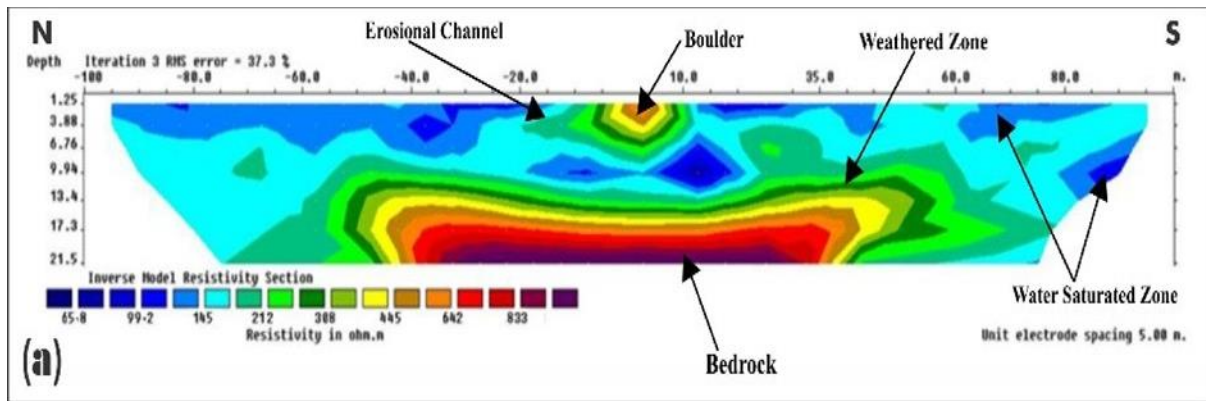
Figure 5.7: (a) Profile 5 electrical resistivity tomography, (b) Geologic cross-section interpreted from the resistivity model within a sequence of horizontal sedimentary sequence (see figure 5.3).

5.4.5 Profile 6

The electrical resistivity tomography section, as shown in Figure 5.8a), was lithologically interpreted based on different resistivity values distributed across the zone and clearly shown by the geologic section in Figure 5.8b. The low resistivity values range was between 10.1 – 55.5Ωm interpreted as the weathered saturated zone located across all the zones from topsoil to the bedrock and formed the bedrock. The lithological composition of this is silt clayey deposit with principal aquifer formation and depot for groundwater. The intermediate resistivity range is the next with the resistivity values between 125 – 546Ωm. This layer interpreted as the weathered zone composed from fine to coarse sandy plus alluvium material. Another range was the high resistivity range with resistivity value greater than or equal to 1126Ωm, interpreted lithologically as the coarse-sandy in a mixture of gravel, located at a distance 280 – 350m, depth 1.25 – 21.5m, and 20.3m depth thickness. It is important to note that this profile crosses both the Benin formation and the alluvial deposits (see Figure 5.1). Profile 7 was omitted because of its geological structural similarities with profile 6.
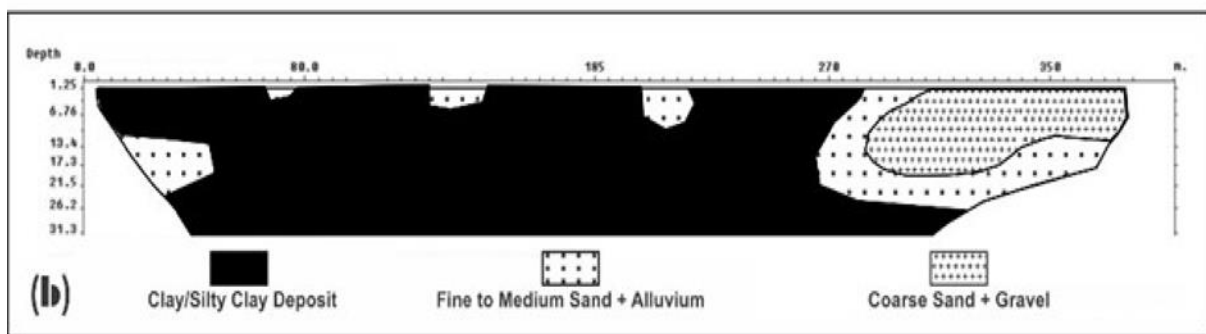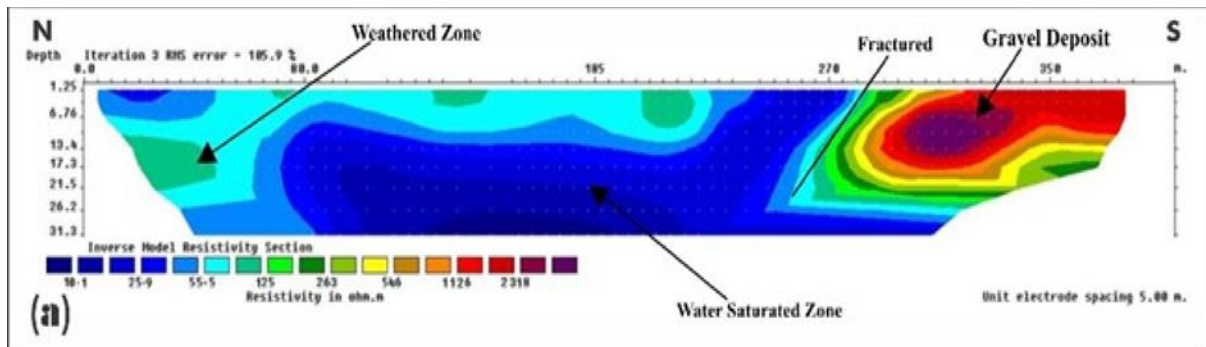
Figure 5.8: (a) Profile 6 electrical resistivity tomography, (b) Geologic cross-section interpreted from the resistivity model within a sequence of horizontal sedimentary sequence (see figure 5.3).

5.4.6 Profile 8

Based on the inversion resistivity model in Figure 5.9a and the perceived geological cross-section in Figure 5.9b, three resistivity ranges can be detected; low resistivity layer, intermediate resistivity layer, and high resistivity layer. The low resistivity value was between 33.6 – 123Ωm, which was interpreted as the saturated zone located at a distance that covered the entire profile with 21.5 - >31.3m depth (i.e. silty clayey-sandstone bedrock). This layer is interpreted as potential groundwater resources in unconfined aquifers in the area. Next, the intermediate resistivity range which was between 234 – 777Ωm. At depth 13.4 – 17.3m with depth thickness of 3.9m, the intermediate zone was interpreted as the weathered saprolite zone (i.e. fine to coarse sandy plus alluvium subsoil). Another range was the high resistivity value > 1422Ωm. This was interpreted as the Coarse sandy mixture with gravel that formed the topsoil located at depth 0 – 13.4m. The high resistivity values >2738Ωm interpreted as the Coarse sandstone mixture with gravel that formed the topsoil, which covered the profile. This is typical of rocks that are underlain by the Nanka formation.
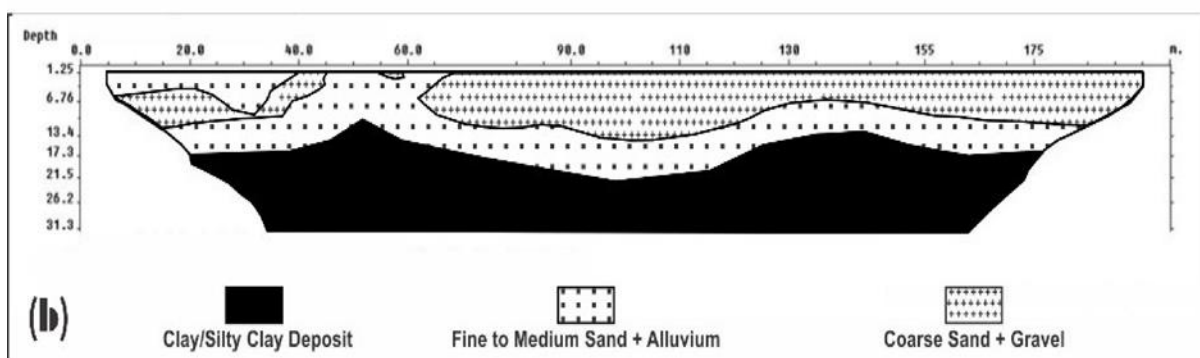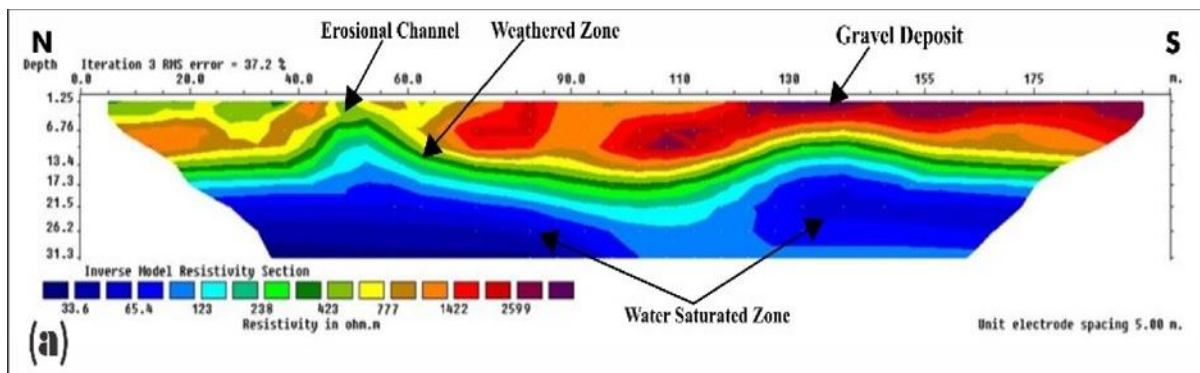
Figure 5.9: (a) Profile 8 electrical resistivity tomography, (b) Geologic cross-section interpreted from the resistivity model within a sequence of horizontal sedimentary sequence (see figure 5.3).

5.4.7 Profile 9

In this profile, a low resistivity zone (8.97–88.4Ωm) from the centre of the survey lines to the end, between 95–195m mark, extends to depths beyond 13.4m (Figure 5.10a). The lithological interpretation from the resistivity of rocks at this zone showed clayey deposits that combined with sandstone to form the bedrock (Figure 5.10b). The extension of this low resistivity zone from the centre suggests the presence of a fracture weathered zone. A distinct intermediate resistivity section (277 - 878Ωm) between the bedrock and the subsoil mark is found below at depths >31.3m extend to 13.4m. This zone is a potentially water-bearing fracture that feeds the shallow subsurface of the profile. The Imo formation have prolific water bearing capacities (see figure 5.1). Profile 10 and 11 were omitted because of its geological structural similarities with profile 9.
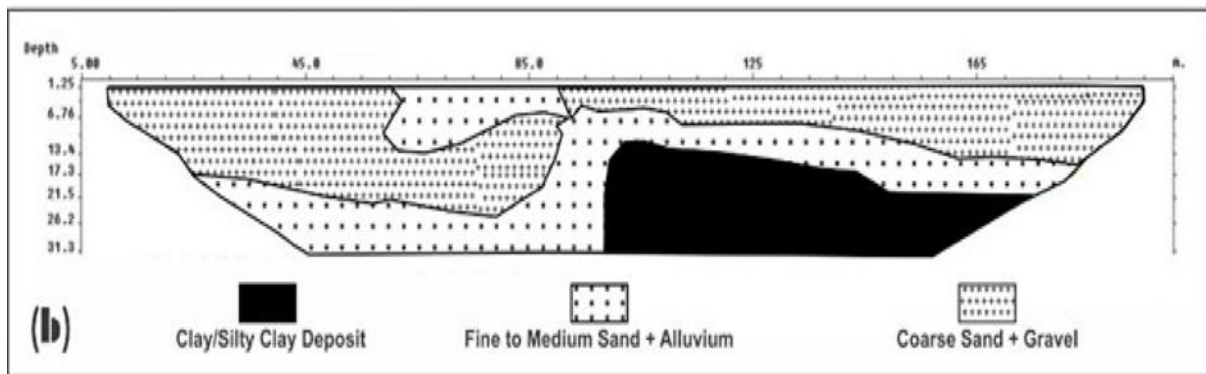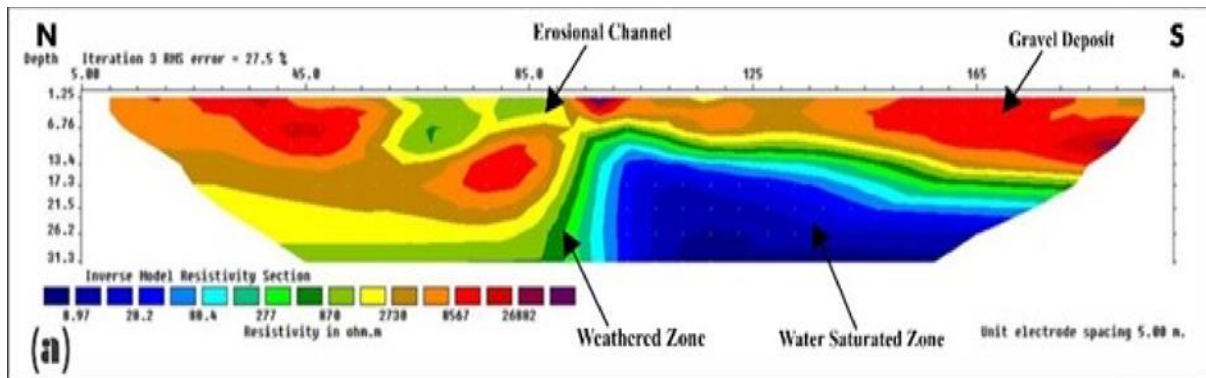
Figure 5.10: (a) Profile 9 electrical resistivity tomography, (b) Geologic cross-section interpreted from the resistivity model within a sequence of horizontal sedimentary sequence (see figure 5.3).

5.5 Conclusions

Geophysical techniques helped us portray and understand the level of destruction caused by the Nanka landslide, Anambra State, Nigeria, to the lives and properties in the area. Geological and geophysical investigations were intimated in this research by using 2D ERT profiling. The profiles were distributed randomly around the study area covering different formations of the Anambra Basin. The results from the research indicated that this landslide is caused by eluvium materials that form a heterogeneous body of clayey-sandstone boulders of various sizes, with the sliding surface (zone) developing along the contact plane between the sandstone bedrock and the eluvium (weathered). The diverse compositions of the tension troughs, such as gravelly soil, talus deposit, weathered fractured rock, and breccias, resulted in variability in the resistivity. The areas with low resistivity corresponded to materials with high soil percentages. The information from profiles 1 to 7 proved that low and intermediate resistivity values are responsible for sliding block, while high resistivity values formed the bedrock. ERT profiles 8 to 11 also indicate that high resistivity values correspond to the sliding block, while low resistivity values correspond to the shale layers and groundwater zones. The groundwater level in various parts of the site was a product of intense rainfall during the rainy season.

The formation of the Nanka landslide is related to the morphology of the terrain, climatic conditions (rainfall), and human intervention. In this way, from the uncontrolled flooding from rainfall and slope saturation by water, in the central parts of the studied area is formed a shallow landslide. It also noted that in the eastern part of the studied area, the cliff was in critical condition to the potential of land-sliding. The existence of features such as fractures and boulders have also the potential of slope failure. Thus, this concludes that this study successfully investigates the landslide slope by using 2D resistivity and geologic characterization.

Bibliography

Andrade, R. (2011). Intervention of Electrical Resistance Tomography (ERT) in resolving hydrological problems of a semi arid granite terrain of Southern India. *Journal of the Geological Society of India, 78*(4), 337.

Asry, Z., Samsudin, A. R., Yaacob, W. Z., & Yaakub, J. (2012). Groundwater Exploration Using 2-D Geoelectrical Resistivity Imaging Technique at Sungai. Udang, Melaka. *Journal of Earth Science and Engineering, 2*(10), 624.

Azhar, A., Hazreek, Z., Aziman, M., Haimi, D., & Hafiz, Z. (2016). *Acidic barren slope profiling using electrical resistivity imaging (ERI) at ayer hitam area Johor, Malaysia*. Paper presented at the Journal of Physics: Conference Series.

Batayneh, A. T. (2006). Use of electrical resistivity methods for detecting subsurface fresh and saline water and delineating their interfacial configuration: a case study of the eastern Dead Sea coastal aquifers, Jordan. *Hydrogeology Journal, 14*(7), 1277-1283.

Bichler, A., Bobrowsky, P., Best, M., Douma, M., Hunter, J., Calvert, T., & Burns, R. (2004). Three-dimensional mapping of a landslide using a multi-geophysical approach: the Quesnel Forks landslide. *Landslides, 1*(1), 29-40.

Binley, A., & Kemna, A. (2005). DC resistivity and induced polarization methods. In *Hydrogeophysics* (pp. 129-156): Springer.

Bruno, F., & Marillier, F. (2000). Geophysical surveys on two landslides in the Swiss Alps, a comparison. *XXV Assembly European Geophysical Society*.

Chambers, J. E., Kuras, O., Meldrum, P. I., Ogilvy, R. D., & Hollands, J. (2006). Electrical resistivity tomography applied to geologic, hydrogeologic, and engineering investigations at a former waste-disposal site. *Geophysics, 71*(6), B231-B239.

Chinweze, C. (2017). Erosion and Climate Change Challenges: Anambra State Nigeria, Case Study Paper presented at the IAIA17 Conference. https://conferences.iaia.org/2017/uploads/presentations/IAIA17%20Erosion_Chizoba. pdf

Coggon, J. (1971). Electromagnetic and electrical modeling by the finite element method. *Geophysics, 36*(1), 132-155.

Cubbage, B., Noonan, G. E., & Rucker, D. F. (2017). A modified Wenner array for efficient use of eight-channel resistivity meters. *Pure and Applied Geophysics, 174*(7), 2705-2718.

Dahlin, T., & Loke, M. H. (1998). Resolution of 2D Wenner resistivity imaging as assessed by numerical modelling. *Journal of Applied Geophysics, 38*(4), 237-249.

Egbueri, J. C., & Igwe, O. (2020). The impact of hydrogeomorphological characteristics on gullying processes in erosion-prone geological units in parts of southeast Nigeria. *Geology, Ecology, and Landscapes*, 1-14.

Gercek, H. (2007). Poisson's ratio values for rocks. *International Journal of Rock Mechanics and Mining Sciences, 44*(1), 1-13.

Gowen, R. A., Smith, A., Fortes, A. D., Barber, S., Brown, P., Church, P., . . . Crawford, I. A. (2011). Penetrators for in situ subsurface investigations of Europa. *Advances in Space Research, 48*(4), 725-742.

Hazreek, M. (2010). Application of Geoelectrical Method in Subsurface Profile Forensic Study. *Proceedings of MUCET*.

Israil, M., & Pachauri, A. (2003). Geophysical characterization of a landslide site in the Himalayan foothill region. *Journal of Asian Earth Sciences, 22*(3), 253-263.

Jongmans, D., & Garambois, S. (2007). Geophysical investigation of landslides: a review. *Bulletin de la Société géologique de France, 178*(2), 101-112.

Kaufmann, O., Deceuster, J., & Quinif, Y. (2012). An electrical resistivity imaging-based strategy to enable site-scale planning over covered palaeokarst features in the Tournaisis area (Belgium). *Engineering Geology, 133*, 49-65.

Kern-Simirenko, C., & Wawro, W. (1990). Reference Materials in Russian and Soviet Area Studies, 1987-88. *Russian Review*, 175-181.

Lapenna, V., Lorenzo, P., Perrone, A., Piscitelli, S., Sdao, F., & Rizzo, E. (2003). High-resolution geoelectrical tomographies in the study of Giarrossa landslide (southern Italy). *Bulletin of Engineering Geology and the Environment, 62*(3), 259-268.

Leontarakis, K., & Apostolopoulos, G. V. (2013). Model Stacking (MOST) technique applied in cross-hole ERT field data for the detection of Thessaloniki ancient walls' depth. *Journal of Applied Geophysics, 93*, 101-113.

Loke, M., & Barker, R. (1996). Practical techniques for 3D resistivity surveys and data inversion1. *Geophysical prospecting, 44*(3), 499-523.

Loke, M. H. (2004). Tutorial: 2D and 3D electrical Imaging Surveys *(Copyright 1996-2004)*, 136.

Loke, M. H., Acworth, I., & Dahlin, T. (2003). A comparison of smooth and blocky inversion methods in 2D electrical imaging surveys. *Exploration geophysics, 34*(3), 182-187.

MacInnes, S., & Raymond, M. (2001). Zonge Data Processing Two-dimensional AMT Modeling Version 4.00.

Muchingami, I., Hlatywayo, D., Nel, J., & Chuma, C. (2012). Electrical resistivity survey for groundwater investigations and shallow subsurface evaluation of the basaltic-greenstone formation of the urban Bulawayo aquifer. *Physics and Chemistry of the Earth, Parts A/B/C, 50*, 44-51.

Muchingami, I., Nel, J., Xu, Y., Steyl, G., & Reynolds, K. (2013). On the use of electrical resistivity methods in monitoring infiltration of salt fluxes in dry coal ash dumps in Mpumalanga, South Africa. *Water SA, 39*(4), 491-498.

Nazaruddin, D. A., Amiruzan, Z., Hussin, H., Khan, M. M. A., & Jafar, M. (2016). Geological Mapping and Multi-Electrode Resistivity Survey for Potential Groundwater Exploration in Ayer Lanas Village and Its Surroundings, Jeli District, Kelantan, Malaysia. *Geophysics, 2016*.

Nicollin, F., Gibert, D., Lesparre, N., & Nussbaum, C. (2010). Anisotropy of electrical conductivity of the excavation damaged zone in the Mont Terri Underground Rock Laboratory. *Geophysical Journal International, 181*(1), 303-320.

Obiadi, I., Nwosu, C., Ajaegwu, N., Anakwuba, E., Onuigbo, N., Akpunonu, E., & Ezim, O. (2011). Gully erosion in Anambra State, south east Nigeria: Issues and solution. *International Journal of Environmental Sciences, 2*(2), 795-804.

Ogbuefi, L., & Ijeomah, O (2019). Gully Erosion in Anambra State: Causes, Effects and Management Approach.

Ola-Buraimo, A.O., Akaegbobi I.M. (2012). Neogene dinoflagellate cyst assemblages of the late Miocne-Pliocene Ogwashi-Asaba sediment in Umuna-1 well, Anambra Basin, Southeastern Nigeria. *Journal of Petroleum and Gas Exploration Research, 2* (6), 115-124

Oyedele, K., Oladele, S., & Okoh, C. (2012). Geo-assessment of subsurface conditions in Magodo brook estate, Lagos, Nigeria.

Ralebakeng, T. (2015). *Research into the capacity of Nanka C10 community council to manage projects performance and origination.* University of Johannesburg,

Ramazi, H., & Jalali, M. (2015). Contribution of geophysical inversion theory and geostatistical simulation to determine geoelectrical anomalies. *Studia Geophysica et Geodaetica, 59*(1), 97-112.

Riwayat, A. I., Nazri, M. A. A., & Abidin, M. H. Z. (2018a). *Application of electrical resistivity method (ERM) in groundwater exploration.* Paper presented at the Journal of Physics: Conference Series.

Riwayat, A. I., Nazri, M. A. A., & Abidin, M. H. Z. (2018b). *Detection of Potential Shallow Aquifer Using Electrical Resistivity Imaging (ERI) at UTHM Campus, Johor Malaysia.* Paper presented at the Journal of Physics: Conference Series.

Saad, R., Nawawi, M., & Mohamad, E. (2012). Groundwater detection in alluvium using 2-D electrical resistivity tomography (ERT). *Electronic Journal of Geotechnical Engineering, 17*, 369-376.

Saleem, M. U. (2012). 2D Reflection Seismic Imaging at a Quick-clay Landslide Site, in Southwest Sweden. In.

Sasaki, Y. (1994). 3-D resistivity inversion using the finite-element method. *Geophysics, 59*(12), 1839-1848.

Sass, O., Bell, R., & Glade, T. (2008). Comparison of GPR, 2D-resistivity and traditional techniques for the subsurface exploration of the Öschingen landslide, Swabian Alb (Germany). *Geomorphology, 93*(1-2), 89-103.

Sastry, R. G., & Mondal, S. K. (2013). Geophysical characterization of the Salna sinking zone, Garhwal Himalaya, India. *Surveys in Geophysics, 34*(1), 89-119.

Sastry, R. G., Mondal, S. K., & Pachauri, A. K. (2006). *2D electrical resistivity tomography of a landslide in Garhwal Himalaya.* Paper presented at the 6th International Conference and Exposition on Petroleum, Kolkata.

Uchechukwu, N. B., Agunwamba, J. C., Tenebe, I. T., & Bamigboye, G. O. (2018). Geography of Udi Cuesta Contribution to Hydro-Meteorological Pattern of the South Eastern Nigeria. In *Engineering and Mathematical Topics in Rainfall*: IntechOpen.

Ukatu, N. N. (2019). *Factors of Gully Expansion in Nanka Gully Site: Orumba North Local Government Area (LGA) Anambra State.* Department of Geography, University of Nsukka, Nigeria.

Unah, L. (2020). Erosion crisis swallows homes and livelihoods in Nigeria. Retrieved from https://www.climatechangenews.com/2020/01/20/erosion-crisis-swallows-homes-livelihoods-nigeria.

Wallace-Wells, D. (2019). *The uninhabitable earth: A story of the future*: Penguin UK.

CHAPTER 6: CONCLUSIONS AND RECOMMENDATIONS

6.1 Introduction

The study was conducted using High-Resolution Geophysical Imaging and Characterization at the severe landslides' vicinities in South-Eastern Nigeria for Uni-Vario-Seasonal degradation monitoring and Civil Engineering remediation. The research work used both geoelectrical '(vertical electrical sounding (VES), 2D Electrical Resistivity Tomography (ERT), and 'Induced polarization)' and geotechnical methods (particle-size analyses, compaction, Atterberg limits, and shear strength tests) to study the landslides at the different parts of South-Eastern Nigeria. The results generated from each research method complement each other in terms of findings and other lithological similarities.

6.2 Summation of the findings

From the course of the research work, the following findings were made;

1. The geoelectrical results from the Nanka landslide proved that the values of recording a continuous spatial pattern, high-resolution VES data for monitoring of the subsurface, demonstrated the advantages of this method over other field techniques and traditional surface mapping. The spatially continuous VES survey of this form allows for volume measurement, separation of different zones, and identification of activities at the gully rim even within the gully interior.

2. The percent increase in the sand with depth at topsoil/subsoil soil was generally not well graded with a high content of fine fraction at the Nanka slide. The textural characteristics of the analysed samples proved that the sand fraction ranges from 69% to 81% with a mean value of 77.8%, gravel ranging from 1% to 2% with approximately 1% mean value, and the silt+clay values also ranging from 18% to 23% with 21.2% mean value.

3. The research results showed that the underlying strata have a low amount of shrinkage potential and plasticity that resulted in the highest instability of the binding materials at sub/topsoil and thereby resulted in the vulnerability of the underlying soil materials to erosion.

4. From the Nanka site, the liquid limit, plastic limit, plasticity index, maximum dry density, and optimum moisture content have average values of 34.92%, 23.31%, 11.61%, 1.86Mg/m^3, and 10.18%; respectively. The low value of the liquid limit of the underlying strata was due to the low amount of fine fraction and suggests that the soil can transition from one state of consistency to another with minimal change in water content. The site's curvature coefficient (Cc) ranged from 0.198 to 0.243, which resulted in uniformly graded soil. This pattern indicates lowering cohesion and soil cracking resistance.

5. The soil shear strength samples decrease with depth at the respective gully sites, which is why the coherent top/subsoil helps to initiate the gully process by encouraging overland flows that lead to the formation of rills and eventual landslides.

6. The regolith thickness contour map and other contour maps showed that the landslide was active, shallow, with material slumps and runout slides. The high void ratio of the cohesion soil resulted in high infiltration rates, resulting in higher flow velocity and internal erosion potential.

7. The landslides in South-Eastern Nigeria showed that the formation of the slides into the top red laterite layer of soil tends to be more controllable than the cut in the sand without cohesion. Soil properties and formations, among other factors, contribute immensely to landslide development. Soil that is predominantly sandy with a high ratio of void and low density is most susceptive to a severe landslide. Once the underlying uncompacted soil with a high void ratio and poor porosity penetrated, the gully formation increases. This is due to the loose nature and failure of the roots of the plant to tie the soil particles together as related to the study locations.

8. The 2D, IP, and geological lithology correlation provided valuable knowledge for studying the hydrogeological model of these landslides' terrains. The formation of the groundwater in the study areas has been affected by creeps' events of the landslide. This survey obtained high values of measured chargeability at different parts of the profiles because of the large and chargeable surface of the sandy particles and the clay mineral composition.

9. These high resistivity values obtained mostly at the bedrock decreases in value with depth, and a boulder of rock fragments with different sizes that weathered into sediments of rocks easily collapsed as the slides plate found at the topsoil. The electric resistivity shriveled with depth as the coarse materials ranged from boulders to sand, and the aquifer system is composed of a layer with a high content of clay.

10. The findings proved that the study areas have the potential for slope failure due to the existence of features such as weathered zones and boulders and that the soil properties and compositions contribute immensely to this geo-environmental hazard.

11. Finally, the lithologies of the vertical geo-electric section showed the slides layers are sandy, clays, gravel, alluvium, natural water (sediments), which was also confirmed by geotechnical results.

6.3 Preventive measures

In view of a thorough investigation of the causes, development, consequences, and remediation of landslides in South-Eastern Nigeria, the following control measures are suggested to assist the agencies, government, researchers, and affected communities, to overcome this geo-environmental problem. They include;

a. The initiation of human-induced landslides activities such as unlawful and imprudent destruction of topsoil, overgrazing, continuous harvesting, disposal of garbage and obstruction of drainage, etc. must be avoided.

b. Annual monitoring of the sliding therein with modern geophysical equipment to offer pre-information on the subsurface conditions is highly needed.

c. The government should provide modern geophysical equipment and money to higher education geophysics and geology students to conduct student research in the impacted areas.

d. Proper scientific documentation of prior events/occurrences at the erosion site is required since they will always serve as a reference for future studies.

e. Government, non-governmental organizations, and community representatives must periodically educate the public, particularly those from impacted areas, about the

implementation of farming and other modes of human action that would not intensify landslide initiation.

f. Laws guiding building construction should be enforced by the governments and organizations involved to prevent future blockage of drainage systems. The agencies need to map out the entire area devastated by landslide to guide property developers and builders to build anti-slide structures.

g. Government at all levels and community leaders should be proactive in stopping the threat of landslides quickly before property and life losses occur.

h. In order to prevent the development of landslide characteristics, proper soil and environmental impact assessment should be carried out prior to the location of any infrastructure.

i. It is vital to promote crop and tree planting on flood plains through afforestation and reduced unnecessary deforestation.

j. Path and drainage maintenance must be imposed on giant control geoengineering systems, as these systems inevitably guide the runoff water that breakdown often, resulting in more severe harm.

6.4 Recommendations for future research

Further geophysical surveys, such as well-logging, seismic, Transient Electromagnetic, and Magnetic Resonance Sounding to determine the mineralogy of the clay in the study areas, should be encouraged. Further studies should include assessing the thickness of the bottom layer with a high clay content and the groundwater/ aquifer boundary conditions. Geotechnical students from other institutions should be encouraged to investigate the landslides phenomena in their environment to suggest to the masses, government, and their communities how to check this global environmental disaster.